PAUL SCHERRER INSTITUT

Progress Report September 2005 to September 2006

Laboratory for Waste Management

Nuclear Energy and Safety Research Department

Preface

The Laboratory for Waste Management has two tasks: (i) to carry out an R&D programme strengthening the scientific basis for nuclear waste management, and (ii) to build and then operate – together with the SLS team – a microXAS beamline.

In its first task, the Laboratory serves an important national role by supporting the Swiss Federal Government and Nagra in their tasks to safely dispose of radioactive wastes from medical, industrial and research applications as well as from nuclear power plants. The activities are in fundamental repository chemistry, chemistry and physics of radionuclides at geological interfaces and radionuclide transport and retardation in geological media and man-made repository barriers. The work performed is a balanced combination of experimental activities in dedicated laboratories for handling radioactive elements and in the field, and theoretical modelling. The work is directed towards repository projects and the results find their application in comprehensive performance assessments carried out by Nagra.

This report summarises the activities and results achieved in the reporting period. It is organised as an overview followed by individual reports on the six waste management sub-programmes and a section on the status of the microXAS beamline.

We gratefully acknowledge the help of the Institute's management and of Nagra in our work.

.

Table of Contents

1 OVERVIEW

M. Bradbury

1.1 Introduction

The progress made in the Laboratory (LES) since September 2005 is summarised in this first section. The work within LES is organised into two projects.

The first is the Waste Management Programme. The progress made in each sub-programme is given in sections 2 to 7. There are strong interactions between the sub-programmes as well as between experimenters and modellers, as can be appreciated from the work descriptions in the different sections. The results of the XAFS sub-programme are integrated into the other activities. It is also the aim in this first section to facilitate for the reader, an appreciation of these interactions.

The second is the microXAS beamline project. The status is presented in section 8. The main incentive for this project was to gain a better understanding and insights into reactions occurring at the molecular level at solid surfaces. X-ray absorption spectroscopy has become an integral tool in the Waste Management Programme.

1.2 General

An important milestone in nuclear waste management in Switzerland was reached on 28 June 2006 when the Bundesrat announced the approval of the Entsorgungsnachweis Bericht (Demonstration of Disposal Feasibility). This decision confirmed that the construction of a deep geological repository for Spent Fuel (SF), Vitrified High-Level Waste (HLW) and Long-lived Intermediate-Level Waste (ILW) is in principle practicable. The Entsorgungsnachweis was submitted to the Bundesrat in December 2002 and since then has undergone intensive review and appraisal procedures from expert groups from the OECD/NEA, HSK (Swiss Federal Nuclear Inspectorate), KNE (Commission for Nuclear Waste Management) and AGNEB (Federal Government Working Group on the Disposal of Nuclear Waste). In addition, numerous consultations with Cantonal authorities and interest groups were carried out.

The Federal Minister for the Department of Environment, Transport, Energy and Communication (UVEK) requested Nagra to evaluate alternatives to the Zürcher Weinland for the siting of a deep geological repository for HLW/SF/ILW, in particular with respect to safety and geology. This “options report”, published in August 2005, identifies the preferred geological-tectonic areas and the possible host rocks in these preferred areas. Criteria such as sufficient lateral extent, suitable depth and sufficiently unperturbed rock were applied in the selections.

In March 2006 the Department of Energy (BFE) presented the first draft of the conceptual part of the Plan for Site Selection for a deep geological repository (Sachplan). The Sachplan is a planning instrument in which the government lays down site selection criteria for the deep geological disposal of low and intermediate level and HLW/SF/ILW waste. The long term safety and the environment are the two priority considerations. The process of site selection should ensure that the public are continually and transparently informed and that there is close cooperation at the Canton, local authority and neighbouring country levels.

Last but not least Nagra is in the process of preparing an Entsorgungsprogramm (Disposal Programme) which has to be submitted to the Bundesrat for approval. The breadth and content of this programme are defined in the Nuclear Energy Law and includes issues such as, radionuclide inventories and their allocation to the different repository types, the required deep geological repositories and their lay outs, repository realisation plans, costs and timescales, financial modalities etc. It is required that the programme be reviewed and readjusted, where necessary, every 5 years and that the HSK and UVEK will have the responsibility of checking and monitoring the compliance of the progress with the planning.

The Entsorgungsprogramm is of particular interest for LES since it contains a longer term R&D part. In order to be correctly represented in this planning, the decision was made to produce a long term (~10 years) research strategy paper divided into time periods of 3, 6 and 10 years. After some intense and fruitful discussions with Nagra a substantial first draft document entitled “LES Research Strategy in Radioactive Waste Management to 2017” was completed in mid June 2006. The production of this strategy paper is also seen as a start to answering some criticisms made at Programme Committee Meetings and in the LES-Audit of 2004.

The document is not only relevant for the above two reasons, but is also important because it will provide clear guidelines for the future scientific research activities and perspectives upon which co-workers can orientate themselves. As with all planning documents,

periodic updates will be required, and the report will form a platform for any necessary changes in the future being transparent and traceable.

In the period up to September 2006 some major and outstanding progress was made at the microXAS beamline at the PSI Swiss Light Source (SLS). The beamline was declared officially commissioned at the end of May 2006. Normal "user operation" started at the beginning of June, and out of some 30 submitted proposals, 18 user proposals were granted beam time between June and December 2006. The beamline joined the pooled facilities in ACTINET and was included in the 5th call for proposals (deadline mid May 2006). Two proposals with radioactive samples were given beamtime at the end of October 2006.

The design aim of a 1x1 μm^2 beam of hard X-rays was always going to be a hard target to reach, given, in particular, the source size and the limited maximum length of any optical beamline system. Nevertheless, a measured spot size of approximately 0.7x1.3 μm^2 has been achieved. This corresponds to the smallest X-ray beam produced at the SLS using achromatic optics (e.g. KB mirrors). A unique feature of the microXAS beamline is the capability of fast switching between the two different beam modes (monochromatic micro-beam and micro-focused white light).

Standard, two-dimensional XRF mapping is commonly based on a "stop-measure-go" procedure advancing from pixel to pixel. An "on-the-fly" fast XRF mapping procedure is being implemented which will reduce total mapping times by up to one order of magnitude. In addition, in cases where the pixel size is larger than the beam size, the continuous scanning mode yields a true averaging over the entire pixel.

The first investigations on radioactive samples were successfully carried out at the microXAS beamline during 11-13 July 2006. A heterogeneous cement sample containing ^{60}Co and a zircaloy sample containing ^{51}Cr, ^{60}Co, ^{103}Ru, ^{125}Sb, ^{132}Te and ^{137}Cs were analysed. Elemental distribution maps were recorded for both samples by collecting two-dimensional micro-XRF data, and the first micro-XAS spectra of a radioactive specimen was collected.

Within the 6th EU Framework Programme, LES is contributing in two main areas:

(1) experimental and modelling studies on the influence of inorganic carbon on the sorption of Ni, Eu and U(VI) on montmorillonite / bentonite (NF-PRO), and illite / Opalinus clay (FUNMIG) and

(2) measuring the diffusive transport characteristics of selected anions (e.g. I^-, Cl^-) and cations (e.g. Na, Cs, Ni) in compacted bentonite (NF-PRO) and Opalinus clay (FUNMIG). Predictive and interpretive modelling in connection with the Diffusion Retardation (DR) experiments at Mont Terri is also being performed within the FUNMIG project.

A further 6th EU Framework activity includes XAS measurements of Se(VI) and Tc(VII) in contact with corroding canister components within NF-PRO. The Integrated Project NF-PRO is due to finish at the end of 2007.

A joint project between JAEA (Japan) and LES has been set up to investigate the partitioning of Ra(II) between aqueous solutions, bentonite and clay sediments, in the presence / absence of minor minerals that could act as sinks for this radionuclide. These minor minerals include barite, calcite and witherite. The duration of the project is fixed at 3 years (official start date 01-04-06) and both partners will finance their own activities within the project.

The University of Mainz, IFR (ROBL) and LES have submitted a joint proposal to ACTINET entitled "Batch experiments and spectroscopic studies of Np(V) sorption on montmorillonite". A PhD student and Post Doc from the University of Mainz will spend 4-5 weeks each at PSI to carry out sorption measurements and modelling.

Bilateral co-operations with external institutions and scientists have continued and are summarized in Table 1.1.

At the end of September 2006, three PhD students were studying in LES. A fourth PhD position has been approved and a student is being actively sought. A proposal for a fifth student has been submitted for approval and it is anticipated that funding for a sixth could be provided as a result of LES's participation in the Geothermal Reservoir Processes project within the Competence Centre Environment and Sustainability. During the past year LES has been particularly successful in its applications for EURATOM Training Fellowships: Inter European Fellowships scheme (Marie-Curie EURATOM Fellowship). Two fellowships have been granted, both beginning in November 2006, and each being fully financed by the EU over a 2 year period. The first project is entitled "Influence of carbonate on actinide sorption on clay minerals" (INCA), in cooperation with INE, FZK and IFR, FZR. The second, "Diffusion of nano-particles in argillaceous media: Assessment of pore structure" (DINAPOR), will be carried out in cooperation with IFR, FZR. A third Marie-Curie EURATOM Fellowship proposal "Microscale investigations of the speciation and mobility of U(VI) in cementitious materials" (MISUC), in cooperation with CEA Saclay/DANS/DPC and IFR, FZR has received very good evaluation marks and is expected to be

successful with the candidate probably starting in Spring 2007. A post doc proposal to implement and optimise the MCOTAC reactive transport code on the massively parallel computer XT3 (HORIZON) and Merlin has also been submitted.

Table 1.1

Co - Operations
Nagra*
Major financial contribution
Various technical working groups
Multinational
6th FP (NoE: ACTINET-6, IP: NF-PRO, FUNMIG),
OECD/NEA TDB III (Fe),
OECD/NEA TDB (solid solutions)
Mont Terri Project (Diffusion Retardation)
Grimsel Test Site (Colloid Formation Migration)
Universities
Bern, Switzerland (mineralogy, petrography)
Irkutsk, Russia (speciation)
UC London, UK (molecular modelling)
Mainz, Germany (cement, montmorillonite)
Strasbourg (glass)
Tübingen (geosphere transport)
Research Centres
CEA*, France (near and far field)
CIEMAT*, Spain (clay systems)
EAWAG, Switzerland (cement)
EMPA*, Switzerland (cement)
INE, FZK*, Germany (near and far field; TRLFS)
JAEA, Japan (Ra in bentonite/argillaceous rocks)
IFR, FZR*, Germany (XAS, TRLFS)
Nuclear Research Centre Mol, Belgium (clays)
VTT, Finland (pH in compacted bentonite)
*formal co-operation agreements

On September 26 and 27, 2005, the Waste Management Programme Committee met for their annual meeting. The work performed within LES and the future plans were discussed as usual (AN-44-05-06). The valuable help and input from the members of the committee, both at the meeting, and throughout the year is appreciated by the whole Laboratory.

1.3 Performance assessment

Although there were no activities in 2005/06 involving direct participation in performance assessment, this situation is expected to change in the years up to approximately 2014. This is a direct result of the implementation of the Sachplan for the deep geological disposal of low and intermediate level and HLW/SF/ILW waste. The site selection procedures laid down in this document for the different types of radioactive waste involve the selection of potential regions and potential sites within these regions. These will involve safety appraisals/evaluations at increasing levels of detail and completeness as the process becomes more and more specific with respect to the selection of a site. Implicit in this process will be reviews and updates of sorption and solubility data bases and transport calculations performed for specific case studies using know how and the sophisticated codes available in LES. Depending on the selections made, whole new data bases may need to be developed involving specifically designed laboratory studies. In any event, the trends in the coming years will be more and more towards site specific studies both in terms of the experimental work and in terms of the application of models and codes.

During the past year a significant portion of the research has been aimed at trying to answer various issues raised in the reviews of the Entsorgungs-nachweis by the OECD/NEA, HSK and the KNE i.e. validity of the use of chemical analogues (e.g. Th(IV) for the tetravalent actinides), gaps in the data base (sorption of Pa), justification of the high sorption values used in the SDBs, Ra solubility, transfer of sorption data and models derived from dispersed systems to intact rock (OPA) and compacted systems (bentonite).

In addition, as a result of discussions with Nagra, a partial re-orientation of the future research work is taking place so that some critical PA related topics, mainly concerned with the dose determining radioelements such as ^{14}C, ^{129}I, ^{79}Se and ^{99}Tc, will be addressed. In particular, an experimental/modelling task force will be set up to investigate the speciation and transport properties of ^{14}C containing aqueous species arising from anaerobic corrosion of carbon steels. Although the information existing in the literature on this topic is very sparse, the indications are that ^{14}C may be released in the form of small organic molecules which could be very mobile. The uncertainties surrounding this topic and the potential safety relevant consequences are the driving forces for the investigations.

1.4 Foundations of repository chemistry

Our participation in international reviews of thermodynamic data within the scope of the OECD/NEA Thermodynamic Data Base Project in 2006 has continued, but at a reduced level. The reviews on selected organic ligands and zirconium were published in November 2005 and the manuscript on the “Scientific guidelines for the evaluation of thermodynamic data for solid solutions” has reached the final stages. LES’s contribution to the NEA TDB review on iron (aqueous complexation of Fe(II)) is still ongoing.

The functionality of the GEMS-PSI code has been further enhanced and the performance and stability of

the GEM-IPM numerical kernel has been increased by ~10% and no longer exhibits the numerical artefacts present in the previous version. Such a "stand alone" version of GEM is a prerequisite for coupling it to fluid mass transport codes. The set up and subroutines for surface complexation sorption models have been improved and calculations with CD-MUSIC on multiple surfaces and site types are possible.

1.5 Repository near field

1.5.1 Clay systems

Although Monte Carlo simulations have shown that NaCl ion pair formation in the interlayer region of Na-montmorillonite increases as the amount of interlayer water decreases, the question as to whether it is energetically favourable to transfer Na^+ and Cl^- ions from the bulk water into the interlayer space remains open. This question is being addressed by free energy perturbation and Gibbs ensemble Monte Carlo simulations, and experiments using chloride K-edge EXAFS studies at the SLS LUCIA beamline. This work could have implications for the diffusion transport of dose determining anions such as Cl-36, if it is shown that diffusion through the interlayer space as neutral (Na^+Cl^-) and charged (Na_2Cl^+) ion pairs is a possible and significant process.

A modified version of the Monte Carlo code provided by N. Skipper (UC London) optimising memory and CPU time usage was used to calculate realisations for a mixed Na, Ca montmorillonite with octahedral charge only. The 6 x 4 clay unit cell contained 1920 atoms in the clay layer and 384 water molecules, 18 Cs and 18 Na ions in the interlayer. Classical molecular dynamics calculations can yield insights into radionuclide diffusion mechanisms in the interlayer space. For example, it was shown that the diffusivity of water and ionic species decreases strongly in a highly non linear manner as the interlayer water content decreases. The effect for Cs is much more pronounced than for Na or water because of the stronger binding of Cs to the surface.

The work on the long term aim of constructing a thermodynamic sorption data base for montmorillonite using the 2SPNE SC/CE sorption model has continued. Surface complexation constants deduced from sorption edge measurements for Am(III), Np(IV) and Pa(V) fit very well onto the previously established linear free energy relation for montmorillonite. It was also demonstrated clearly that Eu(III) is a very good sorption analogue for trivalent actinides. As an important step in being able to model natural bentonite systems, sorption edge measurements for Ni and U(VI) in the presence of inorganic carbon have been carried out, but only partially modelled, as part of the FUNMIG EU Integrated Project.

A series of through-diffusion experiments with $^{22}Na^+$ and $^{85}Sr^{2+}$ across Na-montmorillonite samples at a density of ~1950 kg m^{-3} was completed. A clear effect of the ionic strength of the contacting solution on the diffusive flux was observed. If the data were interpreted assuming that the concentration gradient in the aqueous phase was the driving force for diffusion, then the slopes of the plots of log(effective diffusion coefficient, D_e) against log(conc. NaCl) were -1 and -2 for $^{22}Na^+$ and $^{85}Sr^{2+}$, respectively. Such a dependence on the external salt concentration is very difficult to understand. If however, the hypothesis is made that interlayer diffusion is the dominant process and the driving force is the gradient in the interlayer (essentially determined by cation exchange of the respective diffusing species), then the calculated interlayer diffusion coefficients (D_{IL}) were found to be independent of the composition of the external water phase. Also, the dependence of the diffusive flux on the external water composition could be readily and quantitatively explained. Independent evidence for the interlayer diffusion of Na^+ was obtained from membrane potential experiments.

$^{36}Cl^-$ through-diffusion experiments as a function of the dry density of the bentonite and the chemical composition of the external water indicated that $^{36}Cl^-$ is completely excluded from the interlayer pore space, and partially from the interparticle pore space. The extent of exclusion from the interparticle pore space depends on the chemical composition of the pore water. Unlike cations, the diffusion of anions occurs solely in the interparticle pore space.

The Colloid Chemistry sub-programme is contributing to the Colloid Formation and Transport (CFM) project being carried out at the Grimsel Test Site through laboratory experiments. A series of tests have been carried out using compacted FEBEX pellets in contact with NaCl solutions and Grimsel ground water to investigate the key colloid phenomena of re-suspension (generation) and sedimentation (elimination). In both systems a pseudo equilibrium is reached in which the colloid size distributions are similar.

The focus of the long running glass corrosion experiments (14 years!) is now on EXAFS based investigations of the corrosion products, and aims at determining the distribution and microscopic speciation of safety relevant elements. Although the EXAFS experiments are at an early stage, it has been shown that the distribution of Cs is homogeneous in the unaltered glass and in the corrosion products whereas the distribution of Ni is heterogeneous and tends to be concentrated, in association with Mg, in

alteration products (Mg-smectites) at the periphery of glass grains.

1.5.2 Cement

Hardened cement paste (HCP) is a heterogeneous and chemically complex matrix consisting of a number of different phases. One of the main aims of this work is to identify which phases are predominantly responsible for the often element dependent uptake. To this end, a series of cement minerals were synthesized and characterized, including ettringite (AFt-type phase), calcium monocarboaluminate and calcium monosulfoaluminate (AFm-type phases), tobermorite and xonotlite (crystalline CSH phases) for use in wet chemistry and spectroscopic studies.

The composition and structure of cement phases are affected by many factors - including the composition of the cement, the water-to-cement ratio, the temperature, the degree of hydration, and the presence of chemical and mineral admixtures. Any model for the structure of C(A)SH must account for these observations. As part of an atomistic study of cement phases, the mechanism of water incorporation in the interlayer space of tobermorite, the formation of the Si-tetrahedral chains, the structural position of Al^{3+} impurities and the mechanism of charge compensation in the defects of the Si-tetrahedral chains have been considered. The 14 Å tobermorite was simulated using the ab-initio molecular dynamics technique (MD) starting with atomic positions suggested by X-ray diffraction studies. The obtained MD trajectories will be used to build a thermodynamic sorption model of bivalent cations on CSH and to understand the sorption mechanism of trivalent actinides on the cement phases.

A sorption study on the uptake of the safety relevant element Cs on CSH phases revealed that, in addition to the inverse uptake dependence on the calcium-to-silica ratio due to competition with Ca, a very significant dependence on ageing / crystallinity of CSH phases was determined. Uptake was found to be a factor of 50 higher on a CSH phase (C/S = 1.0) that had been aged for 4 years, than on a fresh CSH having the same C/S ratio, probably due to the formation of an interlayer structure in the aged sample.

The proposed cation exchange model for the uptake of Sr by replacement of Ca in CSH phases, which was also successfully used to interpret Ra sorption data, was extended to include the influence of Na and K. Both of these elements are present at high concentrations in fresh cement porewater.

Although the EXAFS study on U(VI) loaded CSH phases showed that information on the coordination environment of bound U(VI) could be obtained, relatively high U loadings of > 1000 ppm were required due to the limited sensitivity of the technique. Sorption isotherm measurements indicated non linear sorption at loadings less than 1000 ppm and therefore that different sorption mechanism was operating. Time resolved laser fluorescence spectroscopy (TRLFS) studies have begun in cooperation with IFR/FZR to investigate U(VI) speciation in CSH systems at more relevant loadings. In order to obtain the necessary spectral resolution under strongly alkaline conditions, the measurements had to be carried out at temperatures below 150 K.

The observation that the R_d values of lanthanides and trivalent actinides apparently decrease with increasing solid-to-liquid ratio, possibly related to the presence of very small colloids, have not yet been resolved. The intention is to carry out some ultra centrifugation tests at 550000 g. Also, the initial investigations into the uptake of Np on cementitious systems clearly indicated that methodologies need to be developed which enable the sorption experiments to be carried out under well defined redox conditions. Electrochemical methods and chemical poising agents will be investigated. In addition the valence states, both in the aqueous and on the solid phase, need to be checked.

The project to investigate the chemical reactivity of α-isosaccharinic acid (α-ISA) in an artificial cement pore water under repository conditions, was completed at the end of May 2006. The main conclusions drawn were that the chemical transformations to smaller organic molecules were not catalytically promoted by oxygen and complete chemical transformation of α-ISA was only observed when stoichiometric amounts of oxygen were present.

The Ph.D. project of M. Vespa on the speciation of Co and Ni in hydrating cement has been finished and the final Ph.D. examination is scheduled for the end of October 2006.

1.6 Repository far field

The focus of the far field work remains firmly on Opalinus clay (OPA).

The experimental and modelling investigations on illite have been extended to other key radionuclides (Co(II), Sn(IV), Am(III), Th(IV) and Pa(V)) and the work is on track to produce a LFER for illite in a similar way to that for montmorillonite. The experimental work on the influence of inorganic carbon on the sorption of Ni(II) and U(VI) has been completed. Under the assumption that carbonate complexes do not sorb, all of the experimental data could be satisfactorily modelled. These studies were complemented by EXAFS investigations on the

U(VI)/illite system which indicated that U sorbs preferentially to the illite surface via a mononuclear edge-sharing surface complex to one octahedral Fe and one corner-sharing tetrahedral Al site.

Cs sorption experiments on intact OPA samples (13mm and 1.5mm thick) in the concentration range ~10^{-11} to ~10^{-3} M appeared to indicate that the sorption was 2-3 times lower than measured in a dispersed system. The sorption data could however still be satisfactorily modelled with the LES Cs sorption model but with the frayed edge and type II site capacities (where the sorption was predominantly taking place) reduced by a factor of ~2. This could imply that in compacted systems the "edge" sorption sites are less available than the planar cation exchange sites.

In-diffusion experiments of $^{60}Co^{2+}$ and $^{152}Eu^{3+}$ in Opalinus clay samples were started and the $^{60}Co^{2+}$ profiles determined with the "abrasive peeling" technique. The measurements were performed in a glove box under N_2 atmosphere to avoid oxidation of pyrite in OPA. Two different components to the $^{60}Co^{2+}$ profiles were distinguished: ~90% of the Co diffused slowly and ~10% considerably more quickly. No explanation exists for this behaviour at the present time.

In order to model sorption and transport measured in batch sorption experiments and small scale laboratory diffusion and field experiments, and finally also for performance assessment purposes, the in-house 2SPNE-SC/CE mechanistic sorption model was incorporated in the reactive transport model/code MCOTAC. Exhaustive verification tests indicated the successful porting of the sorption model into the coupled code. Cs and Sr diffusion experiments through intact samples of Opalinus clay are being interpreted using mechanistic sorption models and the results will be compared with those from calculations in which the simple K_d-approach for sorption was applied. A further test case being calculated is the reactive transport of protons between the Opalinus clay and the bentonite interface, which is relevant to predicting the temporal evolution of the bentonite porewater. A major advance with far reaching consequences is the planned parallelisation of MCOTAC so that the code can be run on the massively parallel computer HORIZON.

In previous work a thermodynamic analysis of the Eu-calcite system showed the Eu^{3+} forms a solid solution in calcite having two hypothetical Eu end-members depending on the pH. The mechanism of the substitution on an atomistic level remains unknown. The main questions concern the charge compensation mechanism and the local response of the host structure on the guest ions. Atomistic modelling helps to reveal energetically favourable mechanisms of the REE and trivalent actinide substitution in calcite, which complements the information obtained from EXAFS studies and thermodynamic analyses.

Continued support to the Mont Terri field diffusion experiments has been provided through laboratory studies (diffusion coefficient and sorption values, sorption on test materials, evaluation of water chemistry) and through 2D scoping calculations using "Flotran" for radial anisotropic diffusion. Also, a new task, "Analysis of Geochemical Data" has been initiated for Phase 12 of the Mont Terri Project. LES's role in this activity is to quantitatively evaluate the effects of parameter uncertainties and perturbing processes on the water chemistry using Monte Carlo type methods and the impact of such uncertainties and heterogeneities on reactive transport calculations.

The concepts for long-term diffusion experiments as presented in MAMOT are under critical review. A viable alternative could be "large block" laboratory diffusion tests carried out in carefully extracted and preserved OPA cores from Mont Terri. If such experiments were to be performed in the hotlab then strongly sorbing radioactive tracers, including actinides, could be used.

Finally, the PhD study of Ralph Mettier in the area of radionuclide transport in fractured porous media was finished in September 2006 after three and a half years of intensive work.

Laboratory for Waste Management: Sub-Programme Structure 2006

Waste Management Programme

Management 4440xx
Mike Bradbury, OFLA/203a (2290)
Beatrice Gschwend, OFLA/203 (2417)

Geochemical Modelling 4441xx
Wolfgang Hummel, OFLA/208 (2994)
Urs Berner, OFLA/201a (2432)
Enzo Curti, OFLA/202 (2416)
Dmitrii Kulik, OFLA/201a (4742)
Tres Thoenen, OFLA/208 (2422)

Transport Mechanisms 4442xx
Andreas Jakob, OFLA/202 (2420)
Sergey Churakov, OFLA/204 (4113)
Thomas Gimmi, OFLA/206 (2901)
Georg Kosakowski, OFLA/206 (4743)
Wilfried Pfingsten, OFLA/204 (2418)
*Ralph Mettier, OFLA/205 (2368)

XAFS 4443xx
Rainer Dähn, OHLD/004 (2175)
André Scheidegger, WLGA/221 (2184)
*Marika Vespa, OHLD/004 (2966/4139)

Clay Systems 4444xx
Bart Baeyens, OFLA/207 (4316)
Mike Bradbury, OFLA/207 (2290)
Manuel Binkert, OHLD/003 (4451)
Rainer Dähn, OHLD/004 (2175)
Astrid Schaible, OHLD/005 (4317/2278)

Cement Systems 4445xx
Erich Wieland, OHLD/001 (2291/2274)
Mike Bradbury, OFLA/207 (2290)
Barbara Fontana, OHLD/003 (2289)
Dominik Kunz, OHLD/005 (4182/2274)
*Peter Mandaliev, OHLD/004 (5443)
Jan Tits, OHLD/001 (4314/2277)
*Marika Vespa, OHLD/004 (2966/4139)

Colloid Chemistry 4446xx
Claude Degueldre, OHLD/008 (4176/2276)
Roger Rossé, OHLD/005 (2204)

Diffusion Processes 4447xx
Luc Van Loon, OHLD/002 (2257/2275)
Mike Bradbury, OFLA/207 (2290)
Martin Glaus, OHLD/002 (2293/2275)
*Fatima Gonzaléz, OHLD/111 (2185)
Werner Müller, OHLD/003 (2269/2275)
Roger Rossé, OHLD/005 (2204)
Andriy Yaroshchuk OHLD/111 (5316)

Studies 4449xx
Mike Bradbury, OFLA/203a (2290)

* Ph.D. students

MicroXAS Beamline Project

Management 445xxx
Design and Construction 4451xx
Infrastructure 4452xx
André Scheidegger, WLGA/221 (2184)
Rainer Dähn, OHLD/004 (2175)
Daniel Grolimund, WLGA/221 (4782)
Messaoud Harfouche, WLGA/219 (5289)
Beat Meyer, WLGA/231 (5168)
Markus Willimann, WLGA/231 (3554)

September 2006

2 GEOCHEMICAL MODELLING

W. Hummel, U. Berner, E. Curti, D. Kulik, T. Thoenen

2.1 Overview

Work related to thermodynamic databases and codes and the foundations of thermodynamic modelling was a substantial part of the activities of the Geochemical Modelling sub-programme.

The OECD/NEA TDB reviews on selected organic ligands and zirconium were published in November 2005. The work for the NEA TDB "Guidelines" on solid solutions has reached the final stages. Within the scope of the ongoing iron review, the question of how to treat weak complexes in a consistent manner has been reconsidered.

The GEMS-PSI code was enhanced with new functionality, and the GEM numerical kernel, which had been isolated as a small stand alone programme for coupling with various fluid mass transport codes, was re-structured for better transparency and performance.

The theoretical foundations of GEM surface complexation models have been further developed and tested with several worked examples. The GEM DualTh (Dual-Thermodynamic) approach has been used to model new experimental solid-solution data for cement phases.

Further activities in the field of solid solutions comprised of the synthesis of Nd-doped calcites and measurements of EXAFS spectra. A project concerning radium interaction with clays and minor minerals in collaboration with JAEA, Japan, has just started.

The Monte Carlo simulations of NaCl in the interlayer of Na-montmorillonite have been continued. They will be supplemented by EXAFS investigations for which the samples have been prepared.

Activities related to the long-term glass corrosion experiments, which have been running at PSI for more than 14 years, concentrated on the spectroscopic characterisation of the corrosion products.

2.2 Thermodynamic databases and software

2.2.1 OECD/NEA TDB organics review

Within the scope of the OECD Nuclear Energy Agency (NEA) Thermochemical Data Base (TDB) Project, a comprehensive review of selected organic ligands has been carried out. The selected ligands are oxalate, citrate, ethylenediaminetetraacetate and α-isosaccharinate, and the elements considered in the review are U, Np, Pu, Am, Tc, Ni, Se and Zr, and the necessary basic data concerning protonation of the ligands and interactions with the major competing cations Na, K, Mg, Ca. W. Hummel was the chairman of this review. The project commenced in 1998 and the results were published in November 2005 (HUMMEL et al. 2005).

2.2.2 OECD/ NEA TDB zirconium review

E. Curti contributed to the NEA TDB zirconium review with a chapter on Zr carbonate complexes and solid phases. The project has now been concluded with the last revisions and publication of Volume 8 of the "Chemical Thermodynamics" series in November 2005 (BROWN et al. 2005).

2.2.3 OECD/NEA TDB solid solution guidelines

The aim of the TDBSOL expert group (J. Bruno (chairman), D. Bosbach, D. Kulik and A. Navrotsky) is to produce "Scientific guidelines for the evaluation of thermodynamic data for solid solutions". The "guidelines" should provide researchers in nuclear waste geochemistry with the relevant theoretical background and experimental procedures for investigations on Aqueous – Solid Solution (AqSS) systems. The aim of this work is also to help decision makers to support AqSS related projects in the framework of performance assessment. The last TDBSOL Group meeting was held at PSI on the 15-16 November 2005 where peer reviewers' comments were discussed in detail and the work for 2006 planned. Currently, the group is working on a final version of the manuscript.

2.2.4 OECD/NEA TDB iron review

The NEA TDB review of iron is ongoing. U. Berner has provided contributions to the aqueous complexation of Fe(II). Within the scope of this review work, the question of how to treat weak complexes in a consistent manner has been reconsidered.

Formation constants and SIT coefficients from osmotic data: Formation constants for solute complexes are usually derived from measurements of only some of the component concentrations. A variety of experimental methods has been used to evaluate such concentrations, i.e. spectroscopy, emf, potentiometry, etc. In the case of weak complexes the determination may be a difficult task because rather high concentrations are needed in order to "see" significant amounts of the complexes of interest. And, vice versa, high concentrations require appropriate ionic strength correction models to correct for the non-ideality induced by elevated concentrations. In the NEA TDB project,

the Specific Ion Interaction Theory SIT is used to derive formation constants ($\log_{10}\beta°$) and interaction coefficients (ε) from experimental data reported in the literature.

Ongoing work for the NEA review of thermodynamic properties of iron complexes was faced with the problem of deriving a formation constant for $Fe(II)Cl^+$, a very weak complex that may appear at high chloride concentrations. Only a very limited number of reports, mainly based on spectroscopic (UV/VIS) measurements, are available on this rather "simple" system.

From HEINRICH & SEWARD (1990)

$$\log_{10}\beta_1^0(FeCl^+) = (-0.111 \pm 0.027), \text{ and,}$$

$$\Delta\varepsilon = \varepsilon_{(FeCl^+,Cl^-)} - \varepsilon_{(Fe^{2+},Cl^-)} = (0.045 \pm 0.016)\ [kg/mol]$$

were derived.

Very recently, MOOG et al. (2004) gave a comprehensive overview on osmotic data for the $FeCl_2$-H_2O system at 25 °C. In principle, osmotic data are also suited to derive formation constants of complexes, but to the author's knowledge no such attempts have ever been made for $Fe(II)Cl^+$, nor for other weak complexes.

GRENTHE et al. (1997) provided an integrated form of the Gibbs-Duhem equation that relates the osmotic coefficient Φ of a solution to the SIT coefficients of the solutes. In the particular system consisting of only $FeCl_2$ and H_2O, and under the assumption that only $FeCl^+$ is formed, their equation reduces to:

$$Y = \varepsilon_{(Fe^{2+},Cl^-)} \cdot (2m_{FeCl_2} - m_{FeCl^+}) \qquad \text{(eq. 2.1)}$$

with

$$Y = \frac{(\Phi_{eff} - 1)\cdot(3m_{FeCl_2} - m_{FeCl^+})}{\ln 10 \cdot m_{FeCl_2}} + \frac{2A}{3.375}\cdot \frac{(t - 2\ln t - 1/t)}{m_{FeCl_2}} - \frac{(2m_{FeCl_2} - m_{FeCl^+})\cdot m_{FeCl^+}}{m_{FeCl_2}}\cdot\Delta\varepsilon$$

where $t = 1 + 1.5\sqrt{I_m}$, A is the Debye-Hückel parameter (0.5091 at 25 °C), m_k are molalities of solutes, and I_m is the ionic strength.

Note that Φ_{eff} in eq. 2.1 has to be evaluated from the experimental quantity Φ (i.e. $\Phi_{eff} = \Phi\cdot\sum m_k/3m_{FeCl2}$). At first glance the linear equation 2.1 looks rather simple. Unfortunately, finding a solution revealed some difficulties and required that many nested iterations had to be performed. For example, the quantity m_{FeCl^+} is a function of $\beta_1(FeCl^+)$, which in turn is a function of $\beta_1^0(FeCl^+)$, $\Delta\varepsilon$ and $\varepsilon_{(Fe^{2+},Cl^-)}$. In fact, the sought-after slope $\varepsilon_{(Fe^{2+},Cl^-)}$ finally resulting from the linear regression has to be fed into the model as a starting parameter. In other words, it is tested which set of the three parameters $\log_{10}\beta_1^0(FeCl^+)$, $\Delta\varepsilon$ and $\varepsilon_{(Fe^{2+},Cl^-)}$ best fits the osmotic data. In practice, the formation constant and $\Delta\varepsilon$ were pre-defined and $\varepsilon_{(Fe^{2+},Cl^-)}$ was varied until the linear regression reproduced the very same values. The correlation coefficient r^2 was used to assess the quality of fit. Results are provided in Fig. 2.1.

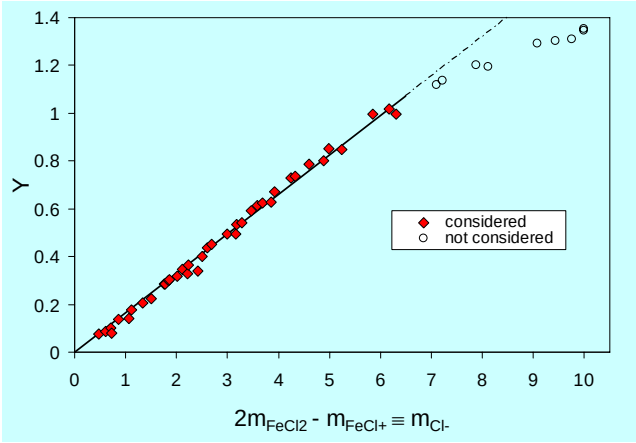

Fig. 2.1: *Determination of $\varepsilon_{(Fe^{2+},Cl^-)}$ from osmotic data in the $FeCl_2$-H_2O system at 25 °C under the assumption that $\log_{10}\beta_1^0(FeCl^+)$ = -(0.111 ± 0.027) as derived from HEINRICH & SEWARD (1990). Experimental systems producing chloride molalities above ~ 6m were not considered (empty symbols). $\varepsilon_{(Fe^{2+},Cl^-)}$ = (0.165 ± 0.002) and $\varepsilon_{(FeCl^+,Cl^-)}$ = (0.370 ± 0.002) [kg/mol] produced the excellent fit shown (r^2 = 0.994).*

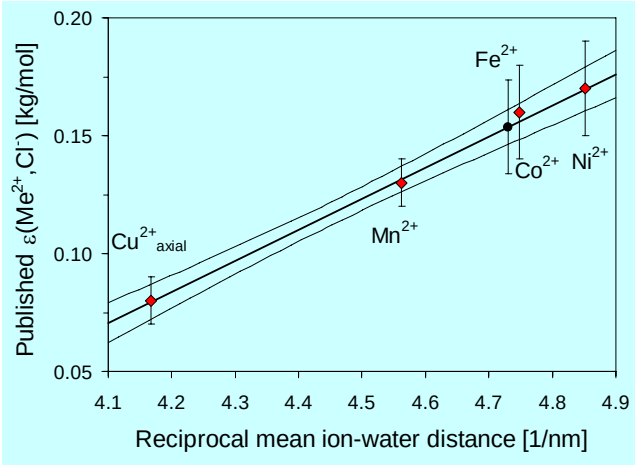

Fig. 2.2: *Weighted linear regression of published SIT coefficients $\varepsilon(Me^{2+},Cl^-)$ against the reciprocal ion-water distance from MARCUS (1988). The confidence interval suggests an uncertainty below ±0.02 [kg/mol].*

A comprehensive sensitivity analysis (varying $\log\beta_1^0$ and $\Delta\varepsilon$) revealed some ambiguities due to parameter correlations. The optimum values for $\varepsilon_{(Fe^{2+},Cl^-)}$ and $\varepsilon_{(FeCl^+,Cl^-)}$ vary slightly with the size of $\log\beta_1^0$, although a "best" pair (using r^2 as a criterion) can be found for every value of $\log\beta_1^0$. An "absolute best" fit is found

for $\log\beta_1^0$ = 0.35, a formation constant which is a factor of 3 larger than the formation constant derived from HEINRICH & SEWARD (1990). However, the differences are not very distinct and the r^2 criterion depends on the actual selection of experimental points to be included in the evaluation. From the sensitivity analysis it was inferred that the data set is well suited to derive SIT coefficients, but it is less conclusive for the derivation of the formation constant. Hence, the HEINRICH & SEWARD (1990) value for $\log\beta_1^0$ was actually selected.

The coefficient $\varepsilon_{(Fe^{2+},Cl^-)}$ was independently estimated by relating published (Me^{2+}, Cl^-)-interaction coefficients (Me = Cu, Mn, Co, Ni) to a reciprocal mean ion-water distance given by MARCUS (1988) (Fig. 2.2). The value of $\varepsilon_{(Fe^{2+},Cl^-)}$ = 0.15 ± 0.02 [kg/mol] from this independent estimate compares very well with the 0.165 ± 0.002 [kg/mol] given above.

2.2.5 GEM-Selektor programme package v.2-PSI

The GEMS-PSI code has been under development in LES since June 2000. With the built-in Nagra/PSI TDB 01/01, the package is well suited for advanced modelling of redox-sensitive systems with aqueous speciation, surface complexation, co-precipitation and solid solution formation. The GEMS-PSI package v. 2.1 (for Win32, Linux and Mac OS X) can be obtained from our homepage (more than 500 downloads have been registered to date). The feedback (user suggestions and bug reports) already allows us to remedy scores of bugs and bottlenecks in the code, which greatly increased its quality, accuracy, performance and value. However, more work on the help system, documentation, test examples and tutorials of GEMS is still necessary.

In three programming sessions (collaborator: S. Dmytrieva), the GEMS code was enhanced with new functionality, and the GEM-IPM numerical kernel was re-structured for better transparency and performance. The GEM kernel has also been isolated into a small standalone C/C++ programme *GEMIPM2K*. The standalone version of GEM is a major prerequisite for coupling it with various fluid mass transport (FMT) codes – a task of growing importance in the LES research programme.

For efficient FMT-GEM coupling, a two-level data exchange interface has been designed, later revised and enhanced with the *Tnode* and *Tnodearray* C++ classes belonging to the GEMIPM2K module prototype version 3. The level of *Tnode* class interface supports only a single GEM IPM call from the FMT part and is optimal for incorporating GEM into an already existing FMT code such as MCOTAC or RockFlow, where the data related to chemical system formulation and the node compositions are in any event kept in the FMT part. The level of *Tnodearray* class makes it possible to keep all chemical and dynamic parameters for all nodes (and two time points) outside the FMT part.

Some tests of the GEM-MCOTAC coupling have already been performed, showing that the GEM chemical system formulation must be checked and tested carefully before starting any extensive coupled modelling, especially in 2D or 3D cases. The GEM2MT module was developed in response to this need. As a minimum, the user can specify the chemical boundary conditions in the form of two or more chemical system compositions, calculate equilibria in all of them, and write on the disk a collection of input files that can be immediately read by the GEMIPM2K programme incorporated in a coupled code. The latest prototype of GEM2MT (July 2006) is also able to perform some simple 1D coupled modelling schemes such as the numerical 1D advection/diffusion using the multi-species finite difference and random walk methods.

Using GEM IPM in coupled FMT-chemistry codes poses very strict requirements on its accuracy, convergence, stability and performance. The substantial restructuring and numerical optimization of the GEM kernel was started by S. Dmytrieva in February 2006. In particular, the customary linear algebra subroutines within GEM IPM were replaced by calls to JAMA C++ package (POZO 2004). This resulted in an unmatched stability of IPM with a circa. 10% speed gain. The source code is now ~2 times smaller and has a more transparent structure. The optimized GEM IPM kernel is used in both GEMS-PSI and GEMIPM2K code variants. Further work on profiling and optimisation of GEMIPM2K is planned.

The GEMS *DualTh* module is an implementation of "dual-thermodynamic" methods which facilitate the retrieval of mixing parameters or thermodynamic properties of solid solution end-members from experimental or geochemical partitioning data. By the end of 2005, the DualTh module prototype was enhanced with least-squares regression calculations for retrieving the interaction parameters of sub-regular and more complex mixing models. Documentation of the module will be completed within the next months. The module is now being used in the evaluation of stoichiometry and g^o values of Na-, K- and Sr-containing end members of the extended CSH AqSS model (see below).

Setup and subroutines for surface complexation models in GEMS have been substantially improved. New surface activity coefficient terms were introduced, i.e. Langmuir, Quasi-Chemical Approximation (QCA) and Frumkin isotherms. Calculation of fully func-

tional CD-MUSIC adsorption models on several surface and site types is made possible.

2.3 Thermodynamic modelling

2.3.1 Dual-thermodynamic methods

The GEM DualTh approach and module prototype are useful in: (i) forward modelling of equilibrium speciation, activities, and element partitioning in a heterogeneous system involving several variable-composition phases; (ii) estimation of interaction parameters of a non-ideal mixing model from known bulk compositions of coexisting aqueous and solid solution phases; and (iii) retrieval of unknown stoichiometries and apparent standard chemical potentials of solid-solution end-members. Inverse modelling tasks, (ii) and (iii), can be performed when the solid solution of interest is shown experimentally to co-exist with the aqueous phase either in equilibrium or in a minimum stoichiometric saturation state. DualTh calculations exploit the ability of the GEM IPM algorithm to compute primal and dual values of the component chemical potentials. For an end-member of a solid solution known to be in equilibrium with the rest of aquatic system, the dual chemical potential can be obtained from a GEM calculation of the *aqueous phase equilibrium alone* if its bulk composition is known (KULIK 2006a). When several experiments are available, a statistical DualTh calculation can retrieve either non-ideal interaction parameters, or optimal end member stoichiometries.

The statistical DualTh approach is currently being applied to determine stoichiometry and g^o_{298} values for Sr, Na and K end members in extending our CSH AqSS model (KULIK & KERSTEN 2001) using new LES experimental data from Tits and Wieland. Preliminary results (based on 24 sorption experiments) include a set of feasible end-member stoichiometries with their g^o_{298} values and solubility products having approximately 0.6 pK unit uncertainty. Further work on this AqSS CSH model extended to Na, K and Sr is in progress.

2.3.2 GEM adsorption modelling (implementing MUSIC SCMs in GEM)

In GEM Surface Complexation Models (SCMs) site mole balance constraints are not used. Instead, the non-electrostatic Surface Activity Coefficient Terms (SACT) (KULIK 2006b, 2006c) provide non-ideal corrections for concentrations of surface complexes according to the availability of binding sites. SACTs are used together with the Coulombic correction terms. SACTs plus new rules for determining elemental stoichiometries of surface species (KULIK 2006c) make the setup and calculation of fully functional multi-surface CD-MUSIC (HIEMSTRA & VAN RIEMSDIJK 2002) adsorption models possible in the GEMS-PSI code. For clay surfaces, this approach is even more promising when combined with the atomistic simulations of surface structures, which can provide site densities, stoichiometries and, eventually, relative stabilities of surface species.

LMA SCMs (e.g. PHREEQC, MINTEQA2) based on site balances are capable of reproducing only competitive Langmuir isotherms, optionally corrected with Coulombic terms (KULIK 2006c). GEM SCMs are far more flexible because they can include QCA (quasi-chemical approximation, multidentate), Frumkin, BET and other isotherm types, all expressed via SACTs instead of site balance constraints. This is a major advance which brings new possibilities in producing sounder yet simpler computer-aided aqueous/surface speciation models, and opens a way to compiling thermodynamic data base of standard molar properties of adsorbed species.

To obtain SACT equations from a classic adsorption isotherm, the idea (applicable to both LMA and GEM SCM implementations) is to split it into "ideal" and "non-ideal" parts, representing the latter as SACT. Such SACT equations have been derived for the Langmuir, the QCA and the Frumkin isotherms (KULIK 2006b, 2006c). The QCA isotherm describes the behaviour of mono-, bi-, tri- and tetradentate surface species, while the Frumkin isotherm accounts for lateral interactions between immobile surface species.

In order to use any surface species in GEM SCM calculations, its elemental stoichiometry must be defined, and standard molal Gibbs energy must be known. We found the rule for determining stoichiometry of the MUSIC inner- and outer-sphere surface species (which often have fractional charges) and checked it on GEM models of surface charge formation on gibbsite, SiO_2, goethite and rutile surfaces. In this rule, the Pauling bond valence concept has been used for the first time for finding elemental stoichiometries of surface complexes on a given crystallographic site type. In turn, this made implementation of CD MUSIC-type SCMs possible in GEM, as described with worked examples in detail by KULIK (2006c).

Results for the worked example of gibbsite $Al(OH)_3$ are shown in Fig. 2.3.

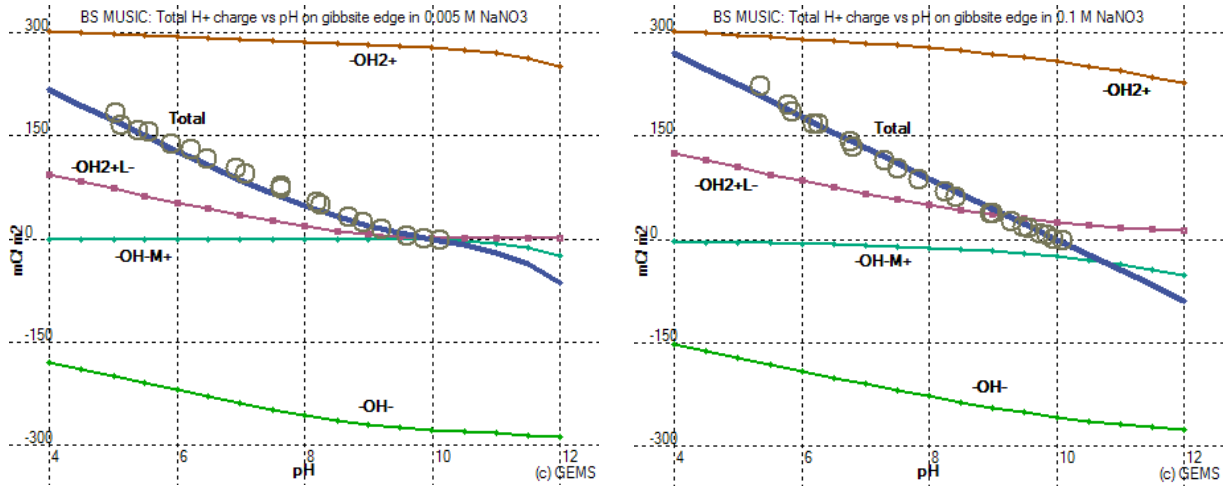

Fig. 2.3: *Surface charge behaviour of gibbsite, modelled at 25 °C using GEM BS SCM at 0.005 M $NaNO_3$ (left) and 0.1 M $NaNO_3$ (right). Open circles: experimental data (Fig. 6 in HIEMSTRA et al. (1999)). Screenshots from a series of GEMS-PSI equilibria calculations.*

2.4 Solid solutions

2.4.1 Synthesis of Nd-calcites

Thermodynamic modelling of Eu-calcite solid solutions (CURTI et al. 2005) and ab initio calculations for Cm(III) substituting for Ca(II) in the calcite lattice (see section 3.4 Transport Mechanisms) suggest a coordination number > 6 for trivalent actinides and lanthanides incorporated in calcites which is an increase with respect to the coordination of Ca(II).

In an effort to verify these model predictions, synthetic Nd-doped calcites (500 to 5000 ppm) were produced at pH ~ 10 with a view to carrying out EXAFS investigations. The synthesis work was quite time-intensive as it required the introduction and testing of the continuous addition method in the LES laboratory. Preliminary spectra, Fig. 2.4, and analyses, Table 2.1, obtained for the highest Nd loading at the X05 micro-XAS beamline (SLS) and at the 10.3.2 beamline (Advanced Light Source, Berkeley) indicate an increased coordination (from 6 to ~ 7) for the first Nd-O shell and a structural expansion around the central Nd atom.

The fitted Nd-O_1 distances of 2.48 ± 0.02 Å are significantly larger than the corresponding Ca-O distances (2.36 Å) observed in the regular calcite lattice. Slightly increased distances are found also for the Nd-O_2 and Nd-C shells, whereas the fitted Nd-Ca distance is consistent with Ca-Ca distances in pure calcite. Nevertheless, the very high energy shift of 12.9 eV is problematic and better spectroscopic data are needed for such dilute samples. A new proposal for measurements at the DUBBLE beamline (ESRF, Grenoble) where cooling with liquid He is possible, has recently been submitted.

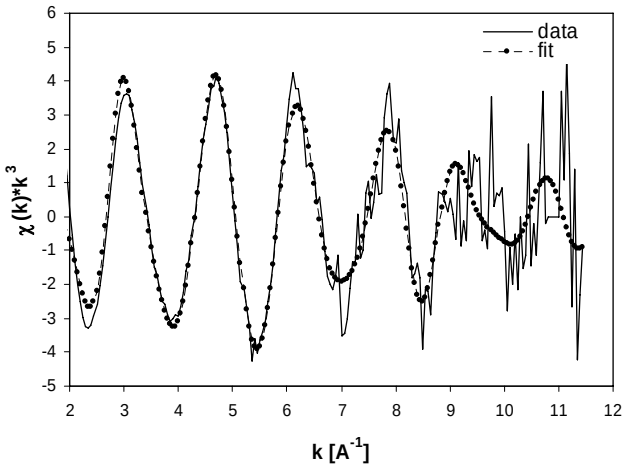

Fig. 2.4: *Best fit to EXAFS data for a synthetic calcite doped with 5000 ppm Nd. Parameters used and obtained in the fit are listed in Table 2.1.*

Table 2.1: *Model parameters with calculated uncertainties for the fit shown in Fig. 2.4. Fixed parameters are shown in bold type.*

	R (Å)	N	σ^2
Nd-O_1	2.48 ± 0.02	6.9 ± 1.8	0.009 ± 0.003
Nd-C	3.38 ± 0.13	**6**	0.020 ± 0.022
Nd-O_2	3.60 ± 0.06	**6**	0.008 ± 0.006
Nd-Ca	4.06 ± 0.12	**6**	0.030 ± 0.018
S_0^2		**1.0**	
ΔE_0		12.9 ± 1.9	

2.4.2 Radium interaction with clays and minor minerals

A cooperation with the Japan Atomic Energy Agency (JAEA) has just started, focusing on the formation of solid solutions between trace concentrations of radium and minor minerals (barite, whitherite, calcite) in the presence of clays (bentonite, Opalinus clay). JAEA has agreed to carry out all the experimental work, whereas LES will take the responsibility for model developments and interpretation of the experiments. The first results from this 3-year project are expected in the coming months.

2.5 Bentonite and clay porewater chemistry

2.5.1 Potential diffusion of chloride species in the interlayer of montmorillonite

Our previous Monte Carlo simulations of Na and Cl in the interlayer of Na-montmorillonite have clearly shown that, given a constant concentration of NaCl in the interlayer, the proportion of neutral NaCl ion pairs increases as the amount of interlayer water is reduced. This suggests that anionic radionuclides could possibly diffuse through the montmorillonite interlayers in compacted bentonite as neutral ion pairs, defying anion exclusion. Since these simulations were done in the NPT- and NVT-ensembles, NaCl was forced to reside in the interlayer throughout the entire simulations. Thus, the crucial question remains as to whether the ion pairs are able to enter the interlayer at all, i.e., whether the free energy of the total system (external bulk water and montmorillonite with interlayer water) is reduced if a Na^+ and a Cl^- ion are transferred from the external bulk water into the montmorillonite interlayer to form a neutral NaCl ion pair.

In order to solve this problem, investigations are underway following two lines (in collaboration with S. Churakov). 1) Free energy perturbation Monte Carlo simulations are currently being used to calculate the free energy changes induced by the formation of NaCl ion pairs in the external water and in the interlayer. 2) Gibbs ensemble Monte Carlo simulations allow the calculation of the equilibrium composition of two phases (in our case montmorillonite with interlayer water, and external bulk water) by exchanging particles during NVT or NPT Monte Carlo simulations. For given initial concentrations of NaCl in the interlayer and in the external bulk water, the exchange of H_2O molecules between interlayer and external water should lead to the equilibrium concentrations of NaCl ion pairs in the interlayer and in the external water.

These molecular modelling studies will be supplemented by chloride K-edge EXAFS investigations (in collaboration with D. Grolimund et al.) at the SLS LUCIA beamline, aiming at the detection of chloride in the interlayer of Na-montmorillonite and the determination of its coordination environment. The samples have been prepared and measurements will take place in mid-September 2006.

2.5.2 Mont Terri porewater chemistry

Nagra has initiated the task "Analysis of Geochemical Data (GD)" for Phase 12 of the Mont Terri Project. T. Thoenen will be concerned with Subtask GD-2 "Parameter Uncertainty". This subtask deals with the interpretation of porewater compositions. The qualitative dependence of calculated parameters on input parameters in geochemical calculations is well established, as well as the influence of perturbing effects (e.g., pyrite oxidation). A quantitative evaluation of parameter uncertainties and perturbing processes, however, is missing. Of particular importance for Mont Terri is the coupled system pH - pCO_2 - alkalinity - clay mineral exchanger population (including protons) - calcite - pyrite oxidation. The planned approach is to use a Monte Carlo-type method to perturb the input parameters of geochemical calculations within a range of known or assumed uncertainties. The statistical evaluation of the resulting output gives the uncertainty on the calculated parameter values. Preliminary investigations concerning the efficient setup of such an approach have been started.

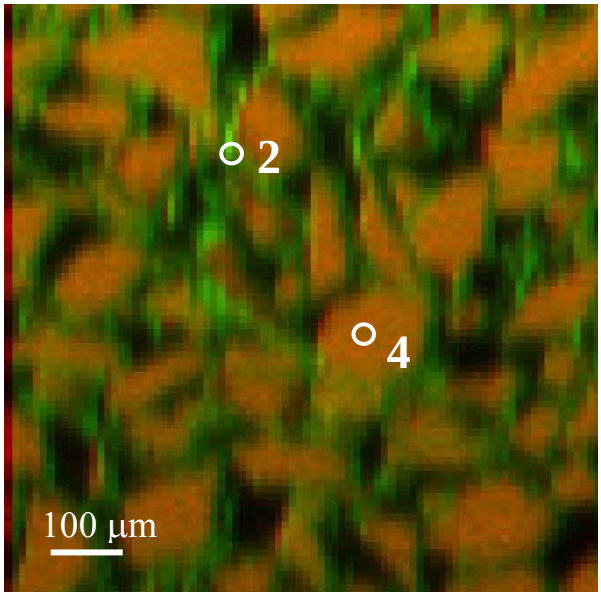

Fig. 2.5: *Bicolour map showing the distribution of Mg (green) and Na (red) in the corroded MW glass. The homogeneous orange areas indicate unaltered glass regions. The Mg-enrichments at the periphery of glass grains correspond to smectite particles formed during the alteration process. Locations 2 and 4 denote the spots at which the absorption spectra shown in Fig. 2.6 were taken.*

2.6 Glass corrosion

Activities related to the long-term glass corrosion experiments, running at PSI for more than 14 years, are now concentrating on the spectroscopic characterisation of the corrosion products. Several beamtime allocations (February and June 2006 at beamline 10.3.2, ALS; May 2006 at LUCIA, SLS) were devoted to this topic during the past year. The main goal of this project is to determine the microscopic distribution and atomic speciation of safety-relevant elements (Ni, Cs) or analogues thereof (Ce, Nd, La) in the corroded and un-corroded glass, as well as their association to major light elements. These light elements (e.g. Mg, Na) are indicators for mineral phases in which the radionuclides might be incorporated. So far, only a small fraction of these data have been analysed and considerable time will have to be invested in this activity in the coming months. However, some interesting findings have already emerged:

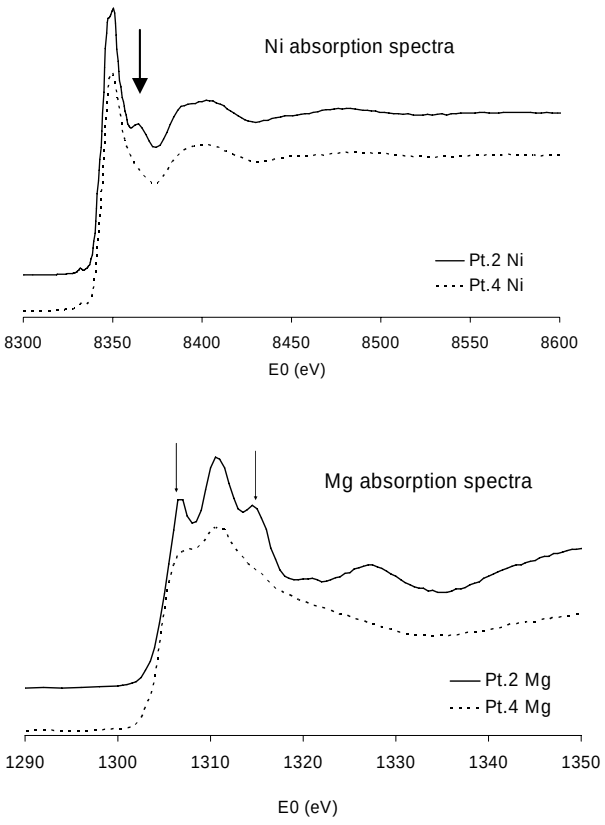

Fig. 2.6: *X-ray absorption spectra recorded at locations 2 and 4 indicated in Fig. 2.5 for (top) Ni, recorded at 10.3.2, ALS and (bottom) Mg, recorded at LUCIA, SLS. Arrows indicate spectral features consistent with 2:1 clay minerals.*

(1) Both Mg (Fig. 2.5) and Ni are heterogeneously distributed and tend to concentrate at the periphery of glass grains. In addition, they are spatially and structurally correlated. Both elements show two types of characteristic distinguishable in XAS spectra in the MW-glass (Fig. 2.6). In the central regions of glass grains, Mg and Ni spectra typical of fresh unaltered silicate glasses were recorded whereas at the periphery of glass grains, where the alteration products reside, Mg and Ni spectra consistent with 2:1 clay minerals were recorded *at identical locations*. This suggests that Ni is associated with the Mg-smectites formed during the glass alteration process.

(2) The distribution of Cs through the MW glass is – in sharp contrast to Ni – remarkably homogeneous, indicating that Cs concentrations are very similar in the corrosion products and in the unaltered glass. The EXAFS spectra are always very similar and show only a single shell.

The documentation of work related to the former EU-project GLASTAB and performed in close co-operation with the Université Louis Pasteur in Strasbourg has been finalised, resulting in a comprehensive publication (CURTI et al. 2006).

2.7 Other activities

IUPAC projects: Within the scope of the IUPAC book project 2005-016-1-100 "Developments and applications in solubility" W. Hummel provided a chapter entitled "Solubility of solids in radioactive waste repositories" (HUMMEL 2006). The book is foreseen to be published in December 2006.

Education activities: D. Kulik, E. Curti and B. Gschwend organised the ACTINET Short Course with Tutorial on Aqueous – Solid Solution Systems Involving Actinides (Thermodynamic and Experimental Aspects) with GEMS-PSI tutorial (lecturers: E. Curti, D. Kulik, A. Navrotsky, S. Churakov; scripts at http://les.web.psi.ch/a_school/index.html, ca. 30 participants, 16-18 November 2005, PSI). The short course was focused on thermodynamic and experimental aspects of solid solution formation in aquatic systems.

Interactions with Swiss universities: In June 2006 W. Hummel submitted his Habilitation thesis "Radioactive Contaminants in the Subsurface: The Influence of Complexing Ligands on Trace Metal Speciation" to the ETH Zürich, Department of Environmental Sciences.

2.8 References

BROWN P.L., CURTI E., GRAMBOW B. (2005)
Chemical thermodynamics of zirconium. OECD/NEA (ed.), Chemical Thermodynamics Vol. 8, Elsevier, Amsterdam, The Netherlands, 512 p.

CURTI E., KULIK D., TITS J. (2005)
Geochimica et Cosmochimica Acta 69, 1721-1737.

CURTI E., CROVISIER J.L., KARPOFF A.M., MORVAN G. (2006)
Applied Geochemistry 21, 1152-1168.

GRENTHE I., PLYASUNOV A.V., SPAHIU K. (1997)
Estimations of Medium Effects on Thermodynamic Data, in: GRENTHE I., PUIGDOMENÈCH I. (eds.): Modelling in Aquatic Chemistry, OECD/NEA Paris, France, pp. 325-426.

HEINRICH C.A., SEWARD T.M. (1990)
Geochimica et Cosmochimica Acta 54, 2207-2221.

HIEMSTRA T., VAN RIEMSDIJK W.H. (2002)
Chapter in: Encyclopedia of Surface and Colloid Science, Marcel Dekker, NY, pp. 3773-3799.

HIEMSTRA T., YONG H., VAN RIEMSDIJK W. (1999)
Langmuir 15, 5942-5949.

HUMMEL W. (2006)
Solubility of solids in radioactive waste repositories. Chapter 21 in: LETCHER T. (ed.): Developments and Applications in Solubility, The Royal Society of Chemistry, Cambridge, UK (in press).

HUMMEL W., ANDEREGG G., PUIGDOMÈNECH I., RAO, L., TOCHIYAMA O. (2005)
Chemical thermodynamics of compounds and complexes of U, Np, Pu, Am, Tc, Se, Ni and Zr with selected organic ligands. OECD/NEA (ed.), Chemical Thermodynamics Vol. 9, Elsevier, Amsterdam, The Netherlands, 1088 p.

KULIK D.A. (2006a)
Chemical Geology 225, 189– 212.

KULIK D.A. (2006b)
Radiochimica Acta (in press).

KULIK D.A. (2006c)
Standard molar Gibbs energies and activity coefficients of surface complexes on mineral-water interfaces (thermodynamic insights). Chapter 7 in: LÜTZENKIRCHEN J. (ed.): Surface Complexation Modelling, Elsevier series, Interface Science and Technology 11, 171-250.

KULIK D.A., KERSTEN M. (2001)
J. Amer. Ceram. Soc. 84, 3017-3026.

MARCUS Y. (1988)
Chemical Reviews 88, 1475-1498.

MOOG H.C., HAGEMANN S., RUMYANTSEV V. (2004)
Zeitschrift für Physikalische Chemie 218, 1063-1087.

POZO R. (2004)
Template Numerical Toolkit - An interface for scientific computing in C++,
http://math.nist.gov/tnt/index.html

3 TRANSPORT MECHANISMS

A. Jakob, S. Churakov, T. Gimmi, G. Kosakowski, R. Mettier, W. Pfingsten

3.1 Overview

Geosphere transport modelling is one of the key activities of the Laboratory for Waste Management and, hence, the working activities in the group cover a wide range of research areas and tackle many important scientific questions.
Our main goal is to achieve an understanding of the most important transport mechanisms and processes and to quantify their effects on the mobility of migrating radionuclides. For this purpose, we use our own and commercial state-of-the-art models and computer codes whose quality is thoroughly investigated by modelling experiments on the laboratory and field scale. Furthermore, we require the predictive quality of such models to be tested in new experiments. Such a procedure leads to refined models, which are highly reliable and can be used for performance assessment purposes.

The main areas of investigations in the last twelve months were:

- The analysis of diffusion experiments on Opalinus clay from Mont Terri at the laboratory and field scale and diffusion data on compacted clay minerals such as montmorillonite, illite and kaolinite;
- reactive transport modelling; application of an extended version of MCOTAC for analysing tracer diffusion through Opalinus clay and bentonite;
- molecular modelling work investigating the mobility of radionuclides through clay minerals and their interaction with solid phases, and
- the derivation of more realistic fracture geometries from the analysis of Grimsel bore cores which can be used in transport modelling.

It is an intrinsic part of the group's philosophy to integrate our investigations with those of other researchers and, hence, there are many in-house interactions – especially with the experimentalists – and in addition there are also strong connections to the Mont Terri facility, universities and other research institutes.

3.2 Modelling diffusion experiments

Modelling Experiments on the laboratory scale

Also this year an extensive series of through- and in-diffusion experiments on Opalinus clay (OPA) and through-diffusion experiments on bentonite and compacted clay minerals at the laboratory scale were analysed. (For further details concerning the experimental aspects of the investigations see Chapter 7 – "Diffusion Processes".)
A broad variety of different tracer tests were analysed for different clay mineral compactions, sample thicknesses and ionic strengths. The goals of these investigations are to obtain further insights into the dominant transport processes and to deduce values for the transport parameters. Such diffusion data for Opalinus clay and bentonite can be used directly in future performance assessments.
All of the experiments required steel filters, and their effects had to be considered in the modelling. In addition, time-dependent boundary conditions and – if required – also non-linear sorption had to be included in the analyses. The experimental conditions for all of the modelled systems are compiled in the following table.

Table 3.1: *Summary of the experimental conditions in the modelled diffusion experiments.*

Type of clay	Tracer	Type of experiment	Degree of compaction [kg m^{-3}]	Sample thickness [mm]	Ionic strength [M]
Na-Montmorillonite	$^{22}Na^{+}$	Through-diffusion	1300, 1600, 1900	5, 10	0.01, 0.1, 0.5, 0.7, 1.0
Na-Montmorillonite	$^{85}Sr^{2+}$	Through-diffusion	2000	1, 5, 10	0.5, 0.7, 1.0
Na-Illite	$^{85}Sr^{2+}$	Through-diffusion	1900	5	0.5, 0.7, 1.0
Kaolinite	$^{85}Sr^{2+}$	Through-diffusion	1900	5	0.5, 0.7, 1.0
Bentonite	$^{22}Na^{+}$	Through-diffusion	1300, 1600, 1900	10	
Bentonite	$^{85}Sr^{2+}$	Through-diffusion	1300, 1600, 1900	5	0.3
Mont Terri OPA	$^{134}Cs^{+}$	Through-diffusion	2400	11	
Mont Terri OPA	$^{134}Cs^{+}$	In-diffusion	2400	13	Different $C_0(t)$
Na-Montmorillonite	Eu	In-diffusion	1600	0.25, 0.5, 1.0	Scoping calculations

Since caesium sorbs non-linearly, a series of experiments with subsequent modelling were carried out for different source concentrations. Due to the strong interaction of caesium with the clay, tracer breakthrough could not be expected on a reasonable time scale and thus the in-diffusion technique was used. Under these circumstances the measured high-resolution tracer distribution profiles across the clay samples (i.e. along the diffusion direction) and the time history of the reservoir concentration provided the basis for the analyses.
In the future, diffusion/sorption studies are planned for strongly sorbing europium in compacted montmorillonite and for that purpose a series of scoping calculations was performed.

A formalism that can be applied to model 'surface' diffusion effects for cation diffusion through compacted and swelling clays was developed. The equations show that the higher mobility of certain cations depend on geometric parameters - e.g., the amount of external versus interlayer pore water - and sorption parameters, but in general it is not possible to determine all the parameter values independently. The relations also show where coefficients obtained from molecular modelling may be of value.

Modelling of Mont Terri field experiments

At the Mont Terri rock laboratory, the new DR diffusion experiments using mobile and sorbing tracers such as HTO, HDO, I^-, $^{22}Na^+$, $^{85}Sr^{2+}$, $^{133}Ba^{2+}$, $^{134}Cs^+$, and $^{60}Co^{2+}$ were started. During the planning and preparation phase, we were involved in a new evaluation of the pore water chemistry, the selection of tracers and the concentrations to be used. Scoping calculations were performed to estimate the most suitable sampling intervals and 2D calculations with "Flotran" for radial, anisotropic diffusion. For this purpose, it was necessary to modify "Flotran" in order to account for heterogeneous diffusion coefficients. This is seen as a longer-term activity which will also continue next year.

Some new modelling was required for the DI-A1 experiments because the dip angle was changed from the initially used value of 45 to 34 degrees. A major issue was the determination of chi-square surfaces (the sum of squares of the residuals between measurements and simulations) for the tracers and the subsequent estimation of values for transport parameters such as the porosity or the rock capacity factor or the pore diffusion coefficient etc. These χ^2-surfaces are indicative, especially for HTO, for slight discrepancies between the borehole and the pore water data in the rock (see Fig. 3.1), which may be associated with model simplifications such as, a homogeneous porosity distribution and a homogeneous pore diffusion coefficient. The methodology of the study, results and conclusions were documented in a technical report.

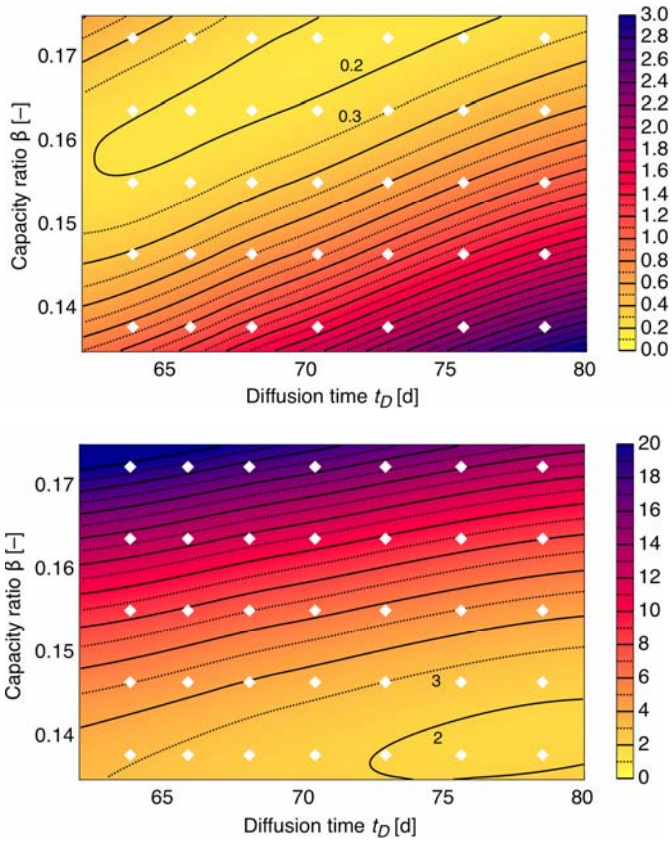

Fig. 3.1: *Contour plots of the χ^2 for HTO for the Mont Terri DI-A1 experiment as a function of the capacity ratio β (which is proportional to the porosity) and the diffusion time t_D (which is inversely proportional to the pore diffusion coefficient).*
Top: Contour plot based on borehole data;
Bottom: Contour plot based on pore water data.
Note, the shift in the locations of the minima in the plots point to effects not adequately accounted for the present modelling (e.g. a heterogeneous porosity distribution).

A new Mont Terri project entitled "Geochemical Data" (GD), has been started in which PSI is also participating. The partners are Nagra, ANDRA (France), SCK (Belgium) and the University of Berne. The project aims at compiling and analysing the newest geochemical and transport data from Mont Terri experiments. Open questions which will be addressed are the pCO_2 and pH of the Opalinus clay pore water; the effects of micro-biological activity; the impact of heterogeneities and uncertainties in the data used to model pore water composition and their influence on reactive transport calculations.

Large-scale isotope profiles

An extensive study of the stable isotope contents in the pore water of the Benken borehole was completed. The results and conclusions from this work were part of a comprehensive paper (submitted to Water Resources Research). The final analysis of the data included new estimates of the errors associated with the method used to obtain isotope contents of pore water which were based on first order error propagation.

3.3 Reactive transport modelling

In order to describe state-of-the-art radionuclide sorption and transport typically measured in batch sorption experiments and small scale laboratory diffusion experiments respectively, and for field experiments and finally also for performance assessment purposes, the in-house 2SPNE-SC/CE mechanistic sorption model by Bradbury and Baeyens was incorporated in the reactive transport model/code MCOTAC.
As part of a complex verification procedure, MINSORB calculations for a simple system (0.01 M $CaCO^3$ in 0.1 M NaCl) were compared to the results from MCOTAC calculations. In addition, reference pore water compositions and site occupancies for Opalinus clay and bentonite were compared for systems having 25 basis species and 55 complexes. The fact that the results always coincided was indicative of a successful adaptation of the 2SPNE-SC/CE model in MCOTAC. A further test case being calculated is the reactive transport of the proton between the Opalinus clay and the bentonite interface. These calculations are relevant to the question of temporal changes in the bentonite pore water in a repository. Currently, laboratory experiments of Cs and Sr diffusion through intact samples of Opalinus clay using mechanistic sorption models are being modelled. These results will be compared with those from calculations in which the simple K_d-approach for sorption was applied

By modifying the GEMIPM internal iteration parameters, the MCOTAC-GEMS coupling has been improved in the sense that solid concentrations calculated by the GEMIPM kernel no longer show small spikes in space where no solid reactions occur. With regard to improving the performance of the MCOTAC-GEMIPM calculations, no further major performance gain could be achieved (10%) although the GEMIPM kernel is now more stable and no longer shows the numerical artefact.

A future strong effort will be made in the direction of parallelisation of MCOTAC so that the code can run on the massively parallel computer HORIZON hosted by the Swiss Centre for Scientific Computing (CSCS) in Manno (Ticino). As a first step, MCOTAC was tailored to the machine specific compilers and operating system. We expect to get additional finances to support a postdoctoral student already experienced and well trained in parallel programming and in the optimisation of sophisticated computer codes. The goal is to port MCOTAC on the high performance computer HORIZON and to take advantage of the expected immediate benefits.

Modelling of column experiments in co-operation with the Institute for Radiochemistry, FZR

1) Migration of U(VI) in a phosphate environment: Column experiment and modelling

The ability of hydroxyapatite $Ca_{10}(OH)_2(PO_4)_6$ (HAP) to immobilize metal ions, particularly lanthanides and actinides, is well known. The long-term stability of this fixation is shown by the results from natural analogue studies. Thus, HAP is a potential back filling material in engineered barriers in abandoned mining areas as well as in the near-field of underground repositories for nuclear and toxic wastes. The interaction of U(VI) with HAP was studied in batch sorption, unsaturated column experiments and by time-resolved and laser-induced fluorescence spectroscopy (TRLFS). MCOTAC was used to analyse the measured U(VI) and tritium breakthrough curves. Assuming two different reaction rates - a fast and a slow one - for the U(VI) interaction with the silanol and the HAP surfaces, it was possible to achieve a reasonable agreement with the measured U(VI) breakthrough curves (see Fig. 3.2). By assuming only reversible equilibrium interaction of the U(VI) with the mineral surfaces, where sorption is expressed in terms of a simple K_d, it was not possible to satisfyingly reproduce the breakthrough data. This emphasised the importance of kinetic processes for the interpretation of breakthrough data of lanthanides and actinides in laboratory column experiments.
In addition, modelling experiments with redox-sensitive tracers such as uranium is very useful in order to test thoroughly our process understanding. The results of such experiments are well suited for benchmark purposes.

2) Use of MCOTAC:

Beate Hollenbach successfully completed her diploma thesis at the Institute for Radiochemistry of the Forschungszentrum Rossendorf, Germany using MCOTAC for the modelling of U(VI) transport through columns filled with gibbsite/quartz mixtures.

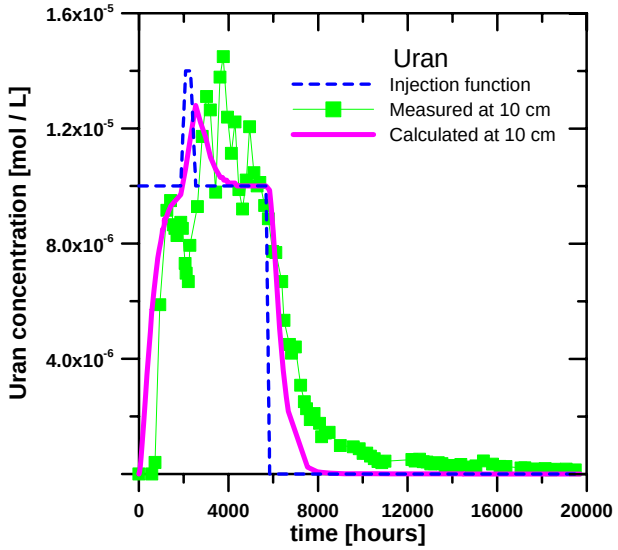

Fig. 3.2: *Measured U(VI) breakthrough curve in a hydroxyapatite/quartz filled column and the calculated best-fit.*

3.4 Molecular modelling

Incorporation of Cm^{3+} in calcite

The rare earth elements (REE) are believed to have a similar chemical behaviour to trivalent actinide species (e.g. Am^{3+}, Cm^{3+}, Pu^{3+}). The use of REEs as analogues avoids some of the difficulties associated with handling actinides in experiments. Despite the difference in the ion charge, the trivalent REEs are known to partition strongly into calcite. The strong affinity is explained by the similarity of the ionic radii of REEs and Ca^{2+}.

Fundamental questions regarding heterovalent substitution concern the charge compensation mechanism and the local response of the host structure on the guest ions. A thermodynamic analysis of the Eu-calcite system showed that the mechanism of the Eu^{3+} incorporation depends on the pH of the solution (CURTI et al. 2005). Two hypothetical Eu end-members were suggested. The $Eu_2(CO_3)_3$ end-member is stable at pH 6. At pH 13 the Eu^{3+} ion is incorporated as the $Eu(OH)_3$ complex. The mechanism of the substitution on an atomistic level remains unknown.

The important information concerning the structure of the local environment around a substituted ion can be obtained from EXAFS measurements. However, the technique is known to have certain limitations. The measurements only provide accurate distances in the first coordination shell of the ions. Although the coordination number can be measured, it is less reliable because it is obtained as an average over possibly different configurations. Particularly in the case of heterovalent isomorphism the uptake of the Eu^{3+} ion is coupled to the incorporation of OH^- and H^+ defects needed for the local charge compensation in the structure of calcite. The light elements defects remain invisible to the EXAFS technique. Thus, the structural information obtained by EXAFS is unfortunately incomplete.

Atomistic modelling helps to reveal energetically favourable mechanisms of the REE and trivalent actinide substitution in calcite which complements the information obtained from EXAFS studies and thermodynamic analyses. Therefore, we performed a series of geometry optimizations of Cm^{3+} defects for a variety of substitution possibilities:

$$3\ Ca^{2+}_{calcite} = 2\ Cm^{3+}_{calcite} \quad (1)$$

$$2\ Ca^{2+}_{calcite} = Cm^{3+}_{calcite} + H^{+}_{calcite} \quad (2)$$

$$Ca^{2+}_{calcite} = CmOH^{2+}_{calcite} \quad (3)$$

$$2\ Ca^{2+}_{calcite} = Na^{+}_{calcite} + Cm^{3+}_{calcite} \quad (4)$$

At present, the computational results are available for the substitution mechanisms given by eqs. 1 and 2. The calculations predict an increase of the Cm^{3+} coordination with oxygen in the first shell from 6 (in ideal calcite) to 7 and higher (Fig. 3.3). This observation is consistent with EXAFS studies of REE doped calcite. For a more detailed comparison of the theoretical results with the experimental data more accurate EXAFS spectra are necessary.

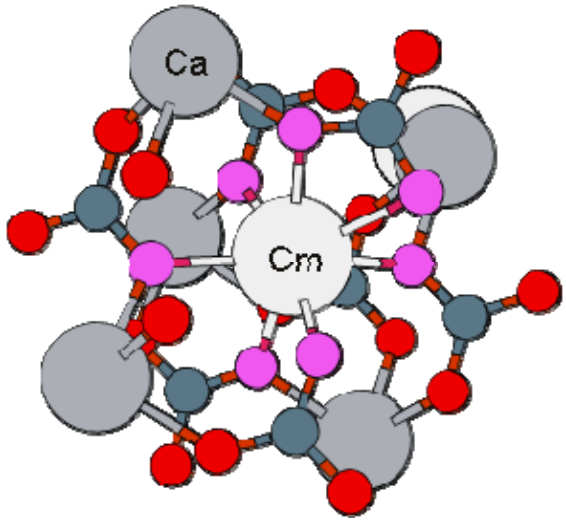

Fig. 3.3: *The structure of Cm^{3+} in calcite formed by the substitution mechanism given in equation (1). The seven oxygen sites building the first coordination shell of the Cm^{3+} ion are marked in pink.*

Structure of cement phases

Hardened cement paste is a main constituent of the engineered barrier systems in low and intermediate level radioactive waste repositories. The ion uptake onto cement phases has been shown to be specific with respect to the element and the composition of the cement used. The mechanism of incorporation and,

this is the most important issue, the possible structural evolution of absorbed ions during the course of alternation processes remains unknown due to the lack of basic structural information of the cement phases. Cement is a complex mixture of calcium (aluminium) silicate hydrates (C(A)SH), portlandite and calcium aluminates. Our present picture of the structure of the C(A)SH phases is based on the crystal structure of tobermorite ($Ca_XH_{2(N+1-X)}Si_NO_{3N+1}zCa(OH)_2 \cdot mH_2O$) and xonotlite ($Ca_6Si_6O_{17}(OH)_2$). The basic structural element of the tobermorite is a banded layer of 6- to 7-coordinated Ca^{2+} ions. Chains of the silicon tetrahedra of variable length are attached at both sides of the Ca-layers. The length of the Si-chains is controlled by the Ca/Si ratio. The alteration processes commonly lead to a decrease of the Ca/Si ratio and results in the formation of infinite $[Si_2O_6]$ chains with a typical three-fold chains ("Dreierketten") pattern. The calcium layers, with attached silicone tetrahedral chains, form loosely bounded layered structures. The stacking is often imperfect and results in the formation of porous channels occupied by water and solvated ions. The C(A)SH phases contain significant amounts of foreign ions, the most important being Al^{3+}. The Al/Ca ratio increases linearly with increasing Si/Ca ratio. The exact composition and structure of cement phases are affected by many factors - including the composition of the cement, the water-to-cement ratio, the temperature, the degree of hydration, and the presence of chemical and mineral admixtures - with the result that there is a tremendous variation in its composition, nanostructure, and morphology. Any model for the structure of C(A)SH must account for these observations. As a preliminary objective for an atomistic study of cement phases we wish to consider the mechanism of the water incorporation in the interlayer space of tobermorite, the formation of the Si-tetrahedral chains, the structural position of Al^{3+} impurities and the mechanism of charge compensation in the defects of the Si-tetrahedral chains.

Tobermorite. In the interlayer of 14 Å tobermorite, where the CSH phase is predominantly formed under water saturated conditions, one half of the available cation sites are occupied by hydrated Ca^{2+} ions, while the other half is occupied by water molecules. Single crystal X-ray diffraction studies of 14 Å tobermorite deliver averaged positions of the interlayer cations and water. Such a static picture is not consistent with the co-existence of partly mobile, weekly bounded water and hydrated interlayer cations. Additionally, X-ray investigations yield no information on hydrogen atoms whose positions are critical for the understanding of the structure of the interlayer which is made up of two dimensional networks of hydrogen bonds.

We simulated the 14 Å tobermorite (see Fig. 3.4) using the ab-initio molecular dynamics technique (MD) starting with atomic positions suggested by X-ray diffraction studies. The preliminary analysis of the atomic trajectories indicates that the experimentally determined structure of tobermorite can be seen as an average over large structural fluctuations of the water molecules and hydration shell of Ca^{2+} ions in the interlayer. The obtained MD trajectories will be used to build a thermodynamic sorption model of bivalent cations on CSH and to understand the sorption mechanism of trivalent actinides on the cement phases.

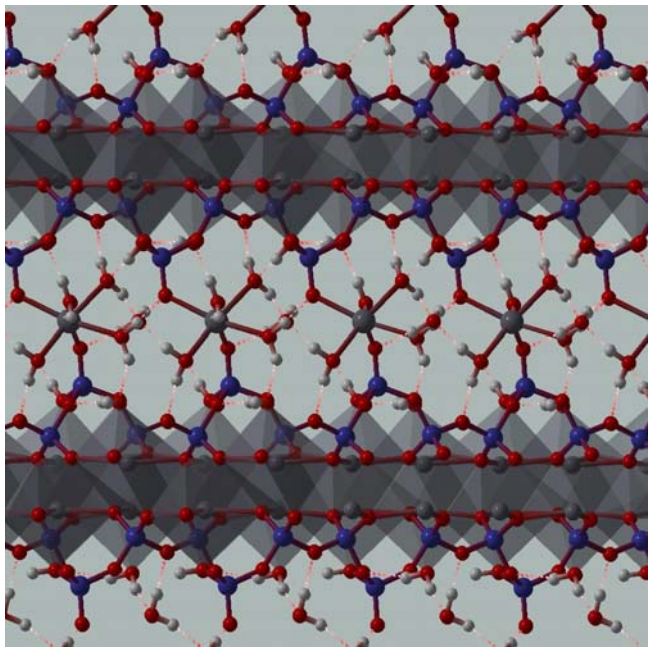

Fig. 3.4: *Snap-shot of a molecular dynamics simulation of 14 Å tobermorite. Oxygen atoms are red, blue represents silicon; and hydrogen is grey. The calcium-polyhedral in the calcium layer are shadowed.*

Xonotlite. The structure and dynamics of OH groups in xonotlite were quantified from ab-initio molecular dynamic simulations. The simulations predicted a single type of hydrogen bonds that is consistent with the experimental thermogravimetric measurements and IR studies. In Fig. 3.5 the calculated IR spectrum is compared with that measured on synthetic xonotlite. Both curves show a single sharp absorption line assigned to the O10-H···O2 hydrogen bond.

The three-fold chains of silicon tetrahedra are formed by two structurally different types of tetrahedra. One third of the Si sites is bonded with three tetrahedra (Q^3-sites), the other two thirds are connected with only two tetrahedra (Q^2-sites). In natural and synthetic xonotlites the Ca/Si ratio is often higher than unity (ideal composition). This is interpreted as a missing tetrahedra in the Si-three-fold chain. Such defects are

the most natural sites for the uptake of radionuclides. The mechanism of defect formation is not understood in detail. In order to determine the energy of defect formation in Q^2 and Q^3 site formed by hydro-garnet substitution mechanism:

$$[SiO_4]^{2-}_{xono} + 2H_2O = [OH]_4^{2-}_{xono} + SiO_2 \qquad (5)$$

the optimal defect geometry was obtained using the ab-initio simulated annealing technique. The calculations predicted that the defects in the Q^3 sites are energetically more stable then the ones in the Q^2 tetrahedra. However, the analysis of the IR spectra and ^1H NMR chemical shift data for the obtained structures provided indirect evidences that the mechanism of charge compensation in the defect might be different from that of equation (5). Hence, further studies will be necessary to resolve the observed discrepancies.

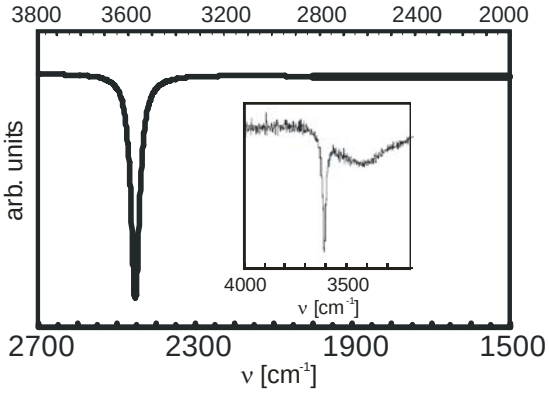

Fig. 3.5: *Calculated IR spectrum of deuterium xonotlite. The upper axis shows the frequency scale corrected for isotopic shift due to deuterium-hydrogen substitution. The measured IR spectrum for synthetic xonotlite is shown in the insert.*

Diffusion of Cs and Na in the montmorillonite interlayer

The Monte-Carlo code of Neal Skipper had to be revised in order to optimise the memory and cpu-time usage and to allow the computation of multiple clay layers.
This new "Monte" version allows us to equilibrate realisations for a mixed Na, Cs-montmorillonite with octahedral charges only. A typical system described by $(Na, Cs)_{0.75}[Si_8][Al_{3.25}Mg_{0.5}]O_{20}(OH)$ with two clay layers, two interlayers and two water layers per interlayer, has a size of (31.68 x 36.45 x 30.12) $Å^3$. The 6 x 4 clay unit cell contains 1920 Atoms in the clay layer, 384 water molecules, 18 Cs and 18 Na atoms. In the modelling, the interlayer water content was systematically varied, and classical molecular dynamic runs of 500 ps length were performed with the DL_POLY code. Such simulations provide appreciable insight into the mechanisms determining radionuclide transport in the interlayer.

One result of the simulations is shown in Fig. 3.6. We calculated values for the three-dimensional interlayer diffusion coefficient for the interlayer species from their mean-square displacements. The ratio of the interlayer diffusion coefficient to that in free water can be interpreted as a retardation coefficient. This ratio, as a function of the interlayer water content is plotted in the Fig. 3.6.

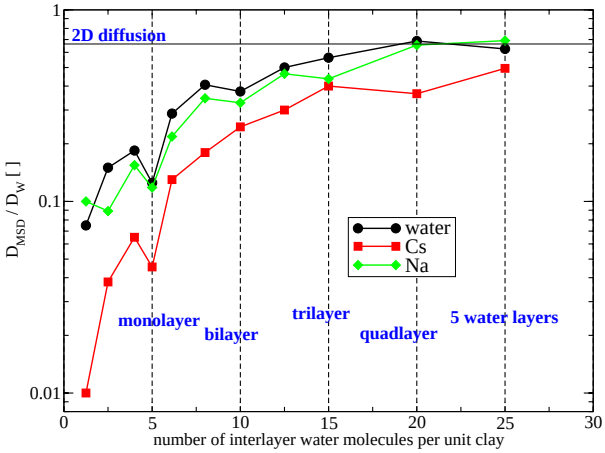

Fig. 3.6: *Values for the diffusion coefficient of water, Na^+ and Cs^+ in the interlayer of the model montmorillonite divided by the corresponding diffusion coefficient in free water. The horizontal line indicates the limit of two-dimensional diffusion in the interlayer.*

The diffusivity of water and ionic species in the interlayer is influenced by several factors, e.g. the interlayer water content, the planar (two-dimensional) geometry of the interlayer and the interaction of the species with the charged clay surface. With decreasing interlayer water content the diffusion coefficient is decreasing in a strongly non-linear manner. For Na and water the diffusion coefficient levels off at a value which is 2/3 of the diffusion coefficient in free water. This value corresponds to two-dimensional diffusion in the "interlayer plane". A stronger binding of Cs to the charged clay surface in the form of "inner sphere complexes", which decreases the mobility of the ions, causes the systematically lower diffusion coefficient of Cs.
It is planned to compare our theoretical data with results from diffusion experiments using montmorillonite.

3.5 Other activities

Long term diffusion experiments on the block scale

Background information and further details of the MAMOT proposal describing long term field diffusion tests at the Mont Terri underground research

laboratory can be found in last year's progress report. In the autumn of 2005, the NES-internal "seed action committee" decided against providing any financial support for this project in this call. A subsequent effort to gain support was made by submitting a revised proposal to the CCEM-CH (The competence centre for energy and mobility which primarily contributes to the development of more sustainable energy systems and in which the lead is taken by PSI.) However, the proposal was subsequently withdrawn due to the lack of interested partners from other ETH domain institutions, which is a necessary selection criterion for the CCEM-CH committee.
At the present time the whole concept of "long time" diffusion experiments with a variety of different tracers, possibly including actinides, is being reviewed. Laboratory experiments on the block scale using carefully extracted and preserved cores with diameters of 10's of centimetres are being considered and evaluated. Advantage could thereby be taken of the PSI hot laboratory infrastructure avoiding the extremely expensive option of constructing a B-laboratory at Mont Terri. The forthcoming elaboration of a detailed proposal for such experiments on the block-scale will be a major task in the near future.

Influence of small-scale heterogeneities on flow and transport in fractured media (PhD study)

The influence of heterogeneous fracture apertures on flow and transport was studied by means of geostatistically generated aperture distributions. The basic log-normal aperture distribution was taken from actual fracture aperture measurements performed on the Grimsel excavation project dataset. Geostatistical modelling allows any number of equivalent realisations to be generated. The variance of the underlying normal distribution was systematically changed and used in a series of numerical models for the Geosys/Rockflow FEM package (KOLDITZ et al. 2004). All models accounting for advection and dispersion were run without (ADE) and with matrix diffusion (ADE + MD), in order to study the interaction of the three processes. The results were also compared to the purely advective model with equivalent aperture distributions discussed in an earlier work (METTIER et al. 2006). Samples of some typical model realisations are shown in Fig. 3.7. At a first glance, the enhanced channelling effect in the more heterogeneous models is obvious. The lower tracer concentrations in the matrix diffusion model is also to be expected due to the large fraction of tracer mass which is residing in the matrix at the time illustrated. The pronounced channelling effect which occurs at high variances also has the effect of reducing the retardation caused by matrix diffusion. The quantification of this effect, among other related observations, is the topic of the still ongoing work and the results will be published in the near future.

Finally, the PhD study of Ralph Mettier will be finished in the autumn of 2006 after three and a half years of intensive work in the area of radionuclide transport in fractured porous media.

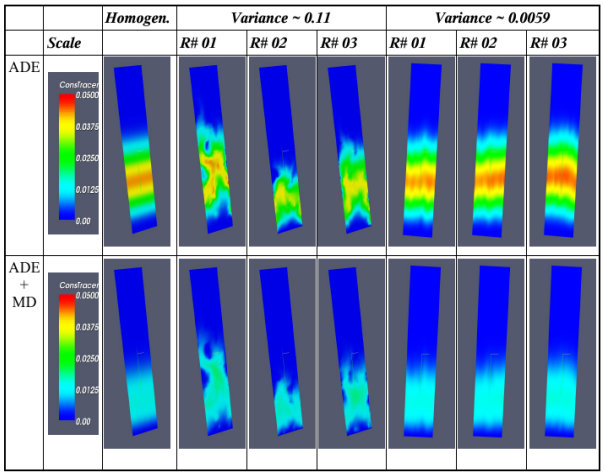

Fig. 3.7: *Seven examples of transport in a single fracture with varying degrees of heterogeneity in fracture aperture, each example shown with, (bottom,) and without, (top), matrix diffusion. Three examples each are taken from two series of realisations with average variances of 0.11 and 0.0059 respectively and compared to the homogeneous reference case. The colour scale is identical in all images, representing normalised tracer concentration (concentration at injection = 1). All images show the same time step, at 1000 seconds after injection of a 50 second rectangular tracer pulse.*

3.6 References

CURTI E., KULIK D.A., TITS J. (2005)
Solid solutions of trace Eu(III) in calcite: Thermodynamic evaluation of experimental data over a wide range of pH and pCO_2. Geochimica et Cosmochimica Acta 69, 1721 – 1737.

KOLDITZ O., BEINHORN M., DE JONGE J., XIE M., KALBACHER T., BAUER S., WANG W., MCDERMOTT C., CHEN C., BEYER C., GRONEWOLD J., KEMMLER D., LEGEIDA D., WALSH R., DU Y. (2004)
GeoSys Rockflow, Open Source Software Design. Technical Report, GeoSys–Preprint [2004-25] http://www.uni-tuebingen.de/zag/geohydrology. GeoSysResearch, Center for Applied Geosciences, University of Tübingen.

METTIER R., KOSAKOWSKI G., KOLDITZ O. (2006)
Influence of small scale heterogeneities on contaminant transport in fractured crystalline rock. Ground Water. 44(5), 687-696. doi:10.1111(g.1745-6584.2006.00236.x

4 CLAY SYSTEMS

B. Baeyens, M. Bradbury, R. Dähn, M. Binkert, A. Schaible

4.1 Introduction

Mechanistic sorption studies on clay minerals constituted the main activities in the Clay Systems sub-programme. An important part of these studies are embedded in the EU 6th Framework Integrated Projects NF-PRO and FUNMIG. Activities within these integrated projects are continuing as scheduled. The main subject in both programmes is the investigation of the influence of the presence of inorganic carbon on the sorption behaviour of Ni(II), U(VI) and Eu(III) on montmorillonite and illite. The near-field studies (montmorillonite/bentonite) are within NF-PRO whereas the far-field studies (illite/ Opalinus clay) are part of the FUNMIG project.

A synthesis on the status of the non-electrostatic sorption modelling approach used to describe metal uptake on clay minerals has been published as a book chapter in the volume Surface Complexation Modelling in the Elsevier series Interface Science and Technology (BRADBURY & BAEYENS, 2006a).

The paper on competitive metal sorption on montmorillonite (BRADBURY & BAEYENS, 2005a) has been published.

Surface analysis (XAS) activities within the sub-programme were severely reduced due to the high level of effort invested in the commissioning work for the microXAS beam line. This work is now finished.

A proposal for a 2 years EURATOM fellowship, fully financed by the EU, at LES and in collaboration with INE (Institut für Nukleare Entsorgungstechnik) of the Forschungszentrum Karlsruhe (FZK) and the Institute for Radiochemistry, (IFR) Forschungs-zentrum Rossendorf (FZR) has been accepted. The candidate, Dr. Maria Marquez, will start in November 2006.

A PhD student (Sonja Dierking) from the Johannes Gutenberg University Mainz spent a one month period in the sub-programme learning the details of clay mineral preparation and sorption techniques. As a result of the excellent co-operation, a proposal on the sorption of Np(V) on montmorillonite was submitted to ACTINET (Joint Research Projects Call 5) and has been successful.

The technician N. Verde left the Clay Systems sub-programme in August 2005, and M. Binkert replaced her in September 2005.

4.2 Performance assessment

Fundamental research with direct relevance to safety analysis studies has continued in the current year.

The longer term aim in the development of future sorption data bases (SDBs) for performance assessment is to move away from ones containing lists of distribution coefficients of radionuclides for specific geochemical conditions, towards SDBs which are founded on thermodynamic parameters for sorption models. There was no work performed directly involved in the development of specific SDBs. However, many of the activities listed below are aimed at resolving open questions with respect to SDBs, and hence have a direct impact on performance assessment. For example the justification of high sorption values in the SDBs (section 4.3.1 & 4.3.2), applicability of mechanistic sorption models to compacted/intact systems (section 4.3.3 & 4.3.4), the effect of inorganic carbonate on metal sorption on clay minerals (section 4.5).

4.3 Mechanistic sorption studies

4.3.1 Sorption of actinides on montmorillonite

Sorption edges for ^{152}Eu(III), and the actinides ^{241}Am(III), ^{239}Np(V) and ^{233}Pa(V) were determined for SWy-1 montmorillonite. Eu(III) is very often used in thermodynamics and sorption studies as a chemical analogue for Am(III). In Fig. 4.1 sorption edge measurements for Eu(III) and Am(III) on Ca-SWy-1 are plotted on the same axes. The measurements clearly indicate that the sorption values for Eu(III) and Am(III) are the same, within the experimental error bands, over the whole pH range from 2.5 to 10.5. Similar results were achieved for Na-SWy-1. These results clearly demonstrate that the sorption of Eu(III) and Am(III) on montmorillonite are essentially the same. The 2SPNE SC/CE sorption model (BRADBURY & BAEYENS, 1997) was used to model the Am(III) data.

In Fig. 4.2 a sorption edge for ^{233}Pa(V) measured on Na-SWy-1 is presented together with the modelled curve. To the best of our knowledge this is the first sorption data set measured and modelled for ^{233}Pa(V) on montmorillonite.

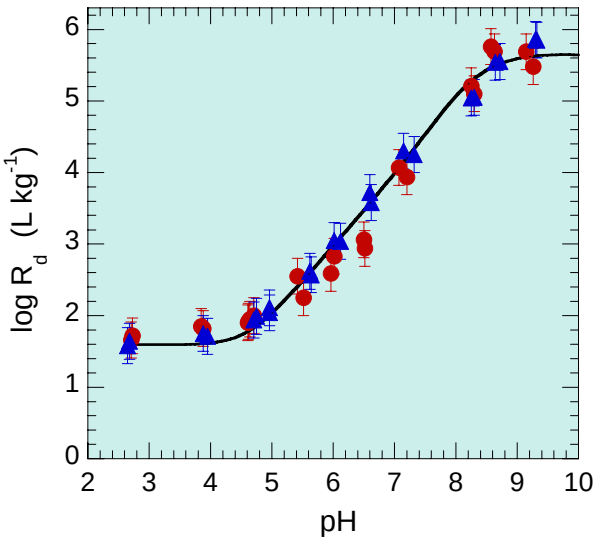

Fig. 4.1: *Sorption edges for ^{241}Am(III) (●) and ^{152}Eu(III) (▲) on Ca-SWy-1 in 0.066 M $CaCl_2$. The continuous curve is the calculated Am(III) sorption edge using the 2SPNE SC/CE model.*

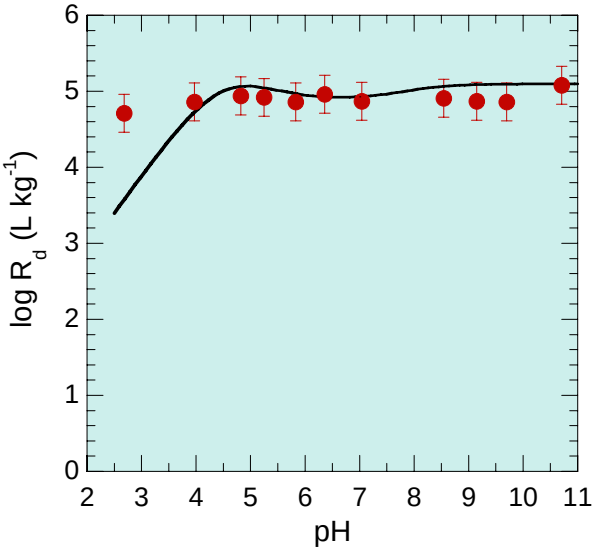

Fig. 4.2: *Sorption edge for ^{233}Pa(V) on Na-SWy-1 in 0.1 M $NaClO_4$. The continuous curve is the calculated Pa(V) sorption edge using the 2SPNE SC/CE model.*

The sorption parameters found for the 2SPNE SC/CE model for the new measurements for ^{241}Am(III), ^{239}Np(V) and ^{233}Pa(V) uptake on montmorillonite, and earlier measurements for ^{241}Am(III) (GORGEON, 1994), ^{237}Np(V) (GORGEON, 1994; TURNER et al., 1998), ^{228}Th(IV) and ^{233}U(VI) (BRADBURY & BAEYENS, 2005b), fit the same linear correlation (LFER) between surface complexation constants of species sorbing on the strong sites (log $^{s}K_y$) and the corresponding hydrolysis constants (log$^{OH}K_x$) established previously. This is illustrated in Fig. 4.3. These results clearly demonstrate, through the LFER,

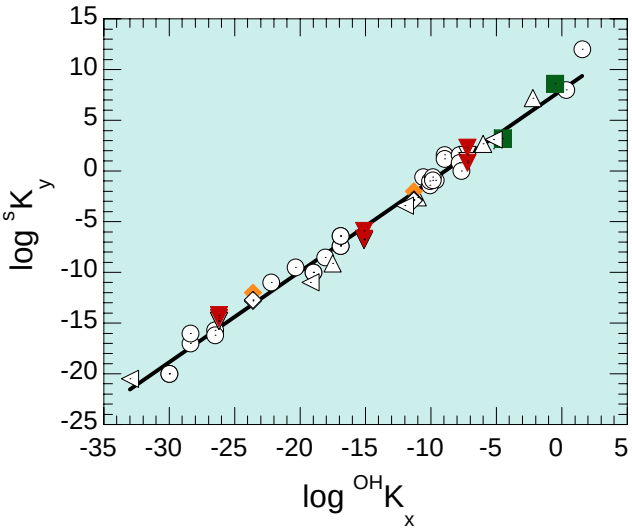

Fig. 4.3: *Correlation of surface complexation constants of species sorbing on the strong sites of montmorillonite with the corresponding hydrolysis constants. Transition and heavy metals (○), ^{241}Am(III) (▽), ^{237}Np(V) (◇), ^{228}Th(IV) (△) and ^{233}U(VI) (◁): BRADBURY & BAEYENS (2005b). The actinides ^{241}Am(III) (▼), ^{239}Np(V) (◆) and ^{233}Pa(V) (■) measured recently fit well on the linear correlation line (log $^{S}K_y$ = 7.99 + 0.89 log $^{OH}K_x$, R = 0.99) and are consistent with previous sorption measurement/modelling results.*

that a chemically consistent picture is emerging explaining quantitatively why different metals sorb to different degrees. For example, very high R_d values are fully expected for strongly hydrolysing metals.

This work was presented at the Migration 2005 Conference, 18-23 September, Avignon, France, and is published as a paper (BRADBURY & BAEYENS, 2006b).

4.3.2 Sorption studies on illite

The experimental and modelling investigations on illite, consisting of the acid/base behaviour and the sorption of Sr(II), Ni(II), Eu(III) and U(VI), have been published as a PSI Bericht / Nagra NTB (BRADBURY & BAEYENS (2005c). These investigations are continuing and have been extended towards other key radionuclides (Co(II), Sn(IV), Am(III), Th(IV) and Pa(V)). The aim is to deduce a LFER for illite in a similar way to the previous work on montmorillonite.

4.3.3 Retention on Opalinus clay

An important aim in the sub-programme is to maintain a close co-operation with the diffusion mechanisms and the transport modelling groups by providing sorption values and mechanistic modelling

input for the interpretation of diffusion results. To this end, a batch sorption isotherm for Cs was carried out on Opalinus clay (OPA) samples which were very similar to those used in the lab diffusion tests and with the same synthetic OPA porewater. The aim was to test the validity of the Cs sorption model applied to diffusion results.

The results are given in Fig. 4.4. The continuous line is the calculated sorption isotherm using the generalised Cs sorption model developed by BRADBURY & BAEYENS (2000) and the same parameters (site type, site capacity and selectivity coefficients) as published in the original work. Only the sorption on the illite fraction of OPA has been taken into account. (Assumption: CEC of illite is 0.2 equiv. kg^{-1}, and the illite fraction in OPA is 18 wt. %). Clearly, the correspondence of the measured data and predicted sorption are good and well within the estimated uncertainty of ±0.2 log units along the whole isotherm. Only at the highest Cs equilibrium concentration of ~10^{-2} M is there a tendency for the model to underpredict the measured sorption.

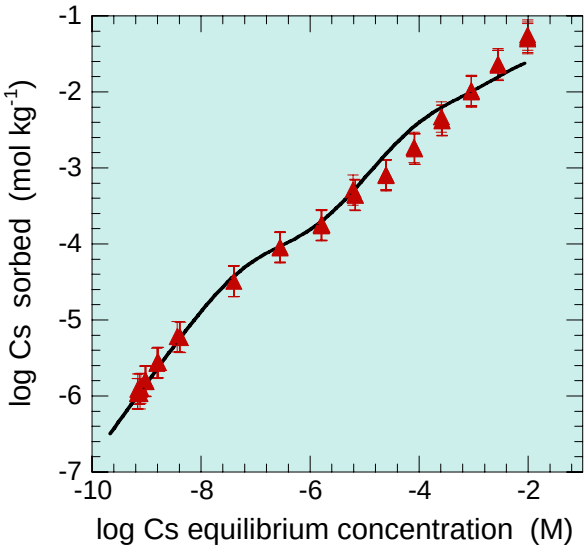

Fig. 4.4: *Cs sorption isotherm on OPA. Experimental conditions: synthetic-OPA porewater, pH ~ 7.4 ±0.2, S:L = 4.9 – 9.8 g L^{-1}, equilibration time = 7 days. The continuous line is the calculated Cs isotherm using the generalised Cs sorption model (BRADBURY & BAEYENS, 2000).*

4.3.4 Sorption on compacted clay minerals

One of the goals of the sub-programme is to try to answer the key question as to whether mechanistic sorption models based on measurements in dispersed systems are directly applicable to compacted systems. In the current year specially designed cells have been constructed to perform sorption measurements on highly compacted clay minerals. The conditions for the tests will be based on predictions from the sorption modelling. The aim is to target specific sorption mechanisms (cation exchange, surface complexation) on a specific set of sites (cation exchange sites, strong sites, weak sites) and compare the measured sorption values with those predicted.

4.4 Surface analysis studies

4.4.1 XAS investigations

XAS activities in the sub-programme were severely reduced because of the time spent for the commissioning of the LES microXAS beamline at the SLS.

One activity related to the sub-programme was the interpretation of some EXAFS measurements of U(VI) uptake on illite obtained earlier within the EU 5th Framework Project ACTAF. These results were presented recently at the international conference XAFS XIII in Stanford (9–14 July, 2006).

U(VI) sorption measurements were carried out on Na-illite, pH = 5 and 6, in a 0.1 M $NaClO_4$ background electrolyte to produce various metal loadings (750-12500 ppm; 3-52 μg/g). All samples were prepared with reaction times of 7 days.

The radial structure functions (RSFs, uncorrected for phase shift) of k^3-weighted L_{III}-edge EXAFS spectra of uranyl treated illite at pH 5 are shown in Fig. 4.5. (The data obtained at pH 6, not shown here, were similar.) Fig. 4.5 shows that there are peaks at R + ΔR ~ 1.4 Å, ~ 1.8 Å, ~ 2.5 Å and ~ 3.0 Å. The peak positions remain essentially unchanged by varying the U(VI) loadings on the clay. The intensity of the peaks at R + ΔR ~ 2.5 Å and ~ 3.0 Å increases with decreasing U(VI) loading which is indicative of a sorption process. In the case of an U(VI) precipitation process, it would be anticipated that the intensity of the peaks C and D would increase with increasing U(VI) loadings.

A thorough data analysis reveals that the U atoms in all samples are coordinated by 2 axial oxygen (O_{ax}) atoms at a distance of ~1.76 Å (see Table 4.1). The U distances between the equatorial oxygen (O_{eq}) atoms are at 2.25-2.3 Å which are far smaller than mononuclear uranyl aquo-complexes with U-O_{eq} distances of 2.41–2.43 Å (CHISHOLM-BRAUSE et al., 1994, DENT et al. 1992). This is a clear indication that inner-sphere complexation process dominates the sorption. The coordination numbers N (U-O_{eq}) are in the range of ~ 4.

Table 4.1: *Structural information derived from the EXAFS analysis of the sorption of U(VI) on Na-illite at pH 5 (f=fixed)*

ppm	U-O_{ax}			U-O_{eq}			U-Al/Si			U-Fe			
	N	R_{U-O} [Å]	s^2 [Å^2]	N	R_{U-O} [Å]	s^2 [Å^2]	N	$R_{U-Al/Si}$ [Å]	s^2 [Å^2]	N	R_{U-Fe} [Å]	s^2 [Å^2]	DE_0 [eV]
1650	2	1.76	0.003	6.2	2.25	0.007	1.1	3.05	0.005 [f]	1.1	3.43	0.005 [f]	-3.4
5500	2	1.76	0.003	5.6	2.25	0.006	1.2	3.07	0.005 [f]	1.1	3.44	0.005 [f]	-3.9
9300	2	1.76	0.003	6.4	2.26	0.011	1.1	3.05	0.005 [f]	0.9	3.42	0.005 [f]	-4.0
12500	2	1.76	0.003	11.2	2.3	0.026	0.3	3.10	0.005 [f]	0.3	3.46	0.005 [f]	-4.5

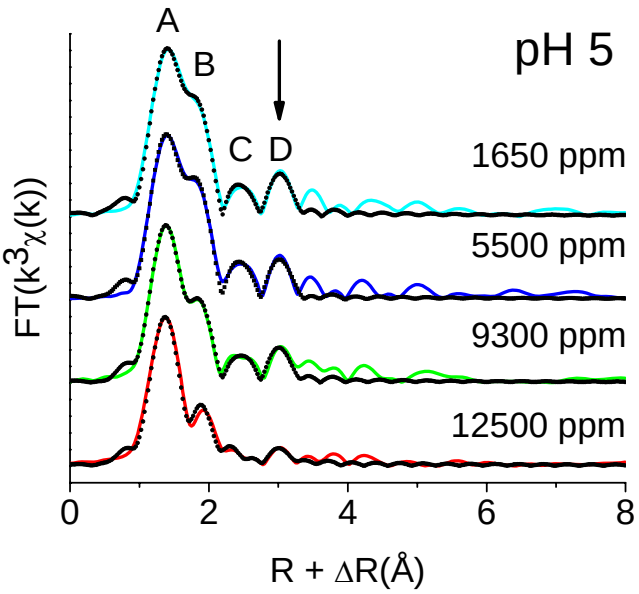

Fig. 4.5: *Radial structure functions of k^3-weighted U L_{III}-edge EXAFS spectra for U sorbed at pH 5 and onto illite (black dotted lines = experimental data; solid lines = fit). The arrow indicates the U-Fe back-scattering contribution.*

For the data analysis of the second shell peaks (R+ΔR = 2.5 Å and 3.0 Å, see Fig. 4.5) the multiple-scattering path of the uranyl moiety was linked to the U-O_{ax} scattering parameters as described in HUDSON et al. (1996) without introducing additional variable fit parameters. Data analysis revealed that the best fits could be obtained with U-Al/Si (EXAFS is unable to distinguish between Al and Si) and U-Fe backscattering pairs at ~3.05 Å and ~3.43 Å, respectively, see Table 4.1. Similar U-Fe distances of 3.40-3.46 Å were observed by CATALANO & BROWN (2005) investigating the uptake of U(VI) by Fe-rich montmorillonites (SWy-1 and SAz-1). However, these authors did not observe any additional peaks from the montmorillonite surface and the U-O_{eq} distances were longer (2.39 Å) compared to this study (2.25-2.3 Å).

A possible explanation for the difference in the structural parameters obtained could be attributed to the structural differences of montmorillonite and illite. In the former, the isomorphic substitution occurs mainly in the octahedral layer (Al^{3+} by Mg^{2+}/Fe^{2+}), whereas in the latter this occurs predominantly in the tetrahedral layer (Si^{4+} by Al^{3+}). In illite the charge deficit is close to the surface of the clay (compared with montmorillonite). This localized charge could cause the sorption of U(VI) to this type of edge site to result in a shorter U-O_{eq} distance (2.25-2.3) compared to the 2.39 Å as reported previously for U uptake by montmorillonite (CATALANO & BROWN, 2005, HENNIG et al., 2002). The fact that the derived coordination numbers for the U-Al/Si and U-Fe backscattering pairs for the samples with low U loading are ~1, indicates that U sorbs preferentially to the illite surface via a mononuclear edge-sharing surface complex to one octahedral Fe and one corner-sharing tetrahedral Al site.

4.4.2 TRLFS investigations

The two part paper on a time resolved laser fluorescence spectroscopy (TRLFS) and modelling investigations of Eu(III)/Cm(III) sorption on illite and montmorillonite (RABUNG et al., 2005, BRADBURY et al., 2005) has been published in Geochimica et Cosmochimica Acta.

4.5 6th EU framework integrated projects (NF-PRO and FUNMIG)

The aim of this work is to investigate and quantify the influence of inorganic carbonate complexation on the uptake characteristics of Ni(II), U(VI) and Eu(III) on illite (NF-PRO) and montmorillonite (FUNMIG). The experimental conditions were selected, with the aid of modelling, so as to yield unambiguous results enabling clear conclusions to be drawn concerning the influence of carbonate complexation in the pH range 6 to 9. This was an essential and important step since the "experimental windows" for such studies

are not large. Although sorption measurements for Ni(II) and U(VI) in the presence of various inorganic carbon concentrations have been measured for both illite and montmorillonite, only the former have been modelled and they are presented below.

Ni(II) sorption and modelling results

Table 4.2 summarises the experimental conditions used in the Ni sorption edge measurements carried out in the presence of different quantities of $NaHCO_3$.

Table 4.2: *Summary of experimental conditions of the Ni(II) sorption measurements on Na-illite.*

Ni(II) total conc. (M)	$NaHCO_3$ total conc. (M)	pH	S:L (g L^{-1})	Time (days)
~10^{-8}	10^{-3}	8.2	2.5	7
~10^{-8}	2 x 10^{-2}	7– 8.5	1.9	21
~10^{-8}	10^{-1}	9.1	2.3	7

The 2SPNE SC/CE model was used for the modelling of the data. Table 4.3 summarises the thermodynamic data used.

Table 4.3: *Aqueous and surface complexation constants for Ni used in the speciation and sorption model calculations.*

Aqueous complexation reactions	log K_0
$Ni^{2+} + H_2O \Leftrightarrow NiOH^+ + H^+$	-9.5
$Ni^{2+} + 2\ H_2O \Leftrightarrow Ni(OH)_2^0 + 2\ H^+$	-18
$Ni^{2+} + 3\ H_2O \Leftrightarrow Ni(OH)_3^- + 3\ H^+$	-29.7
$Ni^{2+} + CO_3^{2-} \Leftrightarrow NiCO_3^0$	4.2
$Ni^{2+} + 2\ CO_3^{2-} \Leftrightarrow Ni(CO_3)_2^{2-}$	6.2
$Ni^{2+} + HCO_3^- \Leftrightarrow NiHCO_3^+$	1.4
Surface complexation reactions	**log K_{SC}**
$\equiv S^SOH + Ni^{2+} \Leftrightarrow \equiv S^SONi^+ + H^+$	0.7
$\equiv S^SOH + Ni^{2+} + H_2O \Leftrightarrow \equiv S^SONiOH^0 + 2\ H^+$	-8.5
$\equiv S^SOH + Ni^{2+} + 2\ H_2O \Leftrightarrow \equiv S^SONi(OH)_2^- + 3\ H^+$	-17.1
Cation exchange reaction	**K_C**
2 Na-illite + $Ni^{2+} \Leftrightarrow$ Ni-illite + 2 Na^+	11

Hydrolysis data are from HUMMEL *et al.* (2002); carbonate data are from Baeyens *et al.* (2003). Note: aqueous polynuclear Ni species are not given because they are insignificant in the model calculations

In order to better understand the predicted Ni sorption modelling results, the aqueous Ni speciation was calculated first, and these results are given in Fig. 4.6. In the pH range 8 to 10 the dominant Ni species are the Ni-monocarbonato and Ni-dicarbonato complexes. Fig. 4.7 presents the experimental and modelling results of Ni sorption on illite in the absence and presence of $NaHCO_3$. The assumption made in the model calculations was that the Ni carbonate complexes do not sorb.

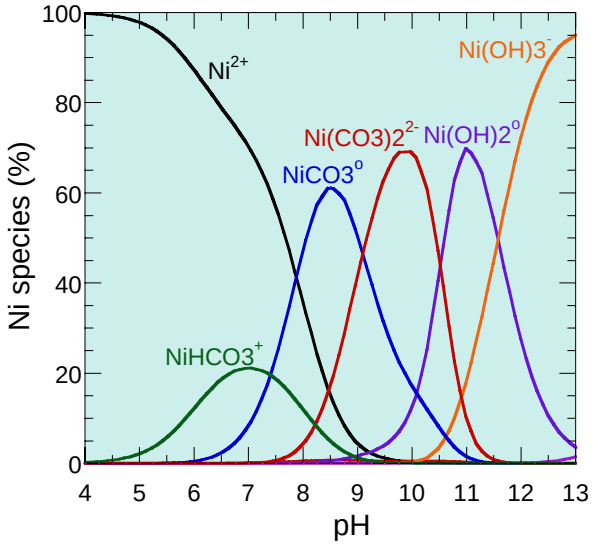

Fig. 4.6: *The Ni aqueous speciation in 0.1 M $NaClO_4$ as a function of pH. The total inorganic carbon concentration is 100 mM.*

Because of the relatively weak Ni carbonate complexation constants, the effect of 1 and 20 mM carbonate on the Ni uptake on illite is also weak, and the predicted data are essentially within the scatter of the measured R_d values. However, in the case where the highest carbonate concentration was used (100 mM), a clear effect is seen if the reference data (no carbonate) are compared with the data in the presence of carbonate. Although there is a rather large scatter in the sorption data, the overall conclusion from these investigations is that the natural carbonate concentrations prevailing in the OPA porewaters (< 30 mM, NAGRA 2002) will not influence Ni uptake in any significant manner.

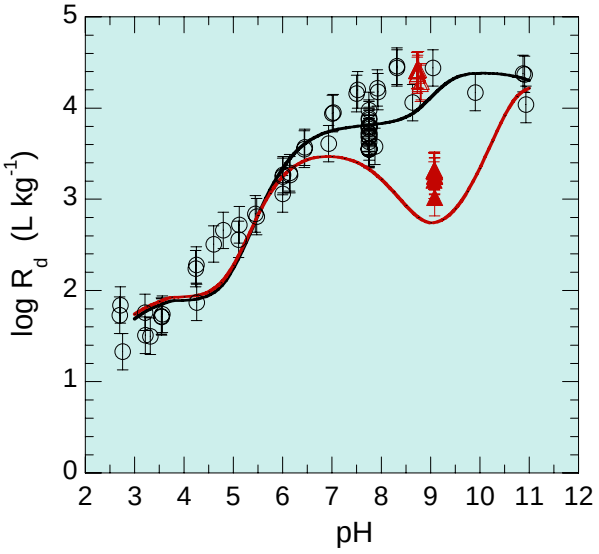

Fig. 4.7: *Effect of $NaHCO_3$ on Ni sorption edges on Na-illite in the absence (O; △) and presence (▲) of 100 mM $NaHCO_3$.*

U(VI) sorption and modelling results

Sorption measurements for U(VI) on Na-illite were determined at trace concentrations in the pH range 7.8 to 9.2 in the absence and presence of various $NaHCO_3$ concentrations. The experimental conditions are summarised in Table 4.4.

Table 4.4: *Summary of experimental conditions of U(VI) sorption on Na-illite.*

U(VI) total conc. (M)	$NaHCO_3$ total conc. (M)	pH	S :L (g L^{-1})	Time (days)
7×10^{-8}	10^{-3}	7.8	2.5	7
6×10^{-8}	1.1×10^{-3}	8.3	2.5	7
7×10^{-8}	10^{-2}	9.2	2.5	7
5×10^{-8}	2×10^{-2}	7.5 – 8.1	1.9	28

As in the case for Ni, the 2SPNE SC/CE model was used for the modelling of the U(VI) data. Table 4.5 summarises the thermodynamic data used**.**

Table 4.5: *Aqueous and surface complexation constants for U(VI) used in the speciation and sorption model calculations.*

Aqueous complexation reactions	log K_0
$UO_2^{2+} + H_2O \Leftrightarrow UO_2OH^+ + H^+$	-5.25
$UO_2^{2+} + 2\ H_2O \Leftrightarrow UO_2(OH)_2^0 + 2\ H^+$	-12.15
$UO_2^{2+} + 3\ H_2O \Leftrightarrow UO_2(OH)_3^- + 3\ H^+$	-20.25
$UO_2^{2+} + 4\ H_2O \Leftrightarrow UO_2(OH)_4^{2-} + 4\ H^+$	-32.4
$UO_2^{2+} + CO_3^{2-} \Leftrightarrow UO_2CO_3^0$	9.94
$UO_2^{2+} + 2\ CO_3^{2-} \Leftrightarrow UO_2(CO_3)_2^{2-}$	16.61
$UO_2^{2+} + 3\ CO_3^{2-} \Leftrightarrow UO_2(CO_3)_3^{4-}$	21.84
Surface complexation reactions	**log K_{SC}**
$\equiv S^SOH + UO_2^{2+} \Leftrightarrow \equiv S^SOUO_2^+ + H^+$	2.6
$\equiv S^SOH + UO_2^{2+} + H_2O \Leftrightarrow \equiv S^SOUO_2OH^0 + 2\ H^+$	-3.6
$\equiv S^SOH + UO_2^{2+} + 2\ H_2O \Leftrightarrow \equiv S^SOUO_2(OH)_2^- + 3\ H^+$	-10.3
$\equiv S^SOH + UO_2^{2+} + 3\ H_2O \Leftrightarrow \equiv S^SOUO_2(OH)_3^{2-} + 4\ H^+$	-17.5
$\equiv S^{W1}OH + UO_2^{2+} \Leftrightarrow \equiv S^{W1}OUO_2^+ + H^+$	0.1
Cation exchange reaction	**K_C**
2 Na-illite + $UO_2^{2+} \Leftrightarrow$ UO_2-illite + 2 Na^+	4.5

Hydrolysis and carbonate data for U(VI) were taken from NEA (2003). Note: polynuclear species are not given because they are insignificant in the model calculations

To facilitate the interpretation of the model predictions, U(VI) speciation was calculated for 1 mM $NaHCO_3$, shown in Fig. 4.8. Clearly, in the pH range from ~6 to ~9.5, the uranyl carbonate complexes are dominant.

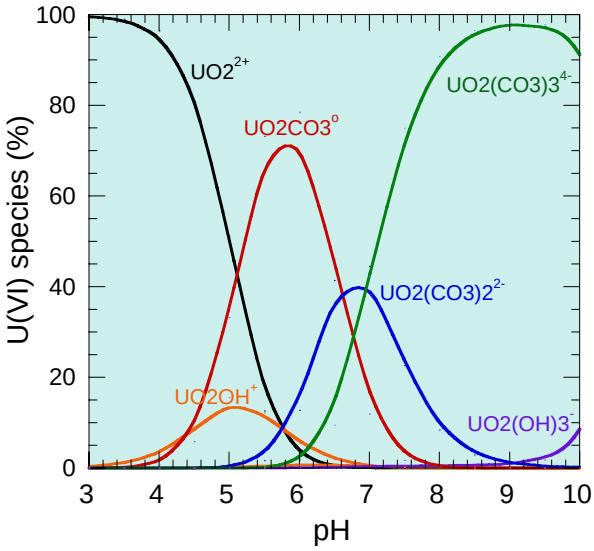

Fig. 4.8: *U(VI) speciation in 0.1 M $NaClO_4$ as a function of pH in the presence of 1 mM $NaHCO_3$.*

Under the assumption that these complexes do not sorb, a decrease in R_d values would be expected. Note that polynuclear species were included in the modelling but have not been plotted in Fig. 4.8 because their contribution was insignificant. Fig. 4.9 shows that U(VI) sorption in the presence of 1 mM and 10 mM $NaHCO_3$ leads to sorption reduction factors of ~10^2 and ~10^4, respectively (pH range 8 - 9). In the presence of 20 mM $NaHCO_3$ there is no measurable U(VI) uptake onto illite (pH ~ 8).

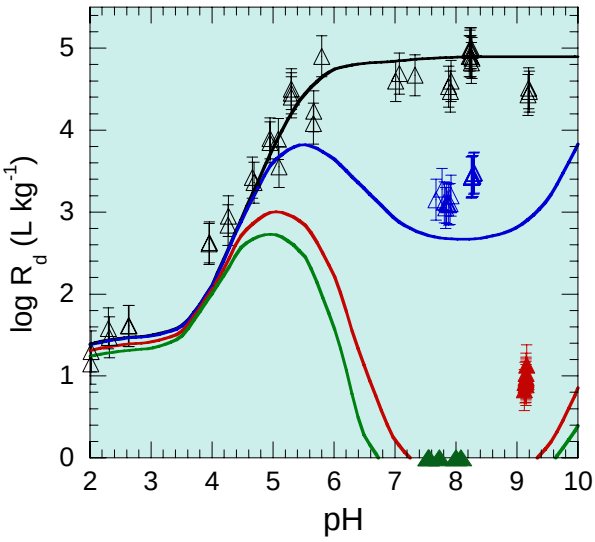

Fig. 4.9: *Effect of $NaHCO_3$ on U(VI) sorption edges on Na-illite in the absence (△) and presence of 1 mM (△), 10 mM (▲) and 20 mM (▲) $NaHCO_3$. The continuous curves are calculated in the absence and the presence of $NaHCO_3$ using the 2SPNE SC/CE model with the parameters given in Table 4.5.*

The model calculations tend to slightly underpredict the measured values under the assumption that uranyl carbonate complexes do not sorb. However, it should be noted that the U(VI)/carbonate thermodynamic data are critical for such a modelling exercise. The rise in the predicted U(VI) sorption at pH > 8 is due to the formation of uranium hydroxy species which sorbs and thereby reduces the overall effect of the aqueous carbonate complexes.

4.6 Other activities

Bentonite porewater modelling: A paper on the pH buffering of the porewater in compacted MX-80 bentonite (BRADBURY & BAEYENS, 2005d) is expected to be published in 2007. As a follow-up to this study, model predictions have been made for pH values in compacted bentonite under different CO_2 partial pressures. In co-operation with VTT, Finland, experiments are on-going and the blind predictions will be compared with the in-situ pH measurements.

Eu sorption on equipment material: In the framework of the Mont Terri field experiments, the use of strongly sorbing traces (e.g. Eu(III)) leads to difficulties because such elements also sorb strongly onto the equipment materials. Applying thin coatings of gold was considered as a potential means of reducing this sorption. This possibility was checked experimentally. The uptake of Eu(III) on gold coated material was slightly less (~ 20 %) compared to the reference material, but was still significant. A second open question was whether the Eu(III) is sorbed reversibly or irreversibly on the materials. The measurement indicated that the desorption kinetics were exceedingly slow if the same water chemistry (pH) conditions were maintained. Only severe acid extractions were able to release the sorbed europium from the materials.

4.7 References

BAEYENS B., BRADBURY M.H., HUMMEL W. (2003)
Determination of aqueous nickel-carbonate and nickel-oxalate complexation constants. J. Soln. Chem. 32, 319-339.

BRADBURY M.H., BAEYENS B. (1997)
A mechanistic description of Ni and Zn sorption on Na-montmorillonite. Part II: Modelling. J. Cont. Hydrol. 27, 223-248.

BRADBURY M.H., BAEYENS B. (2000)
A generalised sorption model for the concentration dependent uptake of caesium by argillaceous rocks. J. Cont. Hydrol. 42, 141-163.

BRADBURY M.H., BAEYENS B. (2005a)
Experimental measurements and modelling of sorption competition on montmorillonite. Geochim. Cosmochim. Acta 69, 4187-4197. Erratum. Geochimica et Cosmochimica Acta 69, 5863-5864.

BRADBURY M.H., BAEYENS B. (2005b)
Modelling the sorption of Mn(II), Co(II), Ni(II), Zn(II), Cd(II), Eu(III), Am(III), Sn(IV), Th(IV), Np(V) and U(VI) on montmorillonite: Linear free energy relationships and estimates of surface binding constants for some selected heavy metals and actinides. Geochim. Cosmochim. Acta 69, 875-892. Erratum. Geochimica et Cosmochimica Acta 69, 5391-5392.

BRADBURY M.H. & BAEYENS B. (2005c)
Experimental and modelling investigations on Na-illite: Acid-base behaviour and the sorption of strontium, nickel, europium and uranyl. PSI Bericht Nr. 05-02 and Nagra NTB 04-02.

BRADBURY M.H., BAEYENS B. (2005d)
pH buffering of the porewater in compacted MX-80 bentonite. Tours conference.

BRADBURY M.H., BAEYENS B. (2006a)
A quasi-mechanistic non-electrostatic modelling approach to metal sorption on clay minerals. Chapter 19 in: *Surface Complexation Modelling* (ed. J. Lützenkirchen) Elsevier Series Interface Science and Technology. Elsevier, Amsterdam, 518-538.

BRADBURY M.H., BAEYENS B. (2006b)
Modelling sorption data for the actinides Am(III), Np(V) and Pa(V) on montmorillonite. Radiochimica Acta, in press.

BRADBURY M.H., BAEYENS B., GECKEIS H., RABUNG TH. (2005)
Sorption of Eu(III)/Cm(III) on Ca-montmorillonite and Na-illite Part 2: Surface complexation modelling. Geochim. Cosmochim. Acta 69, 5403-5412.

CATALANO J, BROWN JR. G.E. (2005)
Uranyl adsorption onto montmorillonite: Evaluation of binding sites and carbonate complexation. Geochim. Cosmochim. Acta 69, 2995-3005.

CHISHOLM-BRAUSE C.J., CONRADSON S.D., BUSCHER C.T., ELLER P.G., MORRIS D.E. (1994)
Speciation of uranyl sorbed at multiple binding sites on montmorillonite. Geochim. Cosmochim. Acta 58, 3625-3631.

DENT A.J., RAMSAY J.D.F., SWANTON W. (1992)
An EXAFS study of uranyl ion in solution and sorbed onto silica and montmorillonite clay colloids. J. Colloid Interface Sci. 150, 45-60.

GORGEON L. (1994)
Contribution à la modélisation physico-chimique de la retention de radioéléments à vie longue par des matériaux argileux. Ph.D. thesis. Université Paris 6.

HENNIG C., REICH T., DÄHN R., SCHEIDEGGER A.M. (2002)
Structure of uranium sorption complexes at montmorillonite edge sites. Radiochim. Acta 90, 653-657.

HUDSON E.A., ALLEN P.G., J.T., DENECKE M.A., REICH T. (1996)
Polarized X-ray-absorption spectroscopy of the uranyl ion: Comparison of experiment and theory. Physical Review B 54, 156-165.

HUMMEL W., BERNER U., CURTI E., PEARSON F.J. THOENEN T. (2002)
Nagra/PSI Chemical Thermodynamic Data Base 01/01. Nagra Technical Report NTB 02-16, Nagra, Wettingen, Switzerland, and Universal Publishers/uPublish.com, Parkland, Florida, USA.

NAGRA (2002)
Project Opalinus clay: Safety Report. Demonstration of disposal feasibility for spent fuel, vitrified high-level waste and long-lived intermediate-level waste (Entsorgungsnachweis). Nagra Technical Report NTB 02-05, Nagra, Wettingen, Switzerland.

NEA (2003) Chemical Thermodynamics Vol.5, Update on the chemical thermodynamics of uranium, neptunium, plutonium, americium and technetium. Elsevier Science Publications B.V, Amsterdam.

RABUNG TH., PIERRET M.C., BAUER A., GECKEIS H., BRADBURY M.H., BAEYENS B. (2005)
Sorption of Eu(III)/Cm(III) on Ca-montmorillonite and Na-illite Part 1: Batch sorption and Time Resolved Laser Fluorescence Spectroscopy experiments. Geochim. Cosmochim. Acta 69, 5393-5402.

TURNER D.R., PABLAN R.T., BERTETTI F.P. (1998)
Neptunium(V) sorption on montmorillonite: An experimental and surface complexation modeling study. Clays Clay Minerals 46, 256-269.

5 CEMENT SYSTEMS

E. Wieland, J. Tits, M.H. Bradbury, B. Fontana, D. Kunz, P. Mandaliev, M. Vespa (μXAS)

5.1 Overview

In the Swiss disposal concept for radioactive waste it is foreseen that long-lived intermediate-level (ILW) and low-level and short-lived intermediate-level (L/ILW) radioactive waste will be disposed of in deep geological repositories with extensive concrete structures. Cement is used to condition (solidify and stabilize) the waste materials and for the construction of the disposal cavern (lining, backfill material). Thus, cement is an important component of the engineered barrier system. Uptake processes by cement and cement phases control radionuclide immobilization in the waste matrix, their retention in the repository near field, and consequently their release into the host rock. In performance assessment (PA) studies it is considered that the source term for radionuclide migration into the host rock is determined by a combination of solubility and sorption constraints in the cementitious near field.

The long-term aim of the sub-programme *Cement Systems* is to develop mechanistic models for the interaction of cementitious materials with safety relevant radionuclides and to improve the current knowledge on the chemical processes in the near field of the planned Swiss ILW and L/ILW repositories. The research programme is directed towards better source term descriptions and strengthening the credibility of the sorption values used in PA studies.

The hardened cement paste (HCP) used in the experimental studies is a heterogeneous matrix consisting of mainly calcium (aluminium) silicate hydrates (C-(A)-S-H), portlandite and calcium aluminates (AFt- and AFm-type phases). In the ongoing research programme wet chemistry and spectroscopic techniques are combined with the aim of gaining a sufficiently detailed understanding of the radionuclide uptake by cementitious materials at the molecular level.

In the following, brief summaries of the main lines of our research in 2006 are presented:

A series of cement minerals were synthesized and characterized, including ettringite, calcium mono-carboaluminate and calcium monosulfoaluminate, as well as tobermorite and xonotlite (crystalline CSH phases). These minerals will be used in future wet chemistry and spectroscopic studies.

A mechanistic sorption study with Cs(I) on HCP and CSH phases was performed in the framework of a "Diplomarbeit" and in cooperation with the Ecole Nationale Supérieure des Ingénieurs en Arts Chimiques et Technologiques (ENSIACET), Toulouse, France. New insight into Cs binding mechanisms was obtained, in particular in conjunction with the effect of CSH ageing on the uptake process.

The uptake studies with actinides and appropriate chemical analogues are ongoing. Progress has been made in connection with the determination of the U(VI) speciation in cementitious systems using X-ray absorption fine structure (XAFS) spectroscopy and time resolved laser fluorescence spectroscopy (TRLFS). The latter measurements were conducted in cooperation with the Institut für Radiochemie (IFR) at the Forschungszentrum Rossendorf (FZR). The XAFS study on U(VI) binding mechanism in CSH phases was completed, and a paper has been published. The first TRLFS measurements with U(VI) doped CSH phases were successfully performed. The results show that U(VI) speciation under alkaline conditions can be investigated using TRLFS if the measurements are carried out at cryogenic temperature.

A Ph.D. project on the influence of the inherent micro-scale spatial heterogeneity of HCP on the immobilization mechanisms of Ni(II) and Co(II) carried out by M. Vespa in the framework of a joint research project with the "XAS beamline" group will be finished in October. In the last year of the project the main activities focussed on completing the experimental investigations and preparing the papers required for submission of the Ph.D. work.

The Ph.D. project on the binding mechanisms of trivalent actinides and lanthanides was successfully started. The structure and dynamics of OH groups in the structure of xonotlite and water molecules in the structure of tobermorite were identified from ab initio molecular dynamics simulations (see Chapter 3), and supporting experimental studies were carried out. Nd(III) uptake by these crystalline CSH phases was investigated using X-ray diffraction (XRD) in combination with the so-called Rietveld analytical approach on highly concentrated samples and XAFS spectroscopy on dilute samples.

A proposal for a 2-year EURATOM fellowship at LES was submitted. The proposal has passed all evaluation thresholds and contract negotiations are expected to start in September 2006.

J.-P. Dobler retired in February 2006. The new technician, Ms. B. Fontana, joined the sub-programme in June 2006.

5.2 Synthesis and characterization of cement minerals

The aims of the cement research programme are focused on elucidating uptake mechanisms by investigating the sorption characteristics of the complex cement matrix and the relevant cement minerals. In this context Ca aluminates and hydrotalcite are considered to be particularly important in conjunction with the retention of the dose-determining anions, i.e., ^{129}I, ^{79}Se, ^{36}Cl, in the cementitious near field. Mechanistic sorption studies with these radionuclides will be an important activity in the future. Thus, the relevant Al-containing cement minerals of the hydrated cement matrix, i.e., ettringite, calcium monocarboaluminate, calcium monosulfoaluminate, were synthesized in 2006 using procedures reported in the open literature, and characterized using scanning electron microscopy coupled with microanalysis (SEM-EDS), thermogravimetric analysis/differential thermoanalysis (TG/DTA) and XRD. Further, the chemical compositions of the materials were determined by acid treatment and analysis of the solutions. The crystalline CSH phases tobermorite and xonotlite were synthesized and characterized in the framework of the Ph.D. project on actinide and lanthanide binding mechanisms. It has been shown that CSH phases play an important role in controlling the uptake of the latter elements in the cement matrix (STUMPF et al. 2004). All minerals were found to be well-crystallised and suitable for use in future wet chemistry and spectroscopic studies.

5.3 Uptake of Cs(I) and Sr(II) by CSH phases and cement

5.3.1 Cs sorption experiments on CSH phases

A large number of studies on the diffusion and sorption of Cs in cementitious systems have been reported (e.g., ATKINSON & NICKERSON 1988; SAROTT et al. 1992; ALBINSSON et al. 1996). Nevertheless, only a few studies report experimental investigations on the binding mechanism of Cs to CSH phases (CRAWFORD et al. 1984; POINTEAU et al. 2001; IWAIDA et al. 2002; VIALLIS-TERRISSE et al. 2002). A comparison of the distribution ratios (R_d values) published for Cs on HCP to date shows that the value is uncertain due to significant variations in the experimental data (OCHS et al. 2006). Evidence has been provided that CSH phases are the main sorbing phase for Cs in HCP (POINTEAU et al. 2001; OCHS et al. 2006). As in the case of the sorption values measured for HCP, the variation in the R_d values for Cs uptake by CSH phases is large. For example, no uptake was reported by CRAWFORD et al. (1984), whereas strong uptake (R_d > 100 L kg^{-1}) was determined by POINTEAU et al. (2001), IWAIDA et al. (2002) and VIALLIS-TERRISSE et al. (2002). The reason for the large variation in the R_d values is poorly understood. It was speculated that, in addition to the solution composition (pH, alkali concentrations) and the degradation state of the cement, unknown material properties may influence the extent of Cs uptake, for example, the crystallinity of CSH phases.

Cs uptake by CSH phases has been addressed in the framework of a "Diplomarbeit" in cooperation with ENSIACET, Toulouse, France. Batch sorption studies were carried out with ^{134}Cs on pure CSH phases and HCP. Although detailed analysis of the data is still ongoing, some findings are already clear. Cs uptake by CSH phases strongly depends on the calcium-to-silica (C/S) ratio of the CSH phases. The sorption values decrease with increasing C/S ratio. This finding is consistent with those of POINTEAU et al. (2001) and OCHS et al. (2006) and is attributed to the competitive effect of Ca in alkali-free solutions and Na/K in alkali-rich solutions on Cs uptake. Note that the same effects were previously observed for Sr(II) and Ra(II) uptake by CSH phases (see section 5.3.2). In contrast to the earlier studies, however, we were able to show that Cs uptake by CSH phases depends also on the crystallinity of the material. Uptake was found to be a factor of 50 higher on a CSH phase (C/S = 1.0) that had been aged for 4 years than on a fresh CSH phase having the same C/S ratio. Note that ageing was carried out under a N_2 atmosphere in a desiccator over saturated $CaCl_2$ solution to maintain the relative humidity at 40 %. XRD showed a broad basal reflection corresponding to a 1.4 nm interlayer distance in the aged CSH phase, which was not detected in the fresh CSH phase. This indicates the presence of an interlayer structure in the aged sample and further suggests that the formation of the interlayer was responsible for the stronger uptake of Cs by the aged material. Note that ageing had no measurable effect on Sr uptake by CSH phases, indicating that Sr is not bound in the interlayer region.

5.3.2 Sr(II) uptake by CSH phases modelled in terms of ion exchange reactions

In the LES Progress Report 2004/2005 an ion exchange model was proposed, which allowed Sr uptake by CSH phases to be modelled in terms of Sr^{2+}–Ca^{2+} replacement at specific cation-exchange sites (for details see TITS et al. 2006a). The same model was applied to successfully predict Ra uptake by cementitious materials (TITS et al. 2006b). In 2006,

the proposed model was extended to include the effect of Na and K on Sr uptake by CSH phases. Note that alkalis are present in significant concentrations in the cement pore water during the early stage of cement degradation. In the experiments artificial cement pore water (ACW) with Na and K concentrations of 0.114 M and 0.18 M, respectively, was used. In the extension of the proposed model it was assumed that the sorption behaviour of Na^+ and K^+ in CSH systems is similar, i.e., binding to the same surface sites and competing with Sr^{2+} and Ca^{2+} for the same exchange sites. The Sr^{2+}–M^+ selectivity coefficient, ${}^{Sr}_{M}K_c$ (M = Na and K), was determined on the assumption that the exchange sites of a CSH phase with a low C/S ratio (0.75 in our studies) are occupied solely by M^+ (i.e. by K^+ and Na^+). Note that the equilibrium Ca concentration in solution is very low for a CSH phase with C/S = 0.75 (TITS et al. 2006a). On the above assumption Sr^{2+}–Ca^{2+} replacement can be neglected, and the R_d value for Sr uptake by CSH phases can be expressed in terms of a Sr^{2+}–M^+ exchange reaction. The selectivity coefficient for the latter reaction was estimated from experimental data determined at low Sr loading (<10^{-2} mol kg^{-1}) using the following equation:

$$ {}^{Sr}_{M}K_C = \frac{2 \cdot R_d(Sr) \cdot [M]^2 \cdot \gamma_M^2}{\gamma_{Sr} \cdot CEC} \qquad (1) $$

The value for ${}^{Sr}_{M}K_c$ was estimated to be 266 using a CEC value of 1.2 eq kg^{-1}, an R_d value of 10^3 L kg^{-1} for Sr uptake by the CSH phase with a C/S ratio of 0.75, and [M] = 0.294 M corresponding to the total Na plus K concentrations in ACW. The activity coefficients of the cations in solution were estimated using the Davies equation. Note that TITS et al. (2006a) determined the selectivity coefficient for the Sr^{2+}–Ca^{2+} exchange reaction, ${}^{Sr}_{Ca}K_c$, to be 1.2.

Sr uptake by CSH phases having other C/S ratios in alkali-free solutions and in ACW can be predicted using the proposed model. Note that in all of these cases both exchange reactions, i.e. Sr^{2+}–Ca^{2+} and Sr^{2+}–M^+, were considered. Fig. 5.1 shows the predicted and experimental R_d values of Sr for CSH phases with different C/S ratios as a function of the equilibrium Ca^{2+} concentration. Note that increasing aqueous Ca^{2+} concentration corresponds to increasing C/S ratios of the CSH phases. The agreement of predicted and experimental data is excellent. The result clearly show that at Ca^{2+} concentrations $\geq 10^{-3}$ M, Sr uptake by CSH phases can be modelled in terms of the Sr^{2+}–Ca^{2+} exchange process. Such conditions are found in high pH, alkali-free solutions. At lower Ca^{2+} concentrations in ACW, however, Sr^{2+}–M^+ replacement cannot be neglected. Under these conditions Sr uptake can be modelled by taking into account both ion exchange reactions, i.e., Sr^{2+}–Ca^{2+} and Sr^{2+}–M^+.

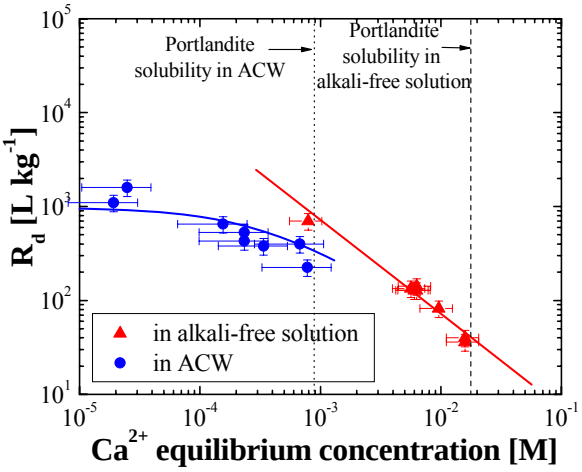

***Fig. 5.1**: Sr uptake by CSH phases in (Na/K) rich ACW and in the absence of alkali metals. R_d values are plotted as a function of the aqueous Ca^{2+} concentration at equilibrium. R_d values are predicted (solid lines) based on Sr^{2+}–Ca^{2+} and Sr^{2+}–M^+ (M= Na, K) ion exchange reactions.*

5.3.3 Sr uptake by cement

In 2006 Sr K-edge XAFS measurement on Sr doped CSH phases (Sr loading ~ 1500 ppm) were carried out to complement the first series of XAFS data on HCP (LES Progress Report 2001/2002). Data analysis showed that the first coordination sphere of the central Sr atom in the Sr doped CSH phases (C/S = 0.7 and 1.1) consists of 5 to 6 oxygen atoms located at a distance of about 2.6 Å. The latter distance corresponds to the Sr-O distance determined for the hydration sphere of Sr in alkaline solution. The coordination number (N) of the sorbed Sr species (N = 5-6) was found to be lower than that for the aqueous species (N ~9). The XAFS data further showed that Sr binds to CSH via two bridging oxygen atoms located at a distance of about 3.6 Å. No further neighbouring atoms were detected in the CSH samples. We were able to interpret the XAFS data collected for the Sr doped HCP samples using the same structural model. This finding suggests that CSH is the uptake-controlling cement phase in the complex cement matrix. A paper on this topic is in preparation.

5.4 Uptake of lanthanides and actinides by cementitious materials

5.4.1 Eu(III) and Nd(III)

Previous investigations have suggested a significant dependence of the R_d values of Eu(III) on the solid-to-liquid (S/L) ratio used in the batch sorption experiments with CSH phases and HCP (LES

Progress Report 2004/2005). It was speculated that in these experiments, strongly sorbing Eu(III) was bound to small cementitious colloids with a diameter < 15 nm, which were present in solution after phase separation (centrifugation for 1 hour at 95000g). On the assumption that the colloid concentration may depend on the S/L ratio, the presence of small Eu sorbing colloids could account for the observed decrease in the R_d value with increasing S/L ratio of the suspensions. Alternative methods for phase separation were tested, e.g., ultrafiltration and the use of dialysis membranes. These tests failed because Eu was found to strongly sorb on the filters, and the dialysis membranes were not stable under the given conditions. In the next step it is foreseen to test ultracentrifugation at increased g forces (up to 550000 g) to improve phase separation.

Recrystallization experiments using ^{45}Ca tracer and Nd L_{III}-edge XAFS measurements were carried out using Nd doped tobermorite ($Ca_5Si_6O_{16}(OH)_2 \bullet 7H_2O$; C/S=0.66-0.83) and xonotlite ($Ca_6Si_6O_{17}(OH)_2$; C/S=1.0) samples. Both crystalline minerals have well-defined structures, which will allow a structural model for Nd(III) uptake by CSH phases to be developed based on the exact knowledge of all atom positions. Note that tobermorite is considered to be an appropriate structural model for aged CSH phases because it has an interlayer. This allows Nd to be sorbed onto the CSH surface and/or be incorporated into the CSH structure. In contrast, xonotlite has no interlayer, and thus, Nd uptake is expected to take place predominantly on the outer surface of the solid.

Ca uptake experiments with ^{45}Ca on xonotlite and tobermorite were carried out to determine the removal of ^{45}Ca from the aqueous solution. The latter process is a measure of the amount of recrystallized solid phases, thus defining the mass of xonotlite and tobermorite accessible to Nd uptake. The data show that recrystallization of the solids was fast over a time period of 14 days after contacting xonotlite and tobermorite with the equilibrium solution. After that, the recrystallization rate decreased with time over a time period of 60 days. XAFS measurements were carried out to determine the coordination environment of Nd taken up by these crystalline CSH phases. Fig. 5.2 shows the Fourier transforms (FTs) of the Nd doped xonotlite and tobermorite samples equilibrated for 1 day and 60 or 90 days, respectively. Data analysis showed that $Nd(OH)_3$ precipitation can be excluded in all samples. After short contact times Si and Ca backscattering contributions (Nd-Si: R = 3.73 Å; N = 3.0) and Nd-Ca (R = 3.79 Å; N = 2.7) were determined besides contributions from the first shell (N-O: R = 2.45 Å; N = 10.1) in the Nd doped tobermorite samples, indicating the formation of a surface complex. With time, however, an additional Ca shell appeared, i.e. Nd-Ca (R = 4.7 Å; N = 1.3), which can be interpreted in terms of the replacement of Ca by Nd in the interlayer of tobermorite. This interpretation is consistent with results from the earlier laser-induced spectroscopic study on Cm(III) uptake by an amorphous CSH phase (C/S=1.0) (TITS et al. 2003). By contrast, the structural parameters determined for the Nd doped xonotlite samples were similar after 1 day and 60 days equilibration. The bond distances were found to be the same within the uncertainty range, i.e., 1st shell: $R_{Nd\text{-}O}$ =2.42-2.45 Å; 2nd shell: $R_{Nd\text{-}Si}$ =3.66 Å; 3rd shell: $R_{Nd\text{-}Ca}$ =3.73 Å; 4th shell: $R_{Nd\text{-}Ca}$ = 3.93-3.95 Å. However, the coordination numbers changed slightly i.e. in the 1st shell from N_O~8.5 to ~6.4, in the 2nd shell from N_{Si}~6 to ~4.5, in the 3rd shell from N_{Ca}~6.5 to ~5, and in the 4th shell from N_{Ca}~2 to ~1. Thus, the structural parameters determined for the Nd doped xonotlite are significantly different from those obtained for Nd doped tobermorite. The above findings suggest the formation of a solid solution with the surface layers of xonotlite rather than the formation of a surface complex. Note that if a Nd surface complex had formed on xonotlite similar structural parameters should result for the Nd doped samples after 1 day equilibration.

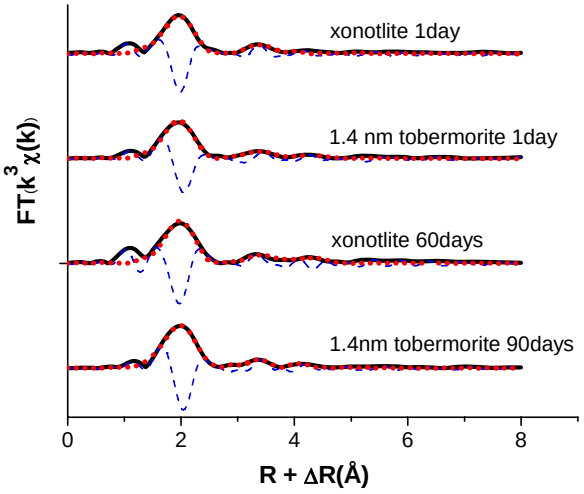

***Fig. 5.2**: Fourier transform of Nd doped tobermorite and xonotlite samples (loading: 5000 ppm; equilibration time: 1 day and 60/90 days).*
Black line: experimental data, red dots: modelled data, broken line: imaginary part.

5.4.2 Spectroscopic investigations with U(VI)

In the past years wet chemistry and XAFS studies on U(VI) uptake by CSH phases were performed in the framework of a cooperation with CRIEPI (Central Research Institute of the Electric Power Industry), Tokyo, Japan (LES Progress Report 2003/2004). The study showed that information on the coordination environment of U(VI) bound to CSH phases can be

obtained using XAFS spectroscopy. A paper on this topic has been published (HARFOUCHE et al. 2006). Nevertheless, the study further showed that for the XAFS measurements relatively high U loadings of > 1000 ppm were required due to the limited sensitivity of the technique. Sorption isotherm measurements with U(VI) on CSH phases, however, revealed that U uptake was not linear at U surface loadings below 1000 ppm (investigated U concentration range = 5 -20000 ppm). This indicates that different sorption mechanisms control U(VI) uptake by CSH phases depending on the U concentration in the system.

In 2006 a cooperation with IFR/FZR was started with the aim of investigating U(VI) speciation in CSH systems at U(VI) loadings below 1000 ppm. This can be achieved due to the lower detection limit of TRLFS. The first part of the planned studies were carried out in 2006 and consisted of a feasibility study with the aim of testing whether or not TRLFS measurements can be performed under strongly alkaline conditions. The spectral resolution of the TRLFS spectra for U sorbed on CSH phases under alkaline conditions was found to be poor if the measurements were carried out at room temperature. The use of a cryostat which allowed measurements to be carried out at temperatures below 150 K, however, significantly improved the fluorescence spectral intensity and the spectral resolution. The test measurements were carried out using suspensions of U(VI) precipitates in 0.3 M NaOH, 0.3 M KOH and 10^{-3}M $Ca(OH)_2$. These solids are expected to be important solubility-limiting phases for U(VI) in cementitious systems. The results show that the TRLFS emission spectra of the two precipitates are almost identical (Fig. 5.3). The precipitate in 10^{-3}M $Ca(OH)_2$, however, did not exhibit any fluorescence U(VI) signal. At the present time, this observation cannot be explained.

TRLFS measurements on samples with U sorbed on CSH phases under different conditions (pH, U loading) had significantly higher fluorescence intensities than the U(VI) precipitates, although the U concentrations in the CSH samples were at least a factor 50 lower. Fig. 5.3 shows that the emission maxima of the U(VI) species bound to CSH phases in alkali-free suspensions (denoted as "in H_2O") are shifted to higher wavelengths compared to the U(VI) precipitates. No influence of the U loading on the spectral characteristics was observed in these samples. By contrast, the spectra of the U doped CSH samples in ACW show a strong influence of the U loading. The spectrum determined at high U loading, i.e., using 50 µM U(VI) in contact with 1 g L^{-1} CSH, is similar to those determined for the U(VI) precipitates. This indicates the formation of U(VI) precipitates in this sample. At lower U loadings, however, the spectra of the two samples are similar to those determined for U(VI) sorbed on CSH phases in the alkali-free suspensions. This could indicate the presence of sorbed U(VI) species under these conditions. Detailed analysis and interpretation of the results is ongoing.

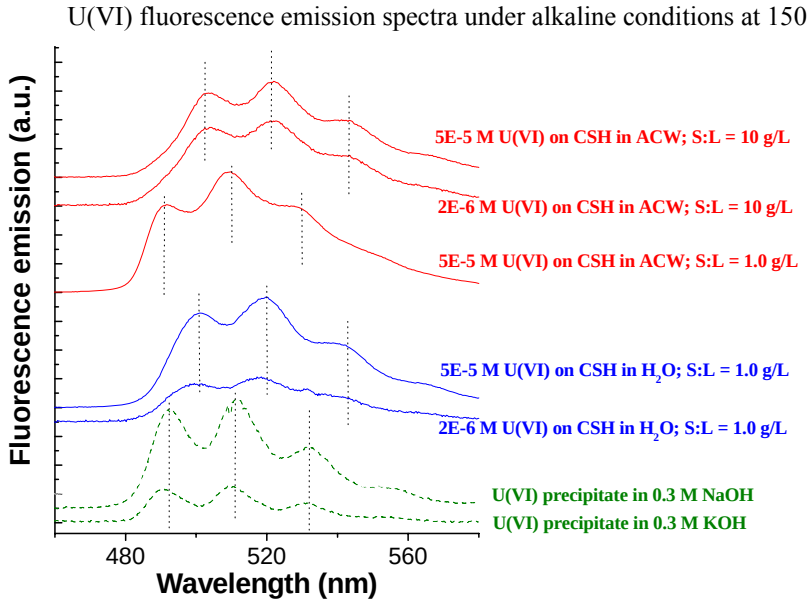

Fig. 5.3: *TRLFS spectra of U(VI) precipitates and U(VI) sorbed on CSH phases under alkaline conditions in alkali-free solution ("in H_2O") and in ACW.In the latter samples the solid-to-liquid ratio (S:L) was varied.*

5.4.3 Neptunium (IV/V) sorption experiments

A first series of sorption experiments with Np(V) carried out in 2005 showed unexpectedly strong sorption of the radionuclide on CSH phases and HCP (LES Progress Report 2004/2005). This strong uptake of Np(V) gave rise to questions concerning the oxidation state of Np in the solution used for sample preparation. The presence of Np(IV) at trace concentration could not be ruled out. For this reason it was decided to repeat the sorption experiments with a fresh Np(V) solution. Np(V) was prepared via oxidation of a Np(IV) solution following a procedure described by RAO et al. (2004). Sorption kinetic tests were carried out with the fresh Np(V) solution on three CSH phases (pH range 10.5-12.5). The sorption data obtained after one week equilibration were compared with those obtained from sorption kinetic tests carried out simultaneously with a Np(IV) solution. It was assumed that Np(IV), available as highly concentrated acidified tracer solution, was stable after adding aliquots of the tracer solution to the alkaline CSH suspensions. The distribution ratios from both series of sorption tests were found to be very similar in magnitude, corroborating the finding of strong uptake by CSH phases (R_d>10^2 m^3 kg^{-1}) in the earlier study. Thus, it is hypothesised that Np(V) was reduced to Np(IV) in the CSH suspensions. Note that E_h was estimated to be in the range between -100 and -300 mV. The results would suggest that Np(V) reduction is fast under alkaline conditions, and therefore, the redox potential has to be buffered at E_h > +100 mV even in the Np(V) doped CSH systems. Further, the tests show that experimental procedures are needed which will allow the oxidation state of Np to be checked at low Np concentrations. Such procedures will be developed in the coming year.

5.5 Co and Ni speciation in hydrating cement

In 2006 the influence of the inherent heterogeneity of the cement matrix on the Ni and Co speciation was investigated using SEM-EDS. The investigations were carried out at the Laboratory of Construction Materials (IMX), Ecole Polytechnique Fédéral de Lausanne (EPFL), and the Laboratory for Materials Behaviour (LWV), PSI, to complement the μ-synchrotron-X-ray fluorescence (μ-XRF) and μ-synchrotron-X-ray absorption spectroscopy (μ-XAS) studies carried out earlier (LES Progress Report 2004/2005). SEM-EDS allows spatially-resolved information on the microstructure of the cement matrix to be gained, and the association of the Ni and Co phases formed in a hydrating cement with specific cement minerals to be investigated. The latter information was not available from the micro-spectroscopic studies.

SEM-EDS investigations on Ni doped cement samples hydrated for 30 days show that for all metal loadings (50 ppm, 500 ppm, 5000 ppm), the Ni phases form rims around inner CSH phase, suggesting a direct association with this cement phase (Fig. 5.4). Note that inner CSH phase denotes CSH material forming around alite, which is the most abundant clinker mineral. In contrast, outer CSH material forms in the pore space of the cement matrix. Ni-rims of a few hundred nanometers up to a few micron thickness and up to ~20 - 50 μm in diameter were observed in the given samples. The elemental distribution maps show that the Ni distribution is extremely heterogeneous and that Ni correlates only with Al.

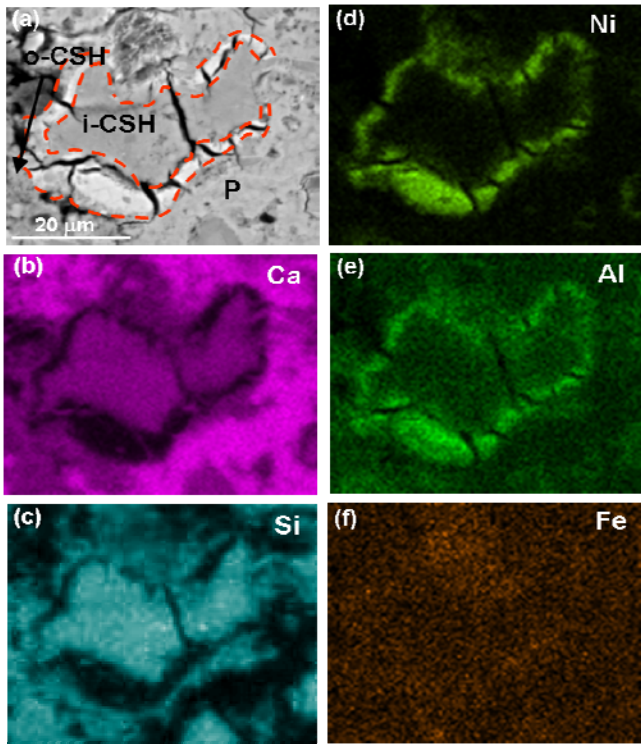

Fig. 5.4: *Back scattered electron (BSE) image (a) and SEM-EDS elemental distribution maps (b-f) of a Ni-rich region in Ni doped HCP samples with a Ni loading of 5000 ppm and hydrated for 30 days. Note that in the SEM-EDS maps (b) to (f) increasing concentrations are indicated by increasing brightness. The red dashed area in (a) represents the Ni-rich region. Notations: P= portlandite ($Ca(OH)_2$), i-CSH=inner-CSH, o-CSH= outer-CSH.*

A tentative explanation for the formation of Ni-rich rims around alite grains can be given by considering some specific features of the mineral. Alite (C_3S) dissolves much faster than the other main clinker mineral, belite (C_2S), which allows inner-CSH type zones to be rapidly formed around C_3S grains in contrast to outer CSH phases (TAYLOR 1997). These reactive zones are expected to have a high specific

surface area. Therefore, a large number of surface sites may be available for Ni binding, which may facilitate Ni accumulation at the grain boundaries of C_3S. The observed correlation of Al and Ni in these regions supports the finding from the earlier μ-XRF/XAS studies which showed the formation of a Ni-Al layered double hydroxide (LDH)-type phase (VESPA et al. 2006). Aluminate (C_3A) is the main Al containing clinker mineral, and thus the main source of Al in hydrating cement. The mineral reacts rapidly and completely with water ((TAYLOR 1997). Note that traces of Mg and Al are also associated with alite (Mg=0.35 wt%). We can speculate that, in addition to Ni, Al accumulates in the reactive zones around C_3S grains due to rapid dissolution of C_3A and the high surface area generated by the hydrating C_3S minerals. Accumulation of the main constituents needed to form hydrotalcite-like phases, i.e., Mg and Al, and the Ni contaminant promotes the formation of Ni containing LDH-type phases. Note, however, that Mg was not observed in the neo-formed Ni-Al LDH by μ-XRF/XAS. The concentration is presumably below the detection limit of these techniques.

In 2006 data analysis of the micro-spectroscopic measurements carried out on the Co doped samples was completed. Additional experiments were carried out to investigate the role of oxidizing agents, in particular O_2, on the oxidation of Co(II) to Co(III) in the Co doped cement samples (LES Progress Report 2004/2005). Fe(III) could be excluded as an oxidizing agent because X-ray absorption near edge spectroscopy (XANES) at the Fe K-edge in the reactive zones of the cement matrix with significant Co(III) accumulation, provided no evidence for Fe(II) formation. Electron paramagnetic resonance (EPR) measurements were carried out to determine the oxidation state of Mn, in particular to check the presence of Mn(II) in Co doped cement samples hydrated for 1 hour, 3, 30 and 150 days. The results showed that the Mn(II) concentration in the cement matrix decreases with increasing hydration time, indicating that involvement of the Mn(IV)/Mn(II) redox couple in the oxidation process can be excluded. Interestingly, both the concentrations of Co(II) and Mn(II) were found to decrease with increasing hydration time. Thus, as in the case of Co(III), the higher oxidation states of Mn tend to form preferentially with time. This finding implies that O_2 is the oxidizing agent in the cementitious systems because oxidation of Co(II) and Mn(II) takes place simultaneously. To further test the influence of O_2 on the Co speciation, one Co doped cement sample, hydrated for 1 hour, was prepared so as to minimize the O_2 concentration in the system. Special measures were taken to reduce the O_2 associated with the cement powder and the Milli-Q water used for sample preparation. (Purging the water for 24 hours with N_2 and repeatedly evacuating a chamber containing the powder under high vacuum). Bulk XAS measurements showed that Co(II) was the dominant oxidation state (~90 %) with some Co(III) impurities in the sample. Thus, this study suggests that oxidation of Co(II) to Co(III) in cementitious systems is fast and can only be suppressed by rigorous measures taken to exclude O_2. A paper on this topic is in preparation.

The above finding has implications for an overall assessment of Co immobilization in cement-stabilized hazardous and radioactive wastes. First, Co(III) is expected to be the dominant valence state of cobalt in waste matrices produced under oxidizing conditions and stored in contact with air, e.g. Co containing residuals from municipal solid waste incineration stabilized with cement prior to landfilling (e.g., BAUR et al. 2001). Secondly, Co(II) is expected to be the dominant valence state in repositories for radioactive wastes in which reducing conditions prevail in the long term (NAGRA 2002). Nevertheless, the results of our investigations clearly show the difficulties which have to be overcome when studying the partitioning of Co(II) in batch-type sorption studies in cementitious systems. An appropriate experimental setup requires that the presence of O_2 is strictly avoided, and that the oxidation state of Co is carefully checked using spectroscopic techniques. To the best of our knowledge, these checks have not been carried out in the sorption studies reported to date.

The Ph.D. project of M. Vespa will be brought to a close with the final Ph.D. examination scheduled in October. Requirements for the submission of the doctoral thesis are fulfilled as the Ph.D. work will include two additional publications presently prepared for submission to *Environmental Science and Technology* and the *Journal of Microscopy*.

5.6 References

ALBINSSON Y., ANDERSSON K., BÖRJESSON S., ALLARD B. (1996)
Diffusion of radionuclides in concrete and concrete-bentonite systems. J. Contamin. Hydrol. 21, 189-200.

ATKINSON A., NICKERSON A.K. (1987)
Diffusion and sorption of caesium, strontium, and iodine in water-saturated cement. Nucl. Technology 81, 100-113.

BAUR I., LUDWIG C., JOHNSON C.A. (2001)
The leaching behaviour of cement stabilized air pollution control residues: A comparison of field and laboratory investigations. Environ. Sci. Technol. 35, 2817-2822.

CRAWFORD R.W., MCCULLOCH C., ANGUS M., GLASSER F.P., RAHMAN A.A. (1984)
Intrinsic sorption potential of cement compounds for ^{134}Cs. Cem. Concr. Res. 14, 595-599.

HARFOUCHE M., WIELAND E., DÄHN R., FUJITA T., TITS J., KUNZ D., TSUKAMOTO M. (2006)
EXAFS study of U(VI) uptake by calcium silicate hydrates. J. Colloid Interface Sci. (in press).

IWAIDA T., NAGASAKI S., TANAKA S., YAITA T., TACHIMORI S. (2002)
Structure alteration of CSH (calcium silicate hydrate phases) caused by soption of caesium. Radiochim. Acta 90, 677-681.

NAGRA (2002)
Project Opalinus clay: Safety Report. Demonstration of disposal feasibility for spent fuel, vitrified high-level waste and long-lived intermediate-level waste (Entsorgungsnachweis). Nagra Technical Report NTB 02-05, Nagra, Wettingen, Switzerland.

OCHS M., POINTEAU I., GIFFAULT E. (2006)
Caesium sorption by hydrated cement as a function of degradation state: Experiments and modelling. Waste Manage. 26, 725-732.

POINTEAU I., MARMIER N., FROMAGE F., FEDOROFF M., GIFFAULT E. (2001)
Cesium and lead uptake by CSH phases of hydrated cement. Mat. Res. Soc. Symp Proc. 663, 105-113.

RAO L., SRINIVASAN T.G., GARNOV A.Y., ZANONATO P., DI BERNARDO P., BISMONDO A. (2004)
Hydrolysis of neptunium(V) at variable temperatures. Geochim. Cosmochim. Acta 68, 4821-4830.

SAROTT F.-A., BRADBURY M.H., PANDOLFO P., SPIELER P. (1992)
Diffusion and adsorption studies on hardened cement paste and the effect of carbonation on diffusion rates. Cem. Concr. Res. 22, 439-444.

STUMPF T., TITS J., WALTHER C., WIELAND E., FANGHÄNEL T. (2004)
Uptake of trivalent actinides (curium(III)) by hardened cement paste: a time-resolved laser fluorescence spectroscopy study. J. Colloid Interface Sci. 276, 118-124.

TAYLOR H.F.W. (1997)
Cement Chemistry. Thomas Telford Publishing, 3rd Ed., London.

TITS J., STUMPF T., RABUNG T., WIELAND E., FANGHÄNEL T. (2003)
Uptake of Cm(III) and Eu(III) by calcium silicate hydrates: a solution chemistry and time-resolved laser fluorescence spectroscopy study. Environ. Sci. Technol. 37, 3568-3573.

TITS J., WIELAND E., MÜLLER C.J., LANDESMANN C., BRADBURY M.H. (2006a)
A wet chemistry study of the strontium binding by calcium silicate hydrates. J. Colloid Interface Sci. 300, 78-87.

TITS J., IIJIMA K., WIELAND E., KAMEI G. (2006b)
Radium binding by calcium silicate hydrates and hardened cement paste. Radiochim. Acta (in press).

VESPA M., DÄHN R., GROLIMUND D., HARFOUCHE M., WIELAND E., SCHEIDEGGER A.M. (2006)
Micro-scale investigations of Ni uptake by cement using a combination of scanning electron microscopy and synchrotron-based techniques. Environ. Sci. Technol. (in press).

VIALLIS-TERRISSE H., NONAT A., PETIT J.-C., LANDESMAN C., RICHET C. (2002)
Specific interaction of cesium with the surface of calcium silicate hydrates. Radiochim. Acta 90, 699-704.

6 COLLOID CHEMISTRY

C. Degueldre, R. Rossé, P. Kunze

6.1 Introduction

The colloid sub-programme is aiming to understand the role of colloids in the migration of radionuclides in the geosphere. Colloids are studied with the emphasis on their properties (concentration, size distribution, nature) in the investigated systems. This report summarises our activities during the last year with emphasis on the cooperative work carried out within the framework of the Grimsel Colloid Project: "Colloid Formation and Migration" (CFM). Activities also included analytical studies on single particles by ICP-MS. This activity has now been discontinued. We are now focusing on colloid generation in batch tests using our analytical tool (single particle counting, SPC) to quantify the phenomena and in the future on colloid characterisation using of EELS.

6.2 The Grimsel "Colloid Formation and Migration Project"

The Colloid and Radionuclide Retardation (CRR) project was discontinued last year. Since 2005 we have participated in the CFM project. The primary aim of this project is to understand the generation of colloids at a bentonite block / groundwater interface under quasi-stagnant water conditions. The CFM experiment detailed goals are:

1. To examine the colloid generation rates and mechanisms at the engineered barrier system (EBS) – host rock boundary under *in-situ* conditions.
2. To evaluate the long-distance migration behaviour of EBS-derived colloids in a water-conducting feature in a repository-relevant flow system (i.e. with a very low flow rate/water flux).
3. To study the long-term geochemical behaviour (mobility, mineralisation, colloid formation, etc) of radionuclides at the EBS-host rock boundary.
4. To examine the influence of radionuclide-colloid interaction mechanisms on colloid-mediated radionuclide migration.
5. To gain experience in long-term monitoring of radionuclide/colloid propagation near a repository.
6. To apply the results to improve repository performance assessments, optimise EBS design and contribute to the "monitoring" debate.

This project involves organisations such as INE/FZK, CIEMAT, ANDRA, JAEA, LANL, AIST, CRIEPI, SolExpert, LES/PSI for the experimental part and several additional groups for the modelling activities.

In the CFM project bentonite is considered to be the main source of colloids from the EBS. Currently we are studying colloid generation in a compacted montmorillonite system at the laboratory scale as part of this study. Fig. 6.1 shows schematically the experiment design being used to investigate the two key phenomena: colloid resuspension (generation) and sedimentation (elimination).

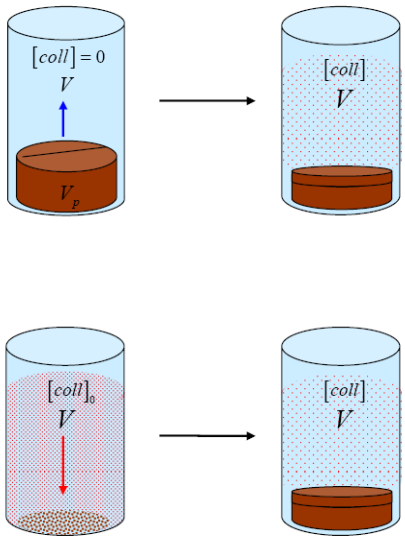

Fig. 6.1: *Colloid generation and sedimentation scheme.*

The generation of FEBEX clay colloids was measured from pellets in contact with various solution compositions and sedimentation was studied in concentrated suspensions. The tests were carried in batch systems. The colloid size distributions in the two systems were measured in the range 50 – 5000 nm as a function of generation and sedimentation time, Figs 6.2 and 6.3. It is striking to observe that the colloid size distributions determined in both the generation and sedimentation experiments trend towards a similar specific size distribution. This suggests a pseudo-equilibrium of the colloid population corresponding to generation - sedimentation coupling. The concentration of particles in the range from 2000 to 200 nm decreases by orders of magnitude, suggesting the elimination of such colloids by sedimentation, while 200 nm colloids may remain in suspension. The colloid size distributions follow a Pareto power law:

$$\delta[coll]_d = a\, d^{-b}\, \delta d \qquad (1)$$

where $[coll]_d$ represents the colloid concentration for a given particle size range, d - $d + \delta d$, in solution, and a and b are constant over a given size range.

In the compacted FEBEX bentonite source tests, the colloid size distributions (suspensions and supernatant after settling) are as shown in Figs. 6.2 and 6.3.

From the series of tests performed for colloid generation and colloid sedimentation, a convergent picture emerges suggesting that after a certain transition time, a pseudo-equilibrium state in the colloid system is reached. As seen in Figs. 6.2 and 6.3, the colloid size distributions recorded in the colloid generation and sedimentation experiments in 10^{-2} M *NaCl* after 312 hr, as well as in Grimsel groundwater (GGW) after 1000 hr, tend to reach similar values.

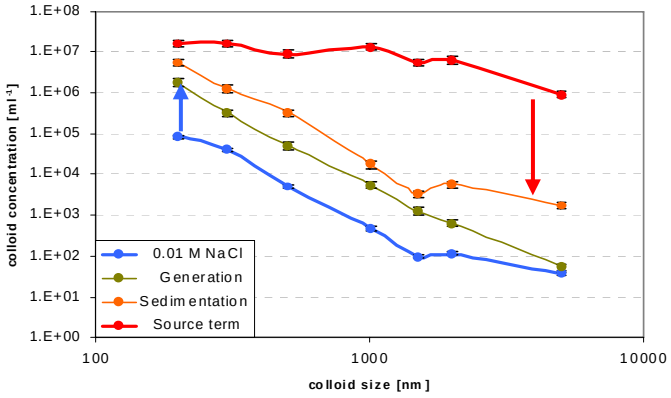

Fig. 6.2: *Bentonite colloid size distributions for colloid generation and sedimentation tests in 0.01 M NaCl after 312 h.*

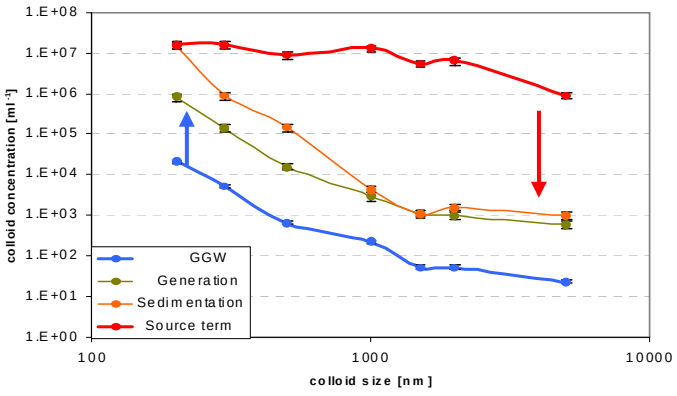

Fig. 6.3: *Bentonite colloid size distributions from colloid generation and sedimentation tests in GGW approximately 1000 h.*

This situation is reached after the small colloids liberated during colloid generation (increases of both *a* and *b* in Eq. 1) and large colloid eliminated from the original suspension during sedimentation (increases of *a* and decreases of *b* in Eq. 1).

6.3 Other colloid activities

Uranium single particle analysis has been performed by inductively coupled plasma - mass spectrometry (ICP-MS). The ICP-MS performances were compared with those achieved by scanning electron microscopy (SEM) and single particle counting (SPC).

In the ICP-MS technique, transient signals induced by the flash of ions due to the ionisation of a uranium colloidal particle in the plasma torch can be detected and measured for selected uranium ion masses ($^{238}U^{+}$, $^{235}U^{+}$ or $^{254}[^{238}U^{16}O]^{+}$) by the mass spectrometer. The signals recorded via time scanning can be analysed as a function of particle size or fraction of the studied element or isotope in the colloid phase. The frequency of the flashes is directly proportional to the concentration of particles in the colloidal suspension. The basic equations for ICP-MS signal s_A analysis of a colloid of size d_{col} are: $s_A = \xi\, d_{col}^{\,3}$

Calibration has been carried out with standard gold colloids, as reported in DEGUELDRE *et al.* (2006a). The tests have been performed on uranium dioxide particles. The study published in Talanta (DEGUELDRE et al., 2006b) describes the experimental conditions and the choice of mass to detect uranium colloids in a single particle analysis mode.

Uranium dioxide colloid distributions derived from the SPC and the ICP-MS data were quantitatively compared. The material distribution could be described by a power law distribution fitted with an exponent $b = 4$. The larger colloid fraction, with a maximum population at d_{col} = 700 nm, was compared with a standard latex bead suspension with d_{col} = 802 nm. The ICP-MS signal s_{238} for $^{238}U^{+}$ were recorded in time scan mode carried out over 20 seconds with signal intensities counted over 10 ms intervals. The signal analysis: $f(s_{238})$ vs s_{238}, was carried out under the following conditions: $\xi = 10^{-5}$ nm^{-3} and for 3 Gaussians distributions with given size maxima and concentrations. This work was published in Talanta for UO_2 colloids, and has also been presented at Actinide 2005 for U_3O_8 colloids.

Comparing the analytical potentials of the different technique used for colloid analysis, it may be stated that SEM allows chemical analysis (colloid sizes >500 nm) and morphological analysis (colloid sizes >50 nm) of colloids in approximately 20 hours. SPC allows the counting of colloids (>30 nm) in only 20 minutes. ICP-MS allows colloid analysis, isotope by isotope, in 20 seconds (for colloid sizes in the range >50-100 nm with a classical torch). This illustrates clearly the potential of this technique.

6.4 References

DEGUELDRE C., FAVARGER P.-Y., ROSSÉ R., WOLD S. (2006a)
Gold colloid analysis by inductively coupled plasma - mass spectrometry in a single particle mode, Analytica Chimica Acta, 555, Issue 2, 263-268.

DEGUELDRE C., FAVARGER P.-Y., ROSSÉ R., WOLD S. (2006b)
Uranium dioxide colloid analysis by single particle inductively coupled plasma - mass spectrometry, Talanta. 68, Issue 3, 623-628.

7 DIFFUSION PROCESSES

L.R. Van Loon, M.A. Glaus, F. González, A. Yaroshchuk, M.H. Bradbury, W. Müller, R. Rossé

7.1 Introduction

The main goal of the "Diffusion Processes" group is to obtain a detailed understanding of the diffusion of radionuclides in compacted argillaceous materials. The clay systems currently under investigation are Opalinus Clay (OPA), compacted bentonite (MX-80), and compacted clay minerals such as montmorillonite, illite and kaolinite.

The work on pure clay minerals was continued. A good set of diffusion data with $^{85}Sr^{2+}$ and $^{22}Na^{+}$ in Na-montmorillonite and Na-illite under different chemical conditions was obtained. Moreover, the first complementary membrane potential measurements on Na-montmorillonite and on kaolinite were also performed. The data indicate a dual porosity diffusion process. Diffusion in the interlayer space, however, dominates the observed fluxes.

The work for the NF-PRO (Near Field Processes) integrated EU-project focused mainly on the diffusion of $^{22}Na^{+}$ and $^{85}Sr^{2+}$ and $^{134}Cs^{+}$ in bentonite at different bulk dry densities. Through-diffusion measurements were combined with out-diffusion and diffusion profile measurement. Additional measurements on $^{36}Cl^{-}$ were also performed. Unlike the diffusion of cations, anions show a single porosity diffusion behaviour. Chloride was found to be excluded from the interlayer and diffuses solely in the interparticle pore space.

Within the framework of the FUNMIG (Fundamentals of Migration) integrated EU-project the diffusion and sorption of $^{134}Cs^{+}$ in intact OPA samples were studied. A sorption isotherm on intact OPA was measured and compared with measurements made in dispersed batch systems. Also, the activation energy for the diffusion of Cs^{+} was measured.

Neutron scattering measurements on the TOF-TOF high resolution time-of-flight spectrometer at the Heinz Maier-Leibnitz neutron source in München were performed, and confirmed the earlier results obtained on the FOCUS time-of-flight spectrometer at the SINQ spallation source at PSI. The structure of ice in different frozen clay samples was measured on the HRPT-diffractometer (High-Resolution Powder Diffractometer for Thermal Neutrons, SINQ).

The work on the reactivity of α-isosaccharinic acid under alkaline conditions (NIREX-SKB-NAGRA-PSI joint project) was finished on time.

7.2 Diffusion in Opalinus Clay

Diffusion experiments in Opalinus Clay were continued. The through-diffusion experiments with $^{134}Cs^{+}$ at a total Cs concentration of 10^{-3} M were finished. The modeling of the data is in progress.
The same system was used to measure the activation energy of the diffusion of $^{134}Cs^{+}$. It was observed that the activation energy (36 kJ mol^{-1}) is twice as large as that for HTO, $^{36}Cl^{-}$ and $^{22}Na^{+}$ (18 - 22 kJ mol^{-1}, VAN LOON et al. 2005). It was further observed that the diffusive flux of $^{134}Cs^{+}$ is significantly higher compared to that of HTO and $^{22}Na^{+}$. Sorption measurements on intact OPA samples indicated that sorption on intact samples is lower by a factor 2-3 than the sorption measured on dispersed OPA. Fig. 7.1 shows the distributions ratio of Cs (R_d) as a function of the equilibrium Cs concentration in solution (Cs_{eq}). Because the sorption is mainly on the frayed edges (FES) and type II sites of the clay (BRADBURY & BAEYENS, 2000), this would mean that in the compact OPA the edge sorption sites are less available.

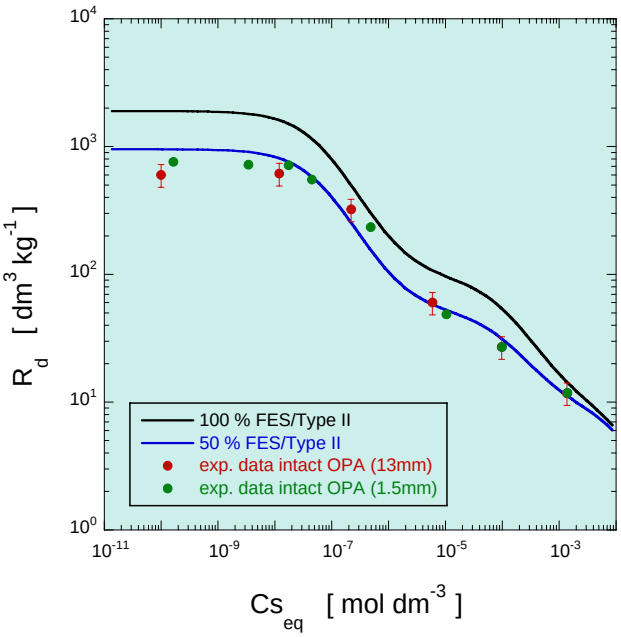

Fig. 7.1: *Sorption of $^{134}Cs^{+}$ on intact OPA from Mont Terri in equilibrium with artificial pore water. The black solid line represents the modelling of the sorption data on crushed OPA. The blue solid line represents the modeling of the data measured on intact OPA. To model the data on intact OPA, the site capacities of FES and type II sites were reduced by a factor of two.*

Experiments on the diffusion of $^{60}Co^{2+}$ and $^{152}Eu^{3+}$ in Opalinus clay were repeated using in-diffusion combined with the abrasive technique recently developed at PSI (VAN LOON & EIKENBERG, 2005). The measurements were performed in a glove box under N_2 atmosphere (O_2 < 2ppm) to avoid oxidation of pyrite in OPA. After a 50 days diffusion time, the profile of ^{60}Co(II) was measured. Two different regions could be observed. In the main region 90 % of the total ^{60}Co(II) diffuses slowly and in a smaller region (10% of total ^{60}Co(II)) diffusion is faster. This confirms the previous observation reported in the annual report from 2005. So far, no explanation for this behaviour has been found. The diffusion of ^{154}Eu(III) is still ongoing.

Texture analysis on OPA samples were performed at the ESRF in Grenoble in cooperation with Prof. H.R. Wenk of the University of California, Berkeley (Earth and Planetary Science). It could be nicely shown that all clay minerals in the OPA are highly textured (preferentially orientated). Moreover, also quartz and calcite were found to be significantly textured. The findings are in agreement with the observed diffusion anisotropy (VAN LOON et al. 2004).

7.3 Diffusion in compacted bentonite

Through-diffusion of $^{36}Cl^-$ was studied as a function of the dry density of the bentonite, and the composition of the external saturating water used in the experiments. The experiments clearly showed that only a small fraction of the total pore space was accessible for $^{36}Cl^-$. This diffusion accessible pore space was hypothesised to be located in the pore space between the clay particles (interparticle pore space). Moreover, it was observed that $^{36}Cl^-$ is also partially excluded from the interparticle pore space. Only at high ionic strengths of the external water, did the diffusion accessible porosity approach the interparticle pore space (Fig. 7.2). The latter was calculated as the difference between the total porosity and the interlayer porosity. For the interlayer porosity, some additional assumptions on the amount of water layers in the interlayer as a function of the bulk dry density of the bentonite had to be made. Up to a bulk dry density of 1300 kg m^{-3}, three layers of water are present. Between a density of 1300 and 1600 kg m^{-3} a change from three to two layers of water in the interlayer was assumed. Beyond 1600 kg m^{-3}, a further decrease to one layer of water was taken. These assumptions were based on basal space measurements reported in KOZAKI et al. (1998). Unlike for cations (GLAUS et al. 2006), it could be shown that the diffusion of anions occurs solely in the interparticle pore space.

Through-diffusion of $^{85}Sr^{2+}$ and $^{22}Na^+$ and $^{134}Cs^+$ was studied as a function of the bulk dry density of the bentonite. As will be shown later (section 7.4), evidence for a dual porosity diffusion process (interparticle and interlayer pore space) was found for these cations.

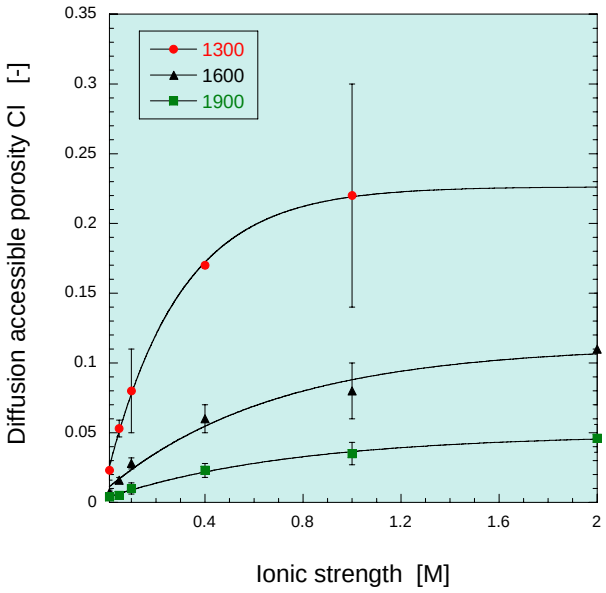

Fig. 7.2: *Effect of ionic strength on the diffusion accessible pore space for $^{36}Cl^-$. For high ionic strength values, the diffusion accessible pore space equals the interparticle pore space.*

7.4 Transport phenomena in compacted clay systems (TRAPHICCS)

A series of through-diffusion experiments with $^{85}Sr^{2+}$ and $^{22}Na^+$ across Na-montmorillonite, Na-illite and kaolinite was finished for a dry density of ~1950 kg m^{-3}. A clear effect of the ionic strength of the contacting solution on the diffusive flux was observed for Na-montmorillonite (Fig. 7.3). For $^{85}Sr^{2+}$ diffusion in Na-montmorillonite, similar relationships were observed, however the corresponding slopes were -2. The observed effects could be explained by a dual porosity diffusion process. However, for the experimental conditions used, interlayer diffusion was the dominating process. Effective diffusion coefficients based on a calculated tracer concentration gradient in the interlayer water of the Na-montmorillonite were found to be independent of the composition of the external water phase.

Independent evidence for interlayer diffusion of Na^+ was obtained from membrane potential measurements. Membrane potentials were measured on Na-montmorillonite compacted to a bulk dry density of 1900 kg m^{-3} after applying salt gradients of NaCl in the feed reservoirs on both sides of the sample.

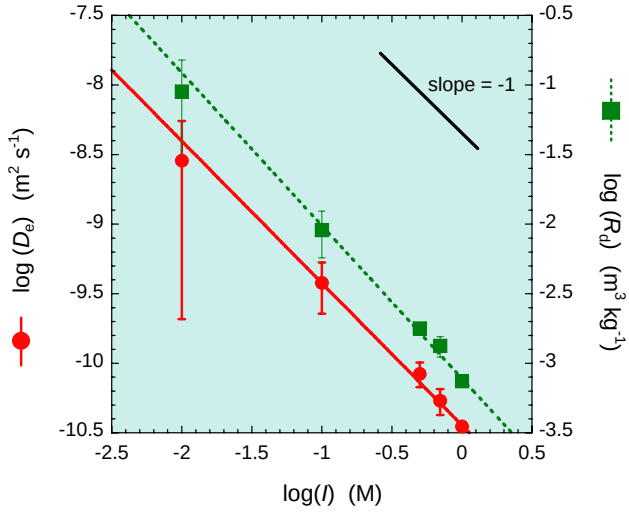

Fig. 7.3: *Effect of ionic strength (I) on the diffusion and sorption of $^{22}Na^+$ in compacted Na-montmorillonite. D_e is an effective diffusion coefficient based on the tracer concentration gradient in the contacting solution.*

After a transient phase of a few hours, during which a steady-state concentration gradient was established across the confining porous filter plates, a constant concentration potential was measured across the clay sample. The relationship between the concentration potential, ΔE, and the ratio of the salt activities in the feed reservoirs is given in Fig. 7.4 and can be described by:

$$\Delta E = \frac{R \cdot T}{F}(2t_+ - 1) \cdot \ln\left(\frac{a_A}{a_B}\right) \qquad (1)$$

where:

ΔE: potential difference between reservoir A and B
R: molar gas constant (8.341 J mol^{-1} K^{-1})
F: Faraday constant ($9.648 \cdot 10^4$ C mol^{-1})
t_+: transport number
a_A, a_B: salt activity in reservoir A and B

The transport number is defined as (BARRY, 1998):

$$t_+ = \frac{u_+}{u_+ + u_-} \qquad (2)$$

where u_+ and u_- are the ionic mobilities of the cation and anion in the clay, respectively. The slope of the line in Fig. 7.4 equals 0.98. From this it can be concluded that the cation transport number, t_+, is almost unity, i.e. the contribution of anions to the current transfer is almost negligible. Such an observation is compatible with the current being transported predominantly in the interlayer water by the charge-compensating cations.

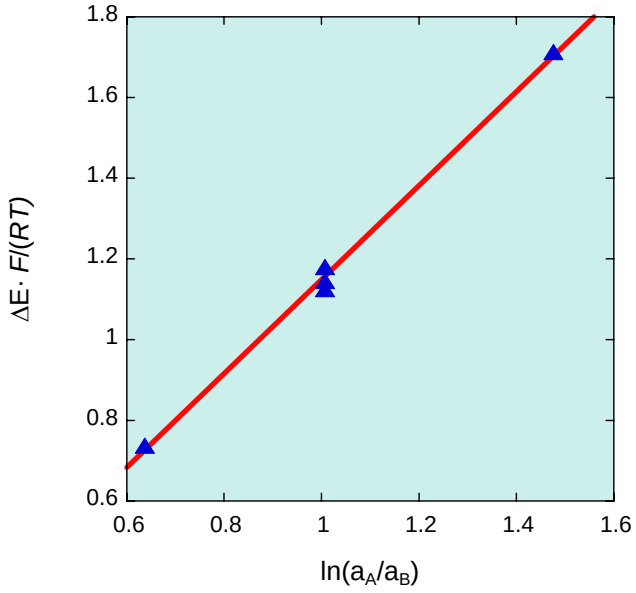

Fig. 7.4: *Membrane potential measurements on compacted Na-montmorillonite: Measured normalised concentration potential as a function of the ratio of salt activities (a" and a') in the feed reservoirs.*

7.5 Dynamics of water in compacted clay systems

Because porewater is the medium through which radionuclides are transported in compacted clay, it is important to know the structure and properties of the confined porewater. The priority question is whether or not confined water has different (or similar) properties to bulk water. Pure clay minerals (montmorillonite, illite, kaolinite, and pyrophyllite) were chosen as model systems for studying the water in clays.

Through-diffusion measurements with HTO were performed on compacted samples of the four materials as a function of temperature. The activation energy for the diffusion of HTO was 22 kJ/mol for montmorillonite. For the other materials, the activation energy was 17 kJ/mol.

Diffraction measurements (HRPT-diffractometer, High-Resolution Powder Diffractometer for Thermal Neutrons, SINQ) on frozen samples showed different ice structures. In montmorillonite – where the water is mainly present in the interlayers – suppression of crystal growth resulted in the formation of amorphous ice. Kaolinite, pyrophyllite and illite, on the other hand, contained ice with a hexagonal (Ice Ih) and a cubic structure.

Time-of-flight measurements on the TOF-TOF spectrometer at FRM II (Garching, Germany) were performed. Because of the larger wavelength of the TOF-TOF neutron beam (λ=10 Å) slower processes such as translational diffusion could be better resolved. The measurements were in good agreement

with earlier measurements performed at the time-of-flight spectrometer FOCUS at PSI, where the beam wavelength is smaller (λ=5.75Å and λ =3.65Å) and therefore the fast rotational movements have a larger contribution to the neutron scattering.

Microscopic data from the time-of-flight instruments (FOCUS and TOFTOF) have been reanalysed separating translational from rotational movement contributions. The diffusion coefficient values were obtained by applying different diffusion models.

7.6 Reactivity of α-isosaccharinic acid

The project investigating the chemical reactivity of α-isosaccharinic acid (α-ISA) in an artificial cement pore water (pH ≈ 12.5) was finished at the end of May 2006. The remaining experiments focused on addressing the role of oxygen in the chemical transformation of α-ISA. Some additional experiments on compacted $Ca(OH)_2$ and hardened cement paste were performed. Both types of experiments led to the conclusion that the chemical transformation was not catalytically promoted by oxygen. Complete chemical transformation of α-ISA was only observed when stoichiometric amounts of oxygen were present. Under strict anaerobic conditions, only parts of α-ISA reacted, probably due to either traces of oxygen or some unidentified oxidising agents present in the solid phase. A microbially mediated process could be excluded because the reactions proceeded in a similar qualitative manner at 90 °C and at room temperature. At 90 ^{o}C, microbial activity is unlikely.

7.7 References

BARRY P.H. (1998)
Derivation of unstirred-layer transport number equations from the Nernst-Planck flux equations. Biophysical Journal 74, 2903-2905.

BRADBURY M.H., BAEYENS B. (2000)
A generalised sorption model for concentration dependent uptake of caesium by argillaceous rocks. J. Contam. Hydrol. 42, 141-163.

GLAUS M., BAEYENS B., BRADBURY M.H., JAKOB A., VAN LOON L.R., YAROSHCHUK A. (2006)
Diffusion of ^{22}Na and ^{85}Sr in montmorillonite: Evidence of interlayer diffusion being the dominant pathway at high compaction. Submitted for publication in Environmental Science and Technology.

KOZAKI T., FUJISHIMA A., SATO S. (1998)
Self-diffusion of sodium ions in compacted sodium montmorillonite. Nuclear technology 121, 63-69.

VAN LOON L.R., SOLER J.M., MÜLLER W., BRADBURY M.H. (2004)
Anisotropic Diffusion in Layered Argillaceous Rocks: A Case Study with Opalinus Clay. Environ. Sci. Technol. 38, 5721-5728.

VAN LOON L.R., MÜLLER W., IIJIMA K. (2005)
Activation energies of the self-diffusion of HTO, $^{22}Na^{+}$ and $^{36}Cl^{-}$ in a highly compacted argillaceous rock (Opalinus Clay). Appl. Geochem. 20, 961-972.

VAN LOON L.R., EIKENBERG J. (2005)
A high-resolution abrasive method for determining diffusion profiles of sorbing radionuclides in dense argillaceous rocks. Applied Radiation and Isotopes 63, 11-21.

8 THE MICROXAS BEAMLINE PROJECT: ON THE WAY TO THE TOP

D. Grolimund, A.M. Scheidegger, M. Harfouche, R. Dähn, B. Meyer, M. Willimann

8.1 Overview

Over the past months, the microXAS beamline team at the Swiss Light Source (SLS) has achieved a number of significant successes with respect to all of the different core objectives of the beamline. The microXAS beamline was originally designed as a hard X-ray microprobe facility dedicated to XAS and XRF with the option of (rudimentary) XRD (SCHEIDEGGER & PRINS, 2000, GROLIMUND et al., 2002). In addition, and going beyond any existing X-ray microprobe instrumentation, the measurement of closed radioactive samples with micro-scale resolution was already foreseen in the original beamline concept. As an important extension to the beamline project, the microXAS beamline became an integral part of the FEMTO project (INGOLD et al., 2004, RIVKIN, 2005). As a result, time-resolved studies with a resolution of ~100 femto seconds will be feasible at the microXAS beamline to study time-dependent phenomena in physics, chemistry, biology, and environmental science (SCHOENLEIN et al., 2000, BRESSLER et al., 2000, SAES et al., 2003).
In the following report, four of the most recent highlights are used to document the considerable progress made during the ongoing commissioning and user operation. These examples illustrate clearly the unique potential of the microXAS beamline.

8.2 Micro-Focusing

Producing a 1x1µm^2 beam of hard X-rays at the SLS represents a demanding optical challenge. This is mainly due to the physical boundary conditions set by the SLS storage ring – in particular the source size and the limited maximum length of any optical beamline system. To overcome these shortcomings, at least partly, a two step focusing concept (MARCUS et al., 2004) tailored to the specific conditions at the SLS was implemented (GROLIMUND et al., 2002). In a first step, a pre-focusing mirror produces a slightly demagnified image of the source. In step two, this image is acting as a secondary source for further, but now pronounced, demagnification by small Kirckpatrick-Baez (KB) mirrors. While such a strategy is favourable in terms of maximizing total acceptance and energy resolution of the beamline, the downside of this arrangement is the demanding requirements concerning optical quality, heat load management as well as mechanical stability of any optical component. Despite all of these potential technical limitations, we have succeeded in producing a (sub-)micron hard X-ray beam at the microXAS beamline. Fig. 8.1 shows derivatives of knife-edge scans yielding the vertical and horizontal beam size and the corresponding spatial intensity distribution. Depicted are measurements for a white beam (almost the entire energy spectrum of the undulator radiation) and for a monochromatic X-ray beam. Note that this capability of fast switching between the two different beam modes (monochromatic micro-beam versus micro-focused white light) represents a unique feature of the microXAS beamline. The measured spot size of approximately 0.7x1.3µm^2 corresponds to the smallest X-ray beam produced at the SLS using achromatic optics (e.g. KB mirrors), which are required to perform spectroscopy.

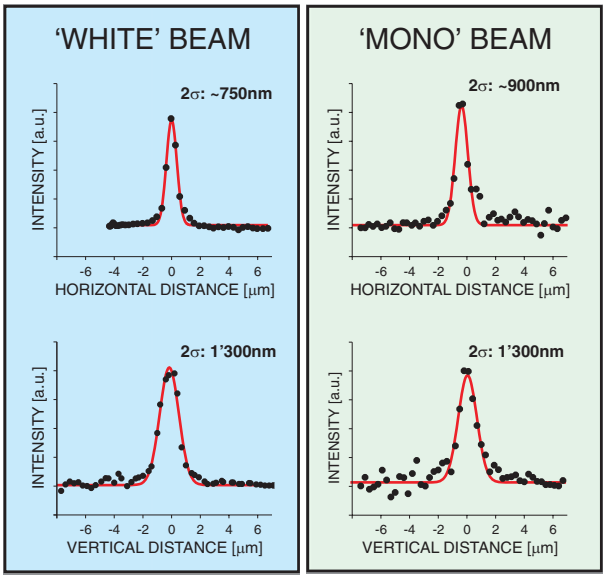

Fig. 8.1: *Beam size at the microXAS beamline as measured by knife-edge scans. Shown are results for micro-focused white light (left panel) and a monochromatic micro-beam (right panel).*

With the achieved beam size of 0.7x1.3µm^2, we have reached the design goal of the microXAS beamline (1x1µm^2, GROLIMUND et al., 2002) and proved our competivness with other synchrotron sources such the ESRF, Spring8 or APS. The slightly increased vertical size of 1.3µm can be explained based on an enlarged vertical source size of the electron beam[#].

[#] The increased vertical source size of the electron beam is caused by an enhanced horizontal/vertical coupling of the SLS storage ring. This coupling will soon be reduced to its lower design value.

Being able to produce a spot size of below 1μm^2 has proven the success of the innovative optical concept of the microXAS beamline. This microXAS concept has already been copied by a micro-beam XAS beamline project at DIAMOND, the new UK synchrotron source.
Currently, further optical and mechanical optimisations are being carried out. It is envisaged to further improve the integrated photon flux and flux density, to simplify and speed-up the alignment of the KB mirror unit (semi-automated alignment), and finally, to improve the robustness of the entire micro-focusing setup during regular user operation.

8.3 Time-efficient XRF mapping

(with major contributions by D. Maden [Controls, SYN])

Standard, two-dimensional XRF mapping is commonly based on a "stop-measure-go" procedure advancing from pixel to pixel. Obviously, due to the high accelerations involved in this 'hopping' process, significant settling times are mandatory after each feed to avoid spatial jittering. We are currently implementing a fast, "**on-the-fly" XRF mapping** procedure. Thereby, the classical, interrupted scanning mode is replaced by a continuous, constant velocity advancing of the scanning motor axis. Pixels are assigned by means of a signal readout triggered by positional feedback signals of the continuously moving scan axis. This improved scheme has two major advantages. First, by avoiding the classical "stop-measure-go" process, a considerable gain in scanning efficiency is obtained. The time penalty due to unproductive scan axis motion and subsequent settling of the system can be reduced to almost zero, and the total mapping time is reduced by up to one order of magnitude. Secondly, in the case of the pixel size being larger than the beamsize, the continuous scanning mode yields a true averaging over the entire pixel.
We have succeeded in recording the first microXRF mapping using this improved scanning scheme. Well-defined, rectangular tantalum structures were used as a micro-structured test pattern. The length-scales of the structures decrease incrementally from 4μm to 1μm. A scanning electron micropcopy image is shown in Fig. 8.2 (*right panel*). The test object was produced by C. David at the laboratory of micro and nano-technology (PSI-LMN).
A two-dimensional elemental distribution map with a pixel resolution of 0.8x2μm^2 was recorded in fluorescence mode using the on-the-fly scanning procedure (beam size of 0.8x1.3μm^2). The recorded Ta L_α fluorescence intensities are depicted in Fig. 8.2 (*left panel*). As is readily apparent, even the 1 micron structures are clearly resolved. Obviously, the resolution in the vertical dimension is limited by the chosen pixel size. In conclusion, the entire microfocus setup, including focusing optics, experimental tables, sample and scanning stages, etc. proved to be extremely precise and stable (free from disturbing vibrations). Furthermore, no systematic distortions were observed, Fig. 8.2 (*left panel*). Accordingly, neither thermal drifts nor mechanical instabilities are diminishing the data quality.
Thus, to summarise, we have demonstrated that the microXAS beamline offers highly stable and precise microXRF mapping capabilities with an outstanding efficiency regarding total recording time.

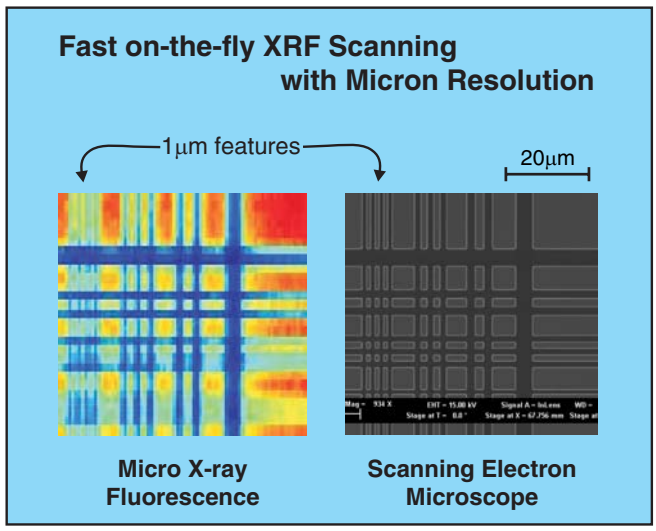

Fig. 8.2: *Time-efficient on-the-fly XRF scanning with micron scale resolution. Tantalum micro-structured test pattern imaged by micro-XRF (left panel) and scanning electron microscopy (right panel).*

8.4 FEMTO installation and slicing

(R&D project lead by G. Ingold, T. Schmidt, S. Johnson, and P.Beaud [FEMTO, SYN]).

During the April 2006 shutdown, the SLS Insertion Device Team finalised the installations within the X05L straight section. All open modifications of the storage ring magnet structure were completed. The wiggler W138 acting as a modulator within the FEMTO slicing scheme was successfully installed and commissioned. Further, crucial electron beam diagnostic devices were added to the straight section. With the completion of the X05L machine-beamline interface, the microXAS beamline project is entering a new era in terms of source and beam stability as well as tunability of the beam trajectory. As an immediate result, the gap of the in-vacuum undulator could be closed for the first time to its design value of 5.5 mm magnetic gap. The insertion device is now delivering a highly brilliant, high intensity X-ray beam over the full spectral range from 4-~23 keV.
As a truly exceptional accomplishment, and only days after the above mentioned extensive hardware

installations, the FEMTO team produced the first femto-second electron beam modulation. The successful interaction of femto-second laser shots with a dedicated bunch of relativistic electrons circling around the SLS storage ring was impressively documented by the measurement of the resulting THz radiation.
After successfully slicing the electron beam, the challenge was to detect femto-second X-ray pulses at the end of the optical system. Key optical elements such as the large mirror unit M1 and the monochromator had to be moved to the proposed femto beam path. To everybody's surprise, the displacement of the optical components out of the path of the core beam could be traced by a live image produced by sliced photons on a fluorescence screen.
Further optimization resulted in a significant improvement regarding the suppression of background contributions. The concept of using both angular separation and source imaging simultaneously as strategies for background noise suppression proved to be highly successful. As depicted in Fig. 8.3, sliced pulse intensity dominates the background contributions of the un-sliced beam as well as the femto-beam halo (storage ring 'memory' of previous slicing events).

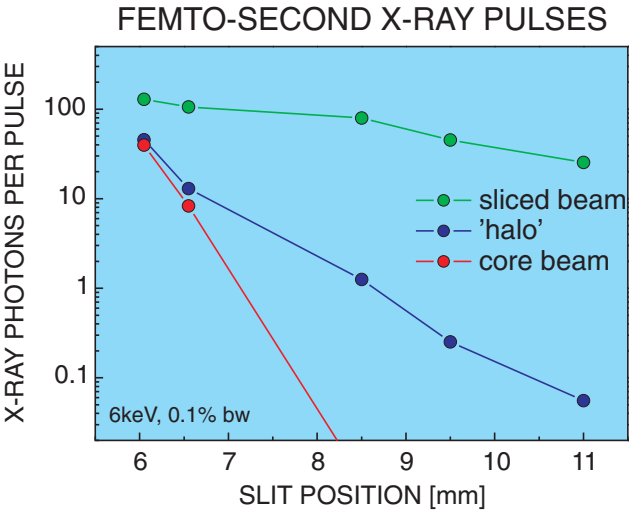

Fig. 8.3: *Femto-second X-ray pulses produced at the microXAS beamline. The ultrafast pulses can be separated from the core beam with an unrivalled pulse-intensity-to-background ratio.*

8.5 Measurements of radioactive samples

(In close collaboration with D. Gavillet, G. Kuri, A. Froideval [LWV, NES], E. Wieland [LES, NES], D. Mohr, A. Fuchs, G. Hauswirth [SU]).

Very recently, investigations on radioactive samples were successfully carried out at the microXAS beamline. A heterogeneous cement sample containing ^{60}Co (total activity: 1300 Bq, dose rate: 2 µSv/h 1cm) as well as a zircaloy sample containing ^{51}Cr, ^{60}Co, ^{103}Ru, ^{125}Sb, ^{132}Te, ^{137}Cs (total activity: 9100 Bq, dose rate: 3 µSv/h 1 cm) were analysed. The beamsize was focused to approximately 10 x 10 µm^2 using the KB focusing mirrors. For both samples elemental distribution maps were recorded by collecting two-dimensional micro-XRF data. Furthermore, we succeeded in collecting the first micro-XAS spectra of a radioactive specimen.
The entire experimental campaign was conducted according to the safety procedure approved by the Federal Office of Health (Bundesamt für Gesundheit, BAG). As requested for the type of samples used, a zone type 1, including a "hand and foot" monitor as well as environmental monitoring, was set up at the microXAS beamline. After the experiments were completed, contamination tests were performed in the experimental hutch and the zone was removed. An impression of the complex experimental setup can be obtained from Fig. 8.4. Most prominent is the removable local shielding (blue and yellow parts), that is obligatory installed during the investigation of active specimens.

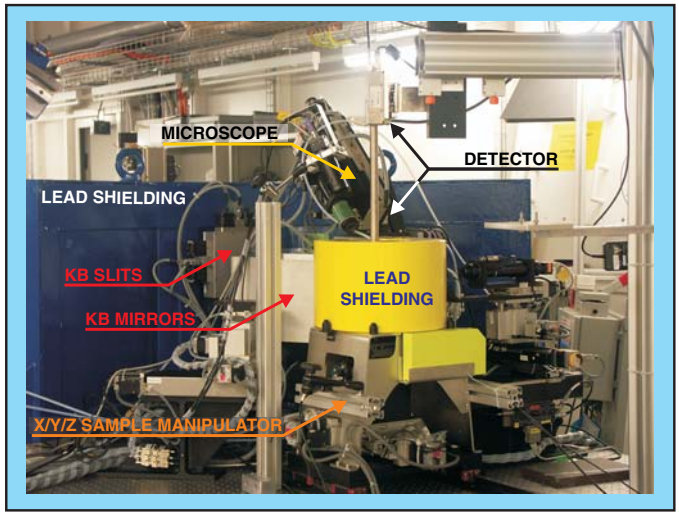

Fig. 8.4: *Experimental setup for the measurement of active samples at the microXAS beamline. Most prominent are the required temporary shielding measures (yellow and blue).*

To illustrate the potential of X-ray micro-probe investigations, Fig. 8.5 shows the spatial distribution of nickel and iron within a radioactive Ni doped cement sample as measured by microXRF. The figure nicely demonstrates the micro-scale heterogeneity within the cement matrix and reveals the heterogeneous distribution pattern of the Ni in cement.

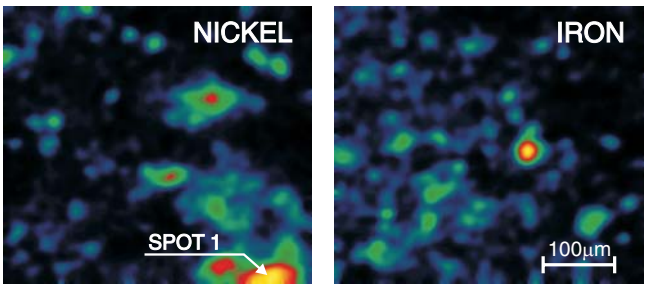

Fig. 8.5: *MicroXRF results showing the spatial distribution of Ni and Fe within a radioactive Ni doped cement sample. The pronounced micro-scale heterogeneity within the cement matrix is readily apparent. The immobilization of Ni in the cement matrix results in Ni-rich micro-domains ('hot spots').*

Micro-XAS experiments were conducted on a Ni rich spot localized within the cement matrix by antecedent micro-XRF mapping. Fig. 8.6 (*top*) depicts the k^3-weighted Ni K-edge EXAFS spectrum while the corresponding Fourier transform is shown in Fig. 8.6 (*bottom*). The chemical speciation observed in the radioactive cement specimen is compared to bulk measurements of Ni reference compounds (α-$Ni(OH)_2$, a natural takovite sample, and a synthesized Ni-Al_2 layered double hydroxide [LDH]). Although a more comprehensive data analysis is still ongoing, preliminary conclusions can be drawn from the inspection of Fig. 8.6. The most important one being that during the hydration process a major part of the aqueous Ni is immobilized in the form of a secondary Ni-Al LDH precipitate.

8.6 More highlights

In addition to the above described highlights, the microXAS beamline has seen a number of successful expert-user experiments. A selection is listed below:

- The Materials Science & Simulation Group at PSI (Prof. H. Van Swygenhoven, R. Maass, S. Van Petegem) has conducted the first successful transmission Laue micro-diffraction experiment using both monochromatic as well as white light micro beams (MAASS et al., 2006).

- Nano-focusing was accomplished by C. David and K. Jefimovs (PSI-LMN) in collaboration with F. Pfeiffer and O. Bunk (PSI-SYN) during a pilot experiment, using zone plates as achromatic focusing devices for hard X-rays. The record focus size achieved at the microXAS beamline so far is approximately 250x250 nm^2.

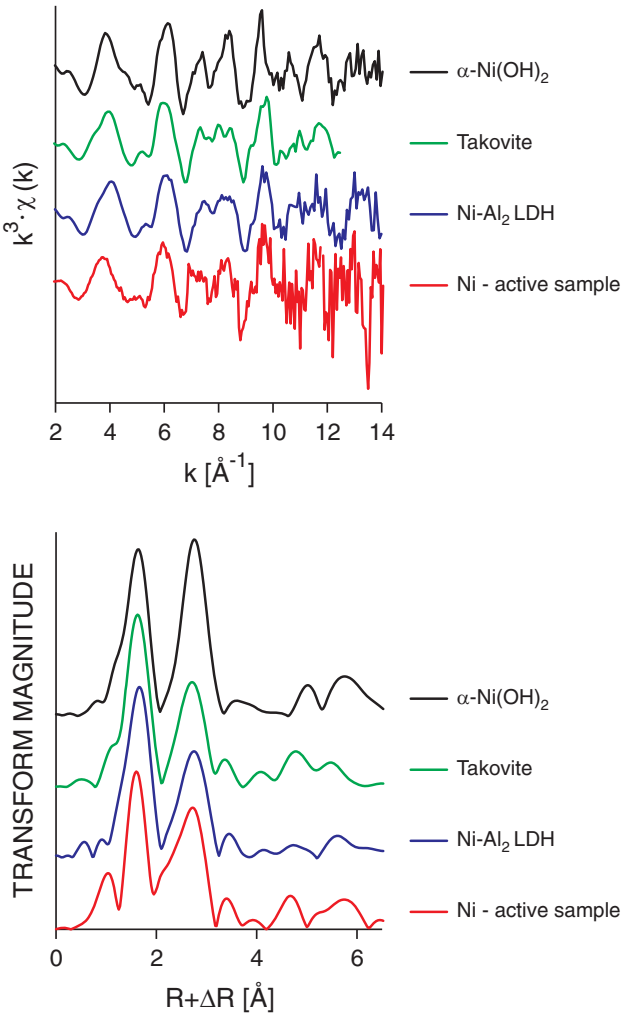

Fig. 8.6: *First micro-XAS spectra obtained from a radioactive specimen. The Ni rich micro-domain indicated in Fig 8.5 was investigated. (top) k^3-weighted Ni K-edge EXAFS spectra and (bottom) the corresponding Fourier transforms. Also shown are bulk measurements of Ni reference compounds for comparison (α-$Ni(OH)_2$, takovite, and a synthesized Ni-Al_2 layered double hydroxide). The results point towards the immobilization of Ni by a newly formed Ni-Al LDH phase.*

- In close collaboration with the SLS-FEMTO team, the research group for Ultrafast Spectroscopy at EPFL (Prof. Ch. Bressler, W. Gawelda, V. Pham, Y. Zaushitsyn, M. Kaiser, and Prof. M. Chergui) produced the world-wide first picosecond time-resolved EXAFS signal up to $k = 10$ Å^{-1}. This extraordinary experimental result in shown in Fig. 8.7. The extended data range allows for the determination of the structure of excited states (GAWELDA et al., 2006).

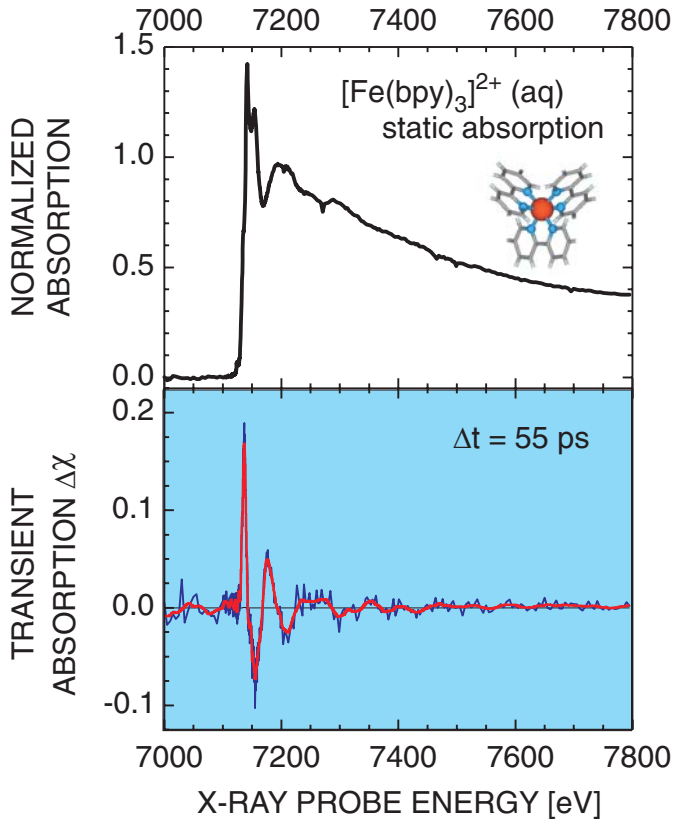

Fig. 8.7: *Ultrafast X-ray absorption of excited states.(top) Raw absorption spectrum for the Fe(bpy) ground state. (bottom) Difference EXAFS signal was recorded 55ps after laser excitation. An evaluable picosecond time-resolved EXAFS signal is observed up to k = 10 Å^{-1}.*

8.7 References

BRESSLER C., SAES M., CHERGUI M., GROLIMUND D., ABELA R., PATTISON P. (2000)
J. Chem. Phys., 116, 2955-2966.

GAWELDA W., PHAM V., BENFATTO M., ZAUSHITSYN Y., KAISER M., GROLIMUND D., JOHNSON S.L., ABELA R., HAUSER A., CHERGUI M., BRESSLER CH. (2006)
Structural Determination of a Short-lived Iron(II) Complex by Picosecond X-ray Absorption Spectroscopy. Physical Review Letters, submitted.

GROLIMUND D., SCHEIDEGGER A.M., VAN DER VEEN J.F., ABELA R. (2002)
Layout of the microXAS beamline at SLS. PSI Scientific Report, 4, 139-148.

INGOLD G., ABELA R., BEAUD P., GROLIMUND D., JOHNSON S.L., RIVKIN L., ROHNER M., SCHLOTT V., SCHMIDT T., SCHULZ L., STREUN A., VAN DER VEEN J.F., CHUBAR O., TARNOVSKY A. (2004)
FEMTO Project : Status of the FEMTO insertion. PSI Scientific Report, 7, 20.

MAASS R., GROLIMUND D., VAN PETEGEM S., WILLIMANN M., JENSEN M., VAN SWYGENHOVEN H., LEHNERT T., GIJS M.A.M., VOLKERT C.A. LILLEODDEN E.T., SCHWAIGER R. (2006)
Applied Physical Letters, in press.

MARCUS M.A., MACDOWELL A.A., CELESTRE R., MANCEAU A., MILLER T., PADMORE H.A., SUBLETT R.E. (2004)
Journal of Synchrotron Radiation, 11, 239-247.

RIVKIN L. (for the SLS team) (2005)
PSI Scientific Report, 1, 86-87.

SAES M., BRESSLER C., ABELA R., GROLIMUND D., JOHNSON S.L., HEIMANN P.A., CHERGUI M. (2003)
Physical Review Letters, 90, 47403.

SCHEIDEGGER A.M., PRINS R. (2000)
Joint proposal by the Swiss XAS user community for an EXAFS beamline for heterogeneous and dilute systems at the Swiss Light Source (SLS), Paul Scherrer Institut, Villigen, Switzerland.

SCHOENLEIN R.W., CHATTOPADHYAY S., CHONG H.H.W., GLOVER T.E., HEIMANN P.A., SHANK C.V., ZHOLENTS A., ZOLOTOREV M. (2000)
Science, 287, 2237-2240.

9 PUBLICATIONS

9.1 Peer reviewed journals and reports

BONHOURE I.[1], BAUR I.[1], WIELAND E., JOHNSON A.[2], SCHEIDEGGER A.M. (2006)
Uptake of Se(IV/VI) oxyanions by hardened cement paste and cement minerals: an X-ray absorption spectroscopy study. Cement and Concrete Research 36, 91-98.
[1] CTB-UPC, Manresa, Spain
[2] EAWAG, Dübendorf, Switzerland

BRADBURY M.H., BAEYENS B. (2005)
Experimental measurements and modelling of sorption competition on montmorillonite. Geochimica et Cosmochimca Acta 69, 4187-4197. Erratum. Geochimica et Cosmochimica Acta 69, 5863-5864.

BRADBURY M.H., BAEYENS B. (2006a)
A quasi-mechanistic non-electrostatic modelling approach to metal sorption on clay minerals. Chapter 19 in: *Surface Complexation Modelling* (ed. J. Lützenkirchen) Elsevier series, Interface Science and Technology 11, 518-538.

BRADBURY M.H., BAEYENS B. (2006b)
Modelling sorption data for the actinides Am(III), Np(V) and Pa(V) on montmorillonite. Radiochimica Acta (in press).

BRADBURY M.H., BAEYENS B., GECKEIS H.[1], RABUNG TH.[1] (2005)
Sorption of Eu(III)/Cm(III) on Ca-montmorillonite and Na-illite. Part 2: Surface complexation modelling. Geochimica et Cosmochimica Acta 69, 5403-5412.
[1]FZK, Karlsruhe, Germany.

BROWN P.L.[1], CURTI E., GRAMBOW B.[2] (2005)
Chemical thermodynamics of zirconium. Nuclear Energy Agency Data Bank, Organisation for Economic Co-operation and Development (ed.), Chemical Thermodynamics Vol. 8, North Holland Elsevier Science Publishers B.V., Amsterdam, The Netherlands, 512 p.
[1] ASIRC, Monash University, Churchill, Australia
[2] Ecole des Mines de Nantes, Nantes, France

CHURAKOV S.V. (2006)
Ab initio study of sorption on pyrophyllite: Structure and acidity of edge sites. Journal of Physical Chemistry B 110(9), 4135-4146.

CURTI E., CROVISIER J.L.[1], KARPOFF A.M.[1], MORVAN G.[1] (2006)
Long-term corrosion of two nuclear waste reference glasses (MW and SON68): A kinetic and mineral alteration study. Applied Geochemistry 21, 1152-1168.
[1] EOST-CGS, University Louis Pasteur, Strasbourg, France

DÄHN R., JULLIEN M.[1], SCHEIDEGGER A.M., POINSSOT C.[1], BAEYENS B., BRADBURY M.H. (2006)
Identification of neoformed Ni-phyllosilicates upon Ni uptake on montmorillonite: A Transmission Electron Microscopy study. Clays and Clay Minerals 54(2), 209-219.
[1] CEA, Saclay, Gif-sur-Yvette, France

DEGUELDRE C., FAVARGER P.-Y.[1], ROSSÉ R., WOLD S.[2] (2006b)
Uranium dioxide colloid analysis by single particle inductively coupled plasma - mass spectrometry. Talanta. 68, Issue 3, 623-628.
[1] University of Geneva, Geneva, Switzerland
[2] Royal Institute of Technology, Stockholm, Sweden

DEGUELDRE C., FAVARGER P.-Y.[1], ROSSÉ R., WOLD S.[2] (2006)
Gold colloid analysis by inductively coupled plasma - mass spectrometry in a single particle mode. Analytica Chimica Acta, 555, Issue 2, 263-268.
[1] University of Geneva, Geneva, Switzerland
[2] Royal Institute of Technology, Stockholm, Sweden

FARGES F.[1], DJANARTHANY S.[1], DE WISPELAERE S.[1], MUNOZ M.[1], MAGASSOUBA B.[1], HADDI A.[1], WILKE M.[2], SCHMIDT CH.[2], BORCHERT M.[2], TROCELLIER P.[3], CRICHTON W.[4], SIMIONOVICI A.[4], PETIT P.-E.[4], MEZOUARD M.[4], ETCHEVERRY M.P.[5], PALLOT-FROSSARD I.[5], BARGAR J.R.[6], BROWN JR. G.E.[6], GROLIMUND D., SCHEIDEGGER A.M. (2005)
Water in silicate glasses and melts of environmental interest: From volcanoes to cathedrals. Physics and Chemistry of Glasses, 46 (4), 350-353.
[1] University Marne Vallee, St Denis, France
[2] University Potsdam, Potsdam, Germany
[3] CEA, Saclay, Gif-sur-Yvette, France
[4] ESRF, Grenoble, France
[5] Musees France, Champs sur Marne, France
[6] Stanford University, Stanford, USA

GAWELDA W.[1], BRESSLER CH.[1], SAES M., KAISER M.[1], TARNOVSKY A.N.[1], GROLIMUND D., JOHNSON S.L., ABELA R., CHERGUI M.[1] (2005)
Picosecond time-resolved X-ray absorption spectroscopy of solvated organometallic complexes. Physica Scripta, T115, 102-106.
[1] EPFL, Lausanne, Switzerland

GEISSMANN CH.[1], YAROSHCHUK A.E., ULBRICHT M.[1] (2006)
Permeability and electrokinetic characterization of poly(ethylene terephthalate) capillary pore membranes with grafted temperature-responsive polymers, Langmuir, published on the Web on July 1, 2006. Doi: 10.1021/la0603774
[1] University of Duisburg, Essen, Germany

GLAUS M.A., LAUBE A., VAN LOON L.R. (2006)
Solid-liquid distribution of selected concrete admixtures in hardened cement pastes. Waste Management 26, 741-751.

GROLIMUND D., BORKOVEC M.[1] (2005)
Colloid-facilitated transport of strongly sorbing contaminants in natural porous media: Mathematical modeling and laboratory column experiments. Environmental Science & Technology 39 (17), 6378-6386.
[1] University of Geneva, Geneva, Switzerland

HARFOUCHE M., WIELAND E., DÄHN R., FUJITA T. [1], TITS J., KUNZ D., TSUKAMOTO M. [1] (2006)
EXAFS study of U(VI) uptake by calcium silicate hydrates. Journal of Colloid and Interface Science (in press).
[1] CRIEPI, Tokyo, Japan

HARFOUCHE M., FARGES F.[1], CROCOMBETTE J.P.[2], FLANK A.M.[3] (2005)
XAFS and molecular dynamics study of natural minerals analogues of ceramics for nuclear waste storage. Physica Scripta T115, 928-930.
[1] University. Marne-la-Vallée, St. Denis, France
[2] CEA, Saclay, Gif-sur-Yvette, France
[3] LURE, Orsay, France

HUMMEL W. (2006)
Solubility of solids in radioactive waste repositories. Chapter 21 in: LETCHER T. (ed.): Developments and Applications in Solubility. The Royal Society of Chemistry, Cambridge, UK (in press).

HUMMEL W., ANDEREGG G.[1], PUIGDOMÈNECH I.[2], RAO L.[3], TOCHIYAMA O.[4] (2005a)
Chemical thermodynamics of compounds and complexes of U, Np, Pu, Am, Tc, Se, Ni and Zr with selected organic ligands. Nuclear Energy Agency Data Bank, Organisation for Economic Co-operation and Development (ed.), Chemical Thermodynamics Vol. 9, North Holland Elsevier Science Publishers B. V., Amsterdam, The Netherlands, 1088 p.
[1] ETH, Zürich, Switzerland
[2] SKB, Stockholm, Sweden
[3] Lawrence Berkeley National Laboratory, Berkeley, USA
[4] IMRAM, Tohoku University, Sendai, Japan

HUMMEL W., ANDEREGG G.[1], PUIGDOMÈNECH I.[2], RAO L.[3], TOCHIYAMA O.[4] (2005b)
The OECD/NEA TDB review of selected organic ligands. Radiochimica Acta 93, 719-725.
[1] ETH, Zürich, Switzerland
[2] SKB, Stockholm, Sweden
[3] Lawrence Berkeley National Laboratory, Berkeley, USA
[4] IMRAM, Tohoku University, Sendai, Japan

HUMMEL W., SCHNEIDER J.W.[1] (2005)
Safety of nuclear waste repositories. Chimia 59, 909-915.
[1] Nagra, Wettingen, Switzerland

KULIK D.A. (2006a)
Dual-thermodynamic estimation of stoichiometry and stability of solid solution end members in aqueous - solid solutions systems. Chemical Geology 225, 189–212.

KULIK D.A. (2006b)
Classic adsorption isotherms incorporated in modern surface complexation models: Implications for sorption of actinides. Radiochimica Acta (in press).

KULIK D.A. (2006c)
Standard molar Gibbs energies and activity coefficients of surface complexes on mineral-water interfaces (thermodynamic insights). Chapter 7 in: Surface Complexation Modelling, (ed. J. Lützenkirchen) Elsevier series, Interface Science and Technology 11, 171-250.

LOTHENBACH B.[1] , WIELAND E. (2006)
A thermodynamic approach to the hydration of sulphate-resisting Portland cement. Waste Management 26, 706-719.
[1] Empa, Dübendorf, Switzerland

METTIER R., KOSAKOWSKI G., KOLDITZ O.[1] (2006)
Influence of small scale heterogeneities on contaminant transport in fractured crystalline rock. Ground Water 44(5), 687-696.
doi:10.1111(g.1745-6584.2006.00236.x
[1] Center for Applied Geoscience, University of Tübingen, Germany

NACHTEGAAL M., SCHEIDEGGER A.M., DÄHN R., CHATEIGNER D.[1], FURRER G.[2] (2005).
Immobilization of Ni by Al-modified montmorillonite: A novel uptake mechanism. Geochimical et Cosmochimica Acta 69, 4211-4225.
[1] CRISMAT, Caen, France
[2] ETH, Zurich, Switzerland

PFINGSTEN W., PARIS B.[1], SOLER J.M.[2], MÄDER U.K.[3] (2006)
Tracer and reactive transport modelling of interactions between high-pH fluids and fractured rock: Field and laboratory experiments. Journal of Geochemical Exploration - Geochemistry for the Safe Isolation of Hazardous Wastes, 90(1-2), 95-113.
[1] ITASCA Consulting, Lyon, France
[2] CSIC, Barcelona, Spain
[3] University of Bern, Bern, Switzerland

RABUNG TH.[1], PIERRET M.C.[1,2], BAUER A.[1], GECKEIS H.[1], BRADBURY M.H., BAEYENS B. (2005)
Sorption of Eu(III)/Cm(III) on Ca-montmorillonite and Na-illite. Part 1: Batch sorption and Time Resolved Laser Fluorescence Spectroscopy experiments. Geochimica et Cosmochimica Acta 69, 5393-5402.
[1] FZK, Karlsruhe, Germany.
[2] Centre de Géochimie de la Surface/Ecole et Observatoire des Sciences de la Terre, Strasbourg, France.

SCHEIDEGGER A.M., GROLIMUND D., CHEESEMAN C.R.[1], ROGERS R.D.[2] (2006)
Micro-spectroscopic investigations of highly heterogeneous waste repository materials. Journal of Geochemical Exploration 88, 59-63.
[1] Imperial College, London, UK
[2] INEEL, Idaho Falls, USA

SCHEIDEGGER A.M., VESPA M. GROLIMUND D., WIELAND E., HARFOUCHE M., DÄHN R. (2006)
The use of (micro)-X-ray absorption spectroscopy in cement research. Waste Management 26(7), 699-705.

SCHEIDEGGER A.M., VESPA M., WIELAND E., HARFOUCHE M., GROLIMUND D., DÄHN R., JENNI A.[1], SCRIVENER K.[1] (2006)
Micro-scale chemical speciation of highly heterogeneous cementitious materials using synchrotron-based X-ray absorption spectroscopy. Chimia 60(3), 149.
[1] IMX, EPFL, Lausanne, Switzerland

SCHINDLER M.[1], MANDALIEV P., HAWTHORNE F.C.[1], PUTNIS A.[2] (2006)
Dissolution of uranyl-oxide-hydroxy-hydrate minerals. I. Curite. The Canadian Mineralogist, 18, 415-431.
[1] University of Manitoba, Winnipeg, Canada
[2] University Münster, Münster, Germany

SCHINDLER M.[1], HAWTHORNE F.C.[1], ALEXANDER M.[2], KUTLUOGLU R.A.[2], MANDALIEV P., HALDEN N.[1], MITCHEL R.H.[2] (2006)
Na-Li-[V_3O_8] insertion electrodes: Structures and diffusion pathways. Journal of Solid State Chemistry, 179, 2616-2628.
[1] University of Manitoba, Winnipeg, Canada
[2] Lakehead University, Thunder Bay, Canada

TITS J., WIELAND E., BRADBURY M.H. (2005)
The effect of isosaccharinic acid and gluconic acid on the Eu(III), Am(III) and Th(IV) retention by calcite. Applied Geochemistry, 20, 2082-2096.

TITS J., WIELAND E., MÜLLER C.J.[1], LANDESMANN C.[2], BRADBURY M.H. (2006)
A wet chemistry study of the strontium binding by calcium silicate hydrates. Journal of Colloid and Interface Science, 300, 78-87.
[1] ETH, Zürich, Switzerland
[2] SUBATECH, Nantes, France

TITS J., IIJIMA K.[1], WIELAND E., KAMEI G.[1] (2006)
Radium binding by calcium silicate hydrates and hardened cement paste. Radiochimica Acta (in press)
[1] JAEA, Tokai, Japan

VAN ISEGHEM P.[1], LEMMENS K.[1], AERTSENS M.[1], GIN S.[2], RIBET I.[2], GRAMBOW B.[3], CROVISIER J.-L.[4], DEL NERO M.[5], CURTI E., SCHWYN B.[6], LUCKSCHEITER B.[7], MCMENAMIN T.[8]
Chemical durability of high-level waste glass in repository environment: Main conclusions and remaining uncertainties from the GLASTAB and GLAMOR projects, in: Scientific Basis for Nuclear Waste Management XXIX, edited by P. Van Isheghem (Mater. Res. Soc. Symp. Proc. 932, Warrendale, PA, 2006), pp. 293-304.
[1] SCK•CEN, Mol, Belgium
[2] CEA-Valrhô, Marcoule, France
[3] Subatech, Nantes France
[4] EOST Centre de Géochimie de la Surface, Strasbourg France
[5] IreS, Strasbourg France
[6] Nagra, Wettingen Swizerland
[7] FZK,Karlsruhe Germany
[8] European Commission, Brussels Belgium

VAN LOON L.R., BAEYENS B., BRADBURY M.H. (2005)
Diffusion and retention of sodium and strontium in Opalinus clay: Comparison of sorption data from diffusion and batch sorption measurements, and geochemical calculations. Applied Geochemistry 20, 2351-2363.

VESPA M., DÄHN R., GROLIMUND D., HARFOUCHE M., WIELAND E., SCHEIDEGGER A.M. (2006)
Speciation of heavy metals in cement-stabilized waste forms: A micro-spectroscopic study. Journal of Geochemical Exploration 88, 77-80.

VESPA M., DÄHN R., GROLIMUND D., WIELAND E., SCHEIDEGGER A.M. (2006)
Spectroscopic investigation of Ni speciation in hardened cement paste. Environmental Science & Technology, 40, 2275-2282.

VESPA M., DÄHN R., GROLIMUND D., HARFOUCHE M., WIELAND E., SCHEIDEGGER A.M. (2006)
Micro-scale investigations of Ni uptake by cement using a combination of scanning electron microscopy and synchrotron-based techniques. Environmental Science & Technology (in press).

VESPA M., DÄHN R., GROLIMUND D., HARFOUCHE M., WIELAND E., SCHEIDEGGER A.M. (2006)
The influence of hydration time on Ni uptake by cement. Czechoslovak Journal of Physics (in press).

WIELAND E., TITS J., ULRICH A.[1], BRADBURY M.H. (2006)
Experimental evidence for the solubility limitation of the aqueous Ni(II) concentration and isotopic exchange of ^{63}Ni in cementitious systems. Radiochimica Acta 94, 29-36.
[1] Empa, Dübendorf, Switzerland

WIELAND E., JOHNSON C.A.[1], LOTHENBACH B.[2], WINNEFELD F.[2] (2006)
Mechanisms and modelling of waste/cement interactions – survey of topics presented at the Meiringen Workshop. Mat. Res. Soc. Symp. Proc. 932, 663-672.
[1] EAWAG, Dübendorf, Switzerland
[2] Empa, Dübendorf, Switzerland

9.2 Conferences/Workshops/Presentations

CHURAKOV S.V., CURTI E.
Mechanism for the substitution of $3Ca^{2+}$ for $2Cm^{3+}$ in calcite. ThUL ACTINET Workshop, INE Karlsruhe, Germany, 25 October 2005.

DÄHN R., BAEYENS B., BRADBURY M.H.
Uptake mechanisms of U(VI) by illite as determined by X-ray absorption spectroscopy. XIII International Conference on X-ray Absorption Fine Structure, Stanford, USA, 9-14 July 2006.

FARGES F.[1,2], ETCHEVERRY M-P.[3,4], HADDI A.[3], TROCELLIER P.[5], CURTI E., BROWN JR G.E.[2]
Durability of silicate glasses: A historical approach. XIII International Conference on X-ray Absorption Fine Structure, Stanford, USA, 9-14 July 2006.
[1] Muséum National d'Histoire Naturelle, CNRS UMR 7160, Paris, France
[2] Stanford University, Stanford, USA
[3] University of Marne la Vallée, St. Denis, France
[4] Laboratoire de Recherche des Monuments Historiques, Champs sur Marne, France
[5] CEA, Saclay, Gif-sur-Yvette, France

GLAUS M.A., JAKOB A., MÜLLER W., VAN LOON L.R., YAROSHCHUK A.
Cation diffusion in highly compacted montmorillonite: Variation of sample thickness and ionic strength. 10th Int. Conf. on Chemistry and Migration Behaviour of Actinides and Fission Products in the Geosphere, Migration 2005, Avignon, France, 18-23 September 2005.

GLAUS M.A., HUMMEL W., RIESER, A.[1], VAN LOON L.R.
PSI contributions to the assessment of natural organic matter from clay. Meeting on 'Dissolved and solid organic matter in argillite from the Opalinus and the Callovo-Oxfordian formations'. (ANDRA–ITÖ–Nagra–PSI–UMR), Zurich, 6-7 October 2005.
[1] Nagra, Wettingen, Switzerland

GLAUS M.A., VAN LOON L.R., YAROSHCHUK A.
Studies of mechanisms of ion transfer in compacted clay by complementary diffusion and electrochemical techniques. ELKIN'06, Intern. Conference on Electrokinetic Phenomena, Nancy, France, 25-29 June 2006.

GONZÁLEZ F.
Translational diffusion of water in compacted clay systems. Seminar Laboratory for Neutron Scattering. 17 March 2006.

GONZÁLEZ F., JURÁNYI F.[1], GIMMI T., VAN LOON L.R.
Translational diffusion of water in compacted clay systems. Confit 2006, 3rd International Workshop on Dynamics in Confinement, Grenoble, France, 23-26 March 2006.
[1] Saarland University, Saarbrücken, Germany.

HARFOUCHE M., FARGES F.[1], MUNOZ M.[2], WILKE M.[3], BROWN JR G.E.[4]
On the coordination of tetravalent actinides in silicate glasses and melts: The "titanite" view. XIII International Conference on X-ray Absorption Fine Structure, Stanford, USA, 9-14 July 2006.
[1] University Marne-la-Vallée, St. Denis, France
[2] University. Grenoble, Grenoble, France
[3] University of Potsdam, Potsdam, Germany
[4] Stanford University, Stanford, USA

HUMMEL W., ANDEREGG G.[1], PUIGDOMÈNECH I.[2], RAO L.[3], TOCHIYAMA O.[4]
The OECD/NEA TDB review of selected organic ligands. 10th Int. Conf. on Chemistry and Migration Behaviour of Actinides and Fission Products in the Geosphere, Migration 2005, Avignon, France, 18-23 September 2005.
[1] ETH, Zürich, Switzerland
[2] SKB, Stockholm, Sweden
[3] Lawrence Berkeley National Laboratory, Berkeley, USA
[4] IMRAM, Tohoku University, Sendai, Japan

JURÁNYI F.[1], GONZÁLEZ F., GVASALIYA S.
Geometrical aspects of QENS experiments in case of anisotropic samples. Confit 2006, 3rd International Workshop on Dynamics in Confinement, Grenoble, France, 23-26 March 2006.
[1] Saarland University, Saarbrücken, Germany

KULIK D.A.
Incorporating classic adsorption isotherms in modern surface complexation models: Implications for sorption of radionuclides. 10th Int. Conf. on Chemistry and Migration Behaviour of Actinides and Fission Products in the Geosphere, Migration 2005, Avignon, France, 18-23 September 2005.

LOTHENBACH B.[1], WINNEFELD F.[1], ALDER C.[1], WIELAND E., LUNK P.[2]
Temperatureinfluss auf die Hydratation von Portlandzementen. 16th IBAUSIL – International Conference on Building Materials, Weimar, Germany, 20-23 September 2006.
[1] Empa, Dübendorf, Switzerland
[2] Holcim, Zürich, Switzerland

MANDALIEV P., CHURAKOV S., DÄHN R., TITS J., WIELAND E.
Application of the bond-valence method, ab initio calculations and XAFS spectroscopy to identify lanthanide binding mechanisms in calcium silicate hydrates. Workshop on X-ray absorption spectroscopy and micro-spectroscopic techniques, Paul Scherrer Institut, Villigen, 20-21 February 2006.

MANDALIEV P., CHURAKOV S., DÄHN R., TITS J., WIELAND E.
Macroscopic and microscopic investigation of Nd binding mechanisms in calcium silicate hydrates (CSH). ThUL-ACTINET School 2006, Lille, France, 15-21 May 2006.

MIBUS J.[1], BRENDLER V.[1], PFINGSTEN W.
Migration of U(VI) in a phosphate environment: Column experiment and modelling. 15th Radio-chemical Conference, Marianske Lazne, Czech Republic, 23-28 April 2006.
[1] Forschungszentrum Rossendorf, Rossendorf, Germany

ROSSANO S.[1], FARGES F.[1,2], TROCERA N.[1], CABARET D.[3], CURTI E., FLANK A.-M.[4], LAGARDE P.[4]
Structural role of Mg in fresh and weathered glasses: A Mg K-edge μ-XANES study. 1st SOLEIL User Meeting, SOLEIL Synchrotron, Gif-sur-Yvette, France, 18-19 January 2006.
[1] University Marne-la-Vallée, St. Denis, France
[2] Stanford University, Stanford, CA, USA
[3] IMPMC, Univ. Paris 6,France
[4] CNRS, UR1, Soleil Synchrotron

SCHEIDEGGER A.M., GROLIMUND D., VESPA M., HARFOUCHE M., WIELAND E., WERSIN P.[1], CUI D.[2]
X-ray micro-spectroscopy: A tool for micro-scale radionuclide speciation in heterogeneous nuclear waste repository materials. 10th Int. Conf. on Chemistry and Migration Behaviour of Actinides and Fission Products in the Geosphere, Migration 2005, Avignon, France, 18-23 September 2005.
[1] Nagra, Wettingen, Switzerland
[2] Studsvik Nuclear AB, Nyköping, Sweden.

STUMPF T.[1], TITS J., FANGHÄNEL TH.[1], WALTHER C.[1], RABUNG TH.[1], WIELAND E. (2005)
Uptake of trivalent actinides (Cm(III)) by hardened cement paste: A time-resolved laser fluorescence spectroscopy (TRLFS) study. 10th Intern. Conf. on Chemistry and Migration Behaviour of Actinides and Fission Products in the Geosphere, Migration 2005, Avignon, France, 18-23 September 2005.
[1] FZK, Karlsruhe, Germany

TITS J., IIJIMA K.[1], WIELAND E., KAMEI G.[1] (2005)
The uptake of radium by calcium silicate hydrates and hardened cement paste. 10th Int. Conf. on Chemistry and Migration Behaviour of Actinides and Fission Products in the Geosphere, Migration 2005, Avignon, France, 18-23 September 2005.
[1] JAEA, Tokai, Japan

TITS J., IIJIMA K.[1], WIELAND E., TOMURA T.[1], KAMEI G.[1]
The role of CSH in the immobilization of strontium and radium by cementitious materials. 29th International Symposium on the Scientific Basis for Nuclear Waste Management, MRS 2005, Ghent, Belgium, 12-16 September 2005.
[1] JAEA, Tokai, Japan

VAN LOON L.R., BAEYENS B., BRADBURY M.H.
Diffusion and retention of sodium and strontium in Opalinus clay: comparision of sorption data from diffusion and batch sorption measurements, and geochemical calculations. 10th Int. Conf. on Chemistry and Migration Behaviour of Actinides and Fission Products in the Geosphere, Migration 2005, Avignon, France, 18-23 September 2005.

VAN LOON L.R.
Endlagerforschung, eine Gratwanderung zwischen Wissenschaft und Anwendung. Fachtagung Schweizerische Gesellschaft der Kernfachleute. ETHZ, Zürich, 28 March 2006.

VAN LOON L.R., GLAUS M.A.
Diffusion of anions and cations in compacted bentonite: towards a mechanistic understanding of diffusion. Technical Meeting (WP2.5, NF-PRO integrated EU Project), BGR, Braunschweig, Germany, 22-23 May 2006.

VESPA M., DÄHN R., GROLIMUND D., HARFOUCHE H., WIELAND E., SCHEIDEGGER A.M.
Micro-XAS study of heterogeneous waste repository materials. SLS User Meeting, Paul Scherrer Institut, Villigen, 17-18 October 2005.

VESPA M., WIELAND E., DÄHN R., GROLIMUND D., SCHEIDEGGER A.M.
Micro-spectroscopic investigation of heavy metal immobilization by cement. Workshop on X-ray absorption spectroscopy and micro-spectroscopic techniques, Paul Scherrer Institut, Villigen, 20-21 February 2006.

VESPA M., DÄHN R., GROLIMUND D., WIELAND E., SCHEIDEGGER A.M.
Micro-XRF/XAS investigation of heavy metals immobilization by hardened cement paste. XIII International Conference on X-ray Absorption Fine Structure, Stanford, USA, 9-14 July 2006.

WERSIN P.[1], GIMMI T., VAN LOON L., SOLER J.M.[2], DEWONCK S.[3], EIKENBERG J., BAEYENS B., HERNÁN P.[4]
Diffusion of HTO, Br^-, I^-, Cs^+, $^{85}Sr^{2+}$, $^{60}Co^{2+}$ and Eu^{3+} in a clay formation: First results from an in-situ experiment in Opalinus Clay. 10th Int. Conf. on Chemistry and Migration Behaviour of Actinides and Fission Products in the Geosphere, Migration 2005, Avignon, France, 18-23 September 2005.
[1] Nagra, Wettingen, Switzerland
[2] CSIC-IJA, Barcelona, Spain
[3] ANDRA, Bure, France
[4] ENRESA, Madrid, Spain

WIELAND E., VESPA M., TITS J., SCHEIDEGGER A.M., DÄHN R., BRADBURY M.H. (2005)
A mechanistic model of the immobilization of nickel radioisotopes in the cementitious near field of an ILW repository. 29th International Symposium on the Scientific Basis for Nuclear Waste Management, MRS 2005, Ghent, Belgium, 12-16 September 2005.

WIELAND E., HARFOUCHE M., FUJITA T.[1], TITS J., KUNZ D., DÄHN R., TSUKAMOTO M.[1] (2006)
A combined wet chemistry and EXAFS study of U(VI) uptake by cementitious materials. 15th Radiochemical Conference Marianske Lazne, Czech Republic, 23-28 April 2006.
[1] CRIEPI, Tokyo, Japan

YAROSHCHUK A.
Advanced characterization of membrane transport properties as input for the modelling. Journée thématique du Club Français des Membranes, Théorie et Modélisation du Transport Transmembranaire, Besançon, France, 14 June 2006.

YAROSHCHUK A.
Concentration polarization phenomena in nano-fluidics. ELKIN'06, Int. Conf. on Electrokinetic Phenomena, Nancy, France, 25-29 June 2006.

9.3 Invited talks

BRADBURY M.H., BAEYENS B.
Modelling the sorption of metals on montmorillonite: Linear free energy relationships. 5th Workshop zum Verbundprojekt "Migration von Actiniden im System Ton, Huminstoff, Aquifer", Leipzig, 4-5 October 2005.

BRADBURY M.H., BAEYENS B.
A quasi-mechanistic non electrostatic modelling approach to metal and actinides sorption on clay minerals: An overview and recent developments. ACTINET Summer school on Geochemistry and Migration of Actinides. Actinide behaviour in Natural Environment, CEA/DPC, Saclay, France, 3-6 July 2006.

GROLIMUND D., INGOLD G., JOHNSON S.L., BEAUD P., ABELA R., BRESSLER CH.[1], GAWELDA W.[1]
Ultra-fast, time-resolved EXAFS: Present capabilities and future prospects. 4th Int. Workshop on Speciation, Techniques, and Facilities for Radioactive Materials at Synchrotron Light Sources, Research Center Karlsruhe, Germany, 18-20 September 2006.
[1] EPFL, Lausanne, Switzerland

GROLIMUND D., HARFOUCHE M., MEYER B., SCHEIDEGGER A.M., WILLIMANN M.
Status and potential of the microXAS beamline. Int. Workshop on X-ray spectroscopic and microscopic methods, Paul Scherrer Institut, Villigen, Switzerland, 20–21 February 2006.

GROLIMUND D., SCHEIDEGGER A.M., HARFOUCHE M., WILLIMANN M., MEYER B.
A new X-ray microprobe facility: The microXAS Beamline at the Swiss Light Source. Synchrotron Environmental Science III, Brookhaven National Laboratory & Stony Brook University, Brookhaven National Laboratory, Long Island, NY, USA, 19-21 September 2005.

HUMMEL W.
Trace metal-humate interactions: The conservative roof approach and its application in performance assessment. 1st Int. Workshop on Organic Matter Modeling, (WOMM'05), Toulon, France, 16-18 November 2005.

KULIK D.A.
Thermodynamics of adsorption. ACTINET workshop on surface complexation on clays (organizer: A.Bauer, FZK INE), Jena, Germany, 14-15 March 2006.

PFINGSTEN W.
MCOTAC applied to gypsum dissolution within a column experiment - code comparison and parameter sensitivity analysis. Réunion Pôle Géochimie-Transport - Workshop of the "Reactive Transport Consortium: International perspectives and new application domains", Saclay, France, 25 November 2005.

SCHEIDEGGER A.M.
Metal speciation in heterogeneous geological media using micro-XRF and micro-XAS. Institut für Geowissenschaften, University of Tübingen, Germany, 8 December 2005.

VESPA M., WIELAND E., DÄHN R., GROLIMUND D., SCHEIDEGGER A.M.
Wet chemistry and micro-XAS studies on radionuclide immobilization in cement-stabilized waste forms. 15th Radiochemical Conference. Marianske Lazne, Czech Republic, 23-28 April 2006.

WIELAND E., JOHNSON C.A.[1], LOTHENBACH B.[2], WÄLLISCH A., WINNEFELD F.[2] (2005)
Conclusions of an international workshop on waste/cement interactions. 29th International Symposium on the Scientific Basis for Nuclear Waste Management, MRS 2005, Ghent, Belgium, 12-16 September 2005.
[1] EAWAG, Dübendorf, Switzerland
[2] Empa, Dübendorf, Switzerland

9.4 Internal reports

GAWELDA W.[1], JOHNSON S.L., GROLIMUND D., ABELA R., KAISER M., PHAM V.T.[1], ZAUSHITSYN Y.[1], VERBRUGGE B.[1], CHERGUI M.[1], BRESSLER CH.[1], CASCELLA M.[1], TAVERNELLI I.[1], HAUSER A.[2]
Ultrafast X-ray absorption spectroscopy at the SLS. PSI Scientific Report 2005, 1, 12-13.
[1] EPFL, Lausanne, Switzerland
[2] University of Geneva, Geneva, Switzerland

RIESER A.B., GLAUS M.A., VAN LOON L.R.
Influence of aqueous extracts from the Callovian-Oxfordian formation at Bure on the sorption and speciation of Ni(II), Eu(III) and Th(IV). PSI Internal Technical Report TM-44-05-02.

SCHEIDEGGER A.M., GROLIMUND D., HARFOUCHE M., WILLIMANN M., MEYER B., DÄHN R., JOHNSON S.L., MOREIRA O., NACHTEGAAL M.
A new hard-X-ray beamline for micro-spectroscopy at the SLS. PSI Scientific Report 2005, 3, 52-53.

SOLER J.M.[1], PFINGSTEN W., PARIS B.[2], MAEDER U.K.[3], FRIEG B.[4], NEALL F.[5], KAELLVENIUS G.[6], YUI M.[7], SHI P.[8], ROCHELLE C. A.[9], NOY D. J.[9] (2006)
Grimsel Test Site - Phase V HPF Experiment: Modeling report. Nagra Technical Report NTB 05-01, Nagra, Wettingen, Switzerland.
[1] CSIC, Barcelona, Spain
[2] ITASCA Consulting, Lyon, France
[3] University of Bern, Bern, Switzerland
[4] Nagra, Wettingen, Switzerland
[5] Neall Consult. United Kingdom
[6] Chalmers University, Gothenburg, Sweden
[7] JNC, Japan
[8] SKB, Stockholm, Sweden
[9] BGS, United Kingdom

9.5 Others/Teachings

DEGUELDRE C., FAVARGER[1] P.-Y., ROSSÉ R., WOLD S.[2]
Uranium Colloid Analysis by Single Particle Inductively Coupled Plasma - Mass Spectrometry, proceedings Actinide 2005, Manchester, 4-8 July 2005, RSC publishing.
[1] University of Geneva, Versoix, Switzerland
[2] Royal Institute of Technology, Stockholm, Sweden

DEGUELDRE C. (2005)
Äspö colloid workshop, Review note, In: The colloid investigations conducted at the Äspö Hard Rock Laboratory during 2000-2004, SKB Technical Report TR-05-20.

KOSAKOWSKI G. (2005)
Geostatistics II. Lecture series for the course “Masters in Applied Environmental Geoscience”.
University of Tübingen, Germany, WS 2005/2006.

KOSAKOWSKI G. (2006)
Geostatistics I. Lecture series for the course “Masters in Applied Environmental Geoscience”.
University of Tübingen, Germany, SS 2006.

KOSAKOWSKI G., KOLDITZ O.[1] (2006)
Models and Applications in Waste Management I and II. Course for masters students. Waste Management Research Center, Graduate School of Environmental Science, University of Okayama, Japan, January 2006.
[1] Center for Applied Geoscience, University of Tübingen, Germany

CHURAKOV S.V. (2005)
Incorporation of foreign elements: ab initio modelling. Molecular modelling: Short Course with Tutorial on Aqueous – Solid Solution Systems Involving Actinides (Thermodynamic and Experimental Aspects). Paul Scherrer Institut, 16-18 November 2005.

KULIK D., CURTI E., CHURAKOV S. (2005)
ACTINET Short Course with Tutorial on Aqueous – Solid Solution Systems Involving Actinides (Thermodynamic and Experimental Aspects) with GEMS-PSI tutorial. Lecturers: E. Curti, D. Kulik, A. Navrotsky, S. Churakov, PSI, Villigen, Switzerland, 16-18 November 2005.
Scripts at: http://les.web.psi.ch/a_school/index.html

WERSIN P.[1], BAEYENS B., BOSSART P.[2], CARTALADE A.[3], DEWONCK S.[4], EIKENBERG J., FIERZ T.[5], FISCH H.R.[5], GIMMI T., GROLIMUND D., HERNÁN P.[6], MÖRI A.[7], SAVOYE S.[8], SOLER J.M.[9], VAN DORP F.[1], VAN LOON L. (2005)
Long-term diffusion experiment (DI-A) – Diffusion of HTO, I^-, $^{22}Na^+$ and Cs^+: Field activities, data and modelling. Mont Terri Technical Report TR 2003-02.
[1] Nagra, Wettingen, Switzerland
[2] Federal Office for Water and Geology, Bern, Switzerland
[3] CEA, Saclay, Gif-sur-Yvette, France
[4] ANDRA, Bure, France
[5] Solexperts, Mönchaltdorf, Switzerland
[6] ENRESA, Madrid, Spain
[7] Geotechnisches Institut, Bern, Switzerland
[8] IRSN, Fontenay-aux-Roses, France
[9] CSIC-IJA, BARCELONA, SPAIN